

Y 3. At7

22/WT-1708

AEC

RESEARCH REPORTS

WT-1708

UNIVERSITY OF
ARIZONA LIBRARY
Documents Collection

NOV 28 1960

Operation

HARDTACK

April - October 1958

Project 26.7

STRUCTURAL RESPONSE AND PERMANENT
DISPLACEMENT MEASUREMENTS

Issuance Date: October 28, 1960

HEADQUARTERS FIELD COMMAND
DEFENSE ATOMIC SUPPORT AGENCY
SANDIA BASE, ALBUQUERQUE, NEW MEXICO

metadc784304

NOTICE

This report is published in the interest of providing information which may prove of value to the reader in his study of effects data derived principally from nuclear weapons tests.

This document is based on information available at the time of preparation which may have subsequently been expanded and re-evaluated. Also, in preparing this report for publication, some classified material may have been removed. Users are cautioned to avoid interpretations and conclusions based on unknown or incomplete data.

PRINTED IN USA

Price \$3.00. Available from the Office of
Technical Services, Department of Commerce,
Washington 25, D. C.

OPERATION HARDTACK II

WT-1708

PROJECT 26.7

STRUCTURAL RESPONSE AND PERMANENT DISPLACEMENT MEASUREMENTS

R. H. Sievers, Jr, Capt, CE, Project Officer
A. R. Stacy, PFC
U. S. Army Engineer Research and Development
Laboratories
Fort Belvoir, Virginia

January 1960

ABSTRACT

Measurements and visual observations made during the Hardtack II series of underground shots provide basis for conclusions regarding shock-resistant design of protection for cavities in rock and qualitative prediction of permanent displacements in rock due to nuclear detonations. Vibration measurements on blast-resistant construction in soil provided non-nuclear test results which apply to shock-resistant design. With varying soil cover, the compressive mode predominated in arch structures and a mass of soil apparently acted with the structure that varied in magnitude in inverse fashion with two depths of cover. Underground structural harmonic response theories were in part verified, for some structures, though the absence of an appreciable flexural mode in buried arch structures was significant.

PREFACE

Project 26.7 was established to (1) provide information relative to material, construction, and geologic features and the effects of range, orientation, and surface location that would enable the design of underground structures to make optimum use of features which might reduce the effects of nuclear shock; (2) determine relative merits of concrete and steel as construction materials for structures in rock; (3) evaluate the use of cushioning material for structures in reduction of accelerations, absorption of transient and permanent strains, spalling, and some block motion without structural damage, and the prevention of concrete spalling; and (4) analyze the nature of block motion in closing a cavity in rock and determine the forces such motion applies to structures together with the possibilities of limiting its magnitude.

Variations in schedule and yields of the Hardtack II series of underground shots prevented collection of data on structures required to cover the objectives of the project. The project was therefore extended to permit investigation by non-destructive testing of existing structures as an approach to these objectives. The project was thus divided by circumstance into results obtained from the nuclear series, Hardtack II, and from investigations of existing structures by non-destructive means.

That portion of the project concerning pre-and post-shot measurements for permanent displacement and strain analysis was conducted as a cooperative effort between the United States Army Engineer Research and Development Laboratories (ERDL) and the United States Coast and Geodetic Survey (USC and GS).

Mr. Walter Helm of USC and GS, as project officer of Project 26.11, was responsible for obtaining movement measurements of the permanent displacement stations. Dynamic structural response measurements during the nuclear tests were recorded in conjunction with measurements of the related Project 26.3, Earth Motion Measurements, Part III, conducted by ERDL. Non-destructive vibration tests were performed on structures constructed for Operation Plumbbob under sponsorship of the Office of Civil and Defense Mobilization and the Office of the Chief of Civil Engineers, United States Navy.

CONTENTS

ABSTRACT	4
PREFACE	5
 PART 1 PERMANENT DISPLACEMENT MEASUREMENTS	13
CHAPTER 1 INTRODUCTION.	13
1.1 Objectives.	13
1.2 Background.	13
1.3 Theory.	14
1.3.1 Accelerations	17
1.3.2 Strain.	18
1.3.3 Permanent Displacement within the Tunnel. . .	18
1.3.4 Permanent Displacement on the Surface	19
 CHAPTER 2 PROCEDURE	26
2.1 Description of Tests.	26
2.2 Instrumentation	28
 CHAPTER 3 RESULTS	41
3.1 General Summary of Tests.	41
3.1.1 Tamalpais Characteristics	41
3.1.2 Neptune Characteristics	42
3.1.3 Logan Characteristics	43
3.1.4 Evans Characteristics	45
3.1.5 Blanca Characteristics.	46
3.1.6 Rainier Characteristics	47
3.2 Forcebeams.	49
3.3 Permanent Displacements	49
 CHAPTER 4 DISCUSSION.	51
4.1 Accuracy of Measurement	51
4.2 Interpretation of Results	52
4.3 Related Work.	56
4.3.1 High Explosive Tests.	56
4.3.2 Nuclear Detonations	58
 CHAPTER 5 CONCLUSIONS AND RECOMMENDATIONS	59
5.1 Displacements	59
5.2 Protective Lining for Cavities.	61
5.3 Confirmation and Continuation	63
 PART 2 STRUCTURAL RESPONSE MEASUREMENTS.	65
CHAPTER 6 INTRODUCTION.	65
6.1 Objectives.	65
6.2 Background.	65
6.3 Theory-Shock Isolation Analysis	66
6.4 Theory-Vibration Testing.	66
6.5 Theoretical Periods-Steel Arch Structures	69
6.5.1 Compressive Mode.	70
6.5.2 Flexural Mode	71

6.6	Theoretical Periods-Buried Culverts.	73
6.6.1	Compressive Mode	74
6.6.2	Flexural Mode.	75
6.7	Theoretical Period-Concrete Dome	76
6.8	Theoretical Period-Underground Garage.	77
CHAPTER 7	PROCEDURE.	82
7.1	Field Operations	82
7.2	Instrumentation.	82
7.2.1	Accelerometer Testing.	82
7.2.2	Gage Mount Tests	84
7.3	Structural Vibration Induction	86
CHAPTER 8	RESULTS.	92
8.1	General.	92
8.2	Steel Arch Structures.	93
8.3	Circular Steel Culvert	97
8.4	Cattlepass Structures.	102
8.5	Circular Reinforced Concrete Culvert	106
8.6	Concrete Dome.	109
8.7	Underground Garage	109
CHAPTER 9	DISCUSSION	124
9.1	Accuracy of Measurement.	124
9.2	Condition of the Structures.	126
9.3	Interpretation of Results-By Structures.	128
9.3.1	Steel Arch Structures.	128
9.3.2	Circular Steel Culvert	132
9.3.3	Cattlepass Structures.	134
9.3.4	Circular Reinforced Concrete Pipe.	135
9.3.5	Concrete Dome.	137
9.3.6	Underground Garage	138
9.4	Interpretation of Damping Measurements	143
9.5	Discussion of Test Procedures.	144
9.6	Discussion of Foam Cushioning.	145
CHAPTER 10	CONCLUSIONS AND RECOMMENDATIONS	149
10.1	Basis	149
10.2	Application of Underground Vibration Theory	149
10.3	Dome Response	151
10.4	Steel Versus Concrete for Underground Structures.	152
10.5	Use of Non-Destructive Testing.	153
10.6	Plastic Foam Cushioning	153
10.7	Confirmation, Continuation, and Related Applications	154
APPENDIX I	VIBRATION MEASUREMENT ON EXISTING STRUCTURES	
	FEASIBILITY STUDY.	156
I.1	Introduction	156
I.1.1	Objective.	156
I.1.2	Background	156
I.1.3	Theory	157
I.2	Procedure.	158
I.2.1	Simple Steel Beam.	158

I.2.2	Massive One-Way Slab.	161
I.2.3	Corrugated-Steel Culvert Pipe	163
I.3	Results	164
I.3.1	Data Sought	164
I.3.2	Analytical Procedure.	165
I.3.3	Measured Structural Responses	165
I.4	Conclusions	168
APPENDIX II SHOCK ISOLATION OF UNDERGROUND STRUCTURES . . .		184
II.1	Introduction	184
II.1.1	Objective and Scope.	184
II.1.2	Background.	184
II.1.3	Theory	185
II.2	Procedure.	187
II.2.1	General.	187
II.2.2	Method I	187
II.2.3	Method II.	188
II.2.4	Method III	188
II.3	Discussion	189
II.3.1	Methods.	189
II.3.2	Results.	190
II.4	Conclusions.	191
II.4.1	Structural	191
II.4.2	Application to Shock Tube or Blast Simulator	192
II.5	Recommendations and Future Work.	192
II.5.1	Design	192
II.5.2	Cost	192
II.5.3	Arches	193
APPENDIX III TABULATED AND GRAPHIC PERMANENT DISPLACEMENT RESULTS.		199
REFERENCES		216
TABLES		
2.1	Description of Bedding.	29
7.1	Testing Schemes	88
8.1	Measured Periods-Steel Arch Structures.	95
8.2	Accelerometer and Loading Positions-Steel Arch Structures.	96
8.3	Measured Periods-Circular Steel Culvert	99
8.4	Accelerometer and Loading Positions-Circular Steel Culvert	101
8.5	Measured Periods-Cattlepass Structures.	103
8.6	Accelerometer and Loading Positions-Cattlepass Structures	105
8.7	Measured Periods-Circular Concrete Culvert.	107
8.8	Accelerometer and Loading Positions-Circular Concrete Culvert	108
8.9	Measured Periods-Underground Garage	110
I.2.1	Steel Beam-Load and Accelerometer Positions	160
I.3.1	Steel Beam-Results of Record Analysis	170
I.3.2	Corrugated Steel Pipe Ten Foot Section-Analysis Summary	171

I.3.3	Corrugated Steel Pipe Thirty Inch Section-Sanborn Unit Records Summary.	172
I.3.4	Corrugated Steel Pipe Thirty Inch Section-Consolidated Unit Records Partial Summary.	173
II.1	Maximum Values of Forcing and Reaction Functions VS Controlling Constants, Method I	194
II.2	Maximum Values of Forcing and Reaction Functions VS Controlling Constants, Method II.	195
II.3	Maximum Values of Forcing and Reaction Functions VS Controlling Constants, Method III	196
III.1	Surface Permanent Displacements, Blanca	199
III.2	Surface Permanent Displacements, Tamalpais.	201

FIGURES

1.1	Predicted Accelerations	21
1.2	Predicted Dynamic Radial Strains.	22
1.3	Predicted Dynamic Tangential Strains.	23
1.4	Permanent Displacements Due to Shot Rainier	24
1.5	Displacement Within Tunnel, Shot Rainier.	25
2.1	Underground Tests Site.	33
2.2	Horizontal Section, Tunnels U12b, U12c.	34
2.3	Horizontal Section, Tunnel U12e	35
2.4	Permanent Displacement Stations on Surface.	36
2.5	Permanent Displacement Stationing	37
2.6	Position of Force-Beams in Alcove	38
2.7	Basic Force-Beam.	39
2.8	Placement of Force-Beams.	40
6.1	Cattlepass Section.	81
7.1	Accelerometer and Turnbuckle Attachment	90
7.2	Plot Plan, Tested Structures.	91
8.1	Unreinforced Steel Arch Structure	111
8.2	Typical High Explosive Placement.	112
8.3	Temporary Flooding at Project Site.	112
8.4	Record of Run 113, Circular Steel Culvert	113
8.5	Four Point Loading in Cattlepass.	115
8.6	Record of Run 100, Circular Concrete Culvert.	117
8.7	Accelerometers and Loading, Concrete Dome	119
8.8	Record of Run 119, Concrete Dome.	121
8.9	Underground Garage Interior.	123
I.2.1	Steel Beam Test	174
I.2.2	Steel Beam Gage Mountings	175
I.2.3	Concrete Magazine Exterior.	176
I.2.4	Loading Column and Gage Mountings, Concrete Magazine.	177
I.2.5	Loading Column Calibration and Release Test	178
I.2.6	Column Release Characteristics.	179
I.2.7	Steel Culvert Field Test.	180
I.2.8	Corrugated Steel Pipe with Circumferential Loading.	181
I.2.9	Corrugated Steel Pipe Gage Mountings.	182
I.3.1	Steel Beam Sample Record Analysis	183
II.1	Typical Foam Isolation Installation	197
II.2	Typical Foam Force-Deflection Curve	197
II.3	Air Pressure Pulse.	198

II.4	Possible Use of Foam in a Shock Tube.	198
III.1	Pre Events to Post Tamalpais, Tunnel U12b	202
III.2	Post Tamalpais to Post Events, Tunnel U12b.	203
III.3	Pre to Post Events, Tunnel U12b	204
III.4	Geologic Section, Tunnel U12c	205
III.5	Neptune Crater Sections Plot Plan	206
III.6	Neptune Crater Sections	207
III.7	Pre Events to Post Events, Tunnel U12e.	208
III.8	Surface Horizontal Displacement Contours, Blanca. .	209
III.9	Surface Vertical Displacement Contours, Blanca. . .	210
III.10	Section along Line-J.	211
III.11	Section along Line-L.	212
III.12	Section thru WP-Blanca.	213
III.13	Section along Line-P.	214
III.14	Section along Line-S.	215

PART 1. PERMANENT DISPLACEMENT MEASUREMENTS

CHAPTER I

INTRODUCTION

1.1 OBJECTIVES

Basic objectives of this project have been stated in the preface. It was planned to obtain the required information by participation in the Hardtack II series in the form of observation of damage to and response of structure arrays. These observations to be backed by dynamic measurements made under ERDL Project 26.3 (Reference 1) and by permanent displacement and strain measurements made under USC and GS Project 26.11 (Reference 2).

1.2 BACKGROUND.

No known structure in rock had been subjected to shock due to a nuclear detonation in that rock prior to the Hardtack II series. Response of underground structures subject to air-induced ground shock or to direct ground shock from a shallow underground burst had been measured in previous test series. Measurements included static, dynamic, and scratch-type records but these could not be correlated to rock because of a lack of scaling data or of justification for use of interaction of soil and structure to represent interaction of rock and structure.

Shock isolation within a rock medium had not been tested. Frangible lining of an underground structure in soil was tested in Operation Plumbbob but with inconclusive results. Use of a flexible foam plastic for protection of an underground structure as was planned for incorporation in this project had received no prior full-scale tests.

Selection of position of the structure installations and, with their deletion, of the force-beams was based on results of Shot Rainier of Operation Plumbbob (References 3, 4, and 5), geologic investigations by the U. S. Geological Survey for the Atomic Energy Commission (References 6, 7, and 8), and the data collected in the Underground Explosions Test Program (Reference 9). Effects of Shot Rainier within the U12b tunnel were such as to indicate that critical structure loading factors within rock are block motion, spalling, and large transient strains. Block motion is used to refer to motion between planes of weakness of an integral mass of rock as opposed to plastic flow, in which geologic structure is lost and viscous flow takes place. The term spalling is used to cover rock movements in the form of flaking and slabbing in which rock adjacent a cavity is loosened along planes roughly parallel the nearest cavity surface, caused by reflection of the shock or excessive shear on planes of weakness.

Permanent displacements and strains due to Shot Rainier were measured (as reported in Reference 4), but the value of these measurements was limited due to uncertainty of survey accuracy, limitations in number and distribution of stations, and lack of reliable data from points on the surface.

1.3 THEORY

Force-beams were situated in an alcove to measure the forces applied across a cavity by the shock. The alcove had a lining of steel ribs with lagging, emplaced in such a manner that the interior was provided protection from such overhead spalling and overbreakage

as might occur prior to the shot. The lining provided no resistance to transient strain or block motion in the range of action of the force-beams. Three beams were placed horizontally in the alcove with their axes essentially radial from the WP of the Evans shot, 280 feet from the alcove. The experiment was intended to provide loading input data for the region of shock effects comparable to that furthest point at which the Rainier tunnel was sealed.

The Rainier tunnel, tangent to a fifty-foot radius from the WP, was sealed by the shot to a range of 200 feet. The same shot produced a crushed zone extending 130 feet from the WP. The cube root scaling law was assumed applicable for extending the Rainier data to the Evans shot. With this assumption, the Rainier shot of 1.7 kilotons (kt) closed the tunnel out to approximately $170 W^{1/3}$ feet, where W is the effective yield of the weapon in kt. Range to the test emplacement was selected using the above scaling, the alcove selected being at a range of $154 W^{1/3}$ (280) feet.

Permanent displacements occurring below the rhyolite cap as a result of the Rainier shot indicated that the material between the WP and the slope underwent a general motion towards the surface of the escarpment. The magnitude of this motion decreased with radial range from the WP except near the surface, where a lessening of confinement allowed an increase in displacement. The increase of the horizontal section as a result of this outward expansion caused a general settlement, which likewise increased nearing the surface. The volume of new voids within the mountain,

as in cracks or the cavity at the WP was thus more than counter-balanced by the increased area of horizontal sections thru the mountain, resulting in a general decrease in elevation.

The net motion of the rock as measured in the tunnel, was towards the nearest surface. The direction of motion indicated no tendency towards being radial from the WP, with the exception of the closest point (at a range of 203 feet). Net motion at this range had twenty-six degrees divergence from radial as opposed to the average divergence of thirty-nine degrees.

The net direction of motion of the points in the tunnel varied only slightly from a point at a range of 216 feet to the furthest point measured, at a range of 1683 feet. The direction of motion of rock was towards the surface but at an angle of greater divergence from a radial from the WP than the direction of the shortest distance to the surface. This motion indicated a large effect of bedding on the direction of net motion, for the general dip of the bedding in the vicinity of the tunnel is down into the mesa, as shown in Figure 2.1. Motion of the points in the tunnel in a direction along the bedding and radial to the WP would consequently have required a sizeable upward component of motion. Similar motion of those same points but towards the nearest surface would have required upward motion but of lesser magnitude. The motion as actually measured, in a direction almost forty degrees from being radial from the WP, required the minimum upward motion that need occur while remaining in the general plane of the bedding and moving towards the surface.

The results described above indicated that the major factors influencing the direction of net motion are the nearness and direction of the surface and the degree and direction of the dip of the bedding. The bedding channeled the thrust of the blast to a great degree, with the resultant motion tending to be in the plane of the bedding. Greater displacements than those which occurred with the Rainier shot would be anticipated if the dip were towards the surface from the WP.

Results from Rainier were used to make some of the following estimates of accelerations, motions, and strains for the Hardtack II series of underground shots.

1.3.1 ACCELERATIONS

Applicable Rainier acceleration records for measurement of peak acceleration were limited, due to the overranging of all but two of the accelerometers in the tunnel during that test. Acceleration records from the vertical drill holes are not considered because of the great variation in rock structure and type between the rock above the shot and that in which the tunnel was situated.

Shot Evans and the alcove in which the force-beams were installed were situated in a rock strata very similar to that in which Rainier took place. The two acceleration readings from within the tunnel for Rainier which were not overranged were used for acceleration prediction. Using a straight-line connection on a logarithmic plot (Figure 1.1) the predicted acceleration on the basis of a six-kt shot was 285 G for the 280-foot range.

1.3.2 STRAIN

No strain measurements of value from within the tunnel were obtained from Rainier, due to equipment failure and adverse shock effects on the gages. The data collected by the Underground Explosion Test Program (Reference 9) from tests in sandstone were therefore used as providing the best available estimate of strain.

These equations are in the form

$$\epsilon = K \left(\frac{L}{W^{1/3}} \right)^n \quad (1.1)$$

where ϵ is the strain in micro-inches per inch, L is the radial distance from the charge in feet, W is the effective yield in pounds of TNT, and K and n are constants dependent upon characteristics of the surrounding medium and direction of strain.

For radial strain in sandstone, the equation is

$$\epsilon_R = 1.5 \times 10^4 \left(\frac{L}{W^{1/3}} \right)^{-2.4} \quad (1.2)$$

and for tangential strain in sandstone the equation is

$$\epsilon_T = 2 \times 10^3 \left(\frac{L}{W^{1/3}} \right)^{-1.9} \quad (1.3)$$

An efficiency of thirty percent was used to compute an equivalent high explosive (HE) yield for scaling purposes. Using the above analysis and assuming that the tuff would act in a manner similar to sandstone, transient radial strain was predicted as 0.92 percent at the 280 foot range (Figure 1.2). Tangential strain, similarly computed, was predicted as 0.14 percent at 280-foot range (Figure 1.3).

1.3.3 PERMANENT DISPLACEMENT WITHIN THE TUNNEL

Measurement of permanent displacements due to the Rainier shot,

for points within the tunnel, provide data only for a line essentially tangent to a fifty-foot radius from the WP and which had a direction other than that in which the largest displacements took place. Furthermore, accuracy of the permanent displacement measurements for Rainier is doubtful due to the order of surveying employed, though the general direction of motion as measured seemed to have been confirmed by the geologic effects of the shot. The measurements obtained from Rainier are as shown in Figure 1.4 and as plotted in Figure 1.5.

The addition of side drifts to the Rainier tunnel following that shot permitted an examination during the Hardtack II series of movements in many different orientations from the points of detonation, enabling measurements of motions inward and outward of the WP for shot Tamalpais in the U12b.02 drift and in many different directions surfaceward for shot Evans in U12b.04.

Permanent strain across the tunnel cavity in the rock was not measured in Rainier. This measurement to have been made in many different locations for each shot in the Hardtack II series, was designed to provide information and to determine occurrence and nature of block motion in squeezing a tunnel section.

1.3.4 PERMANENT DISPLACEMENT ON THE SURFACE.

Measurements of permanent displacement of points on the slope of the escarpment as caused by shot Rainier were for the most part not made on rock continuous with the strata encountered in the tunnel. A comprehensive set of points on outcrops of the bedding was selected to provide coverage of the surface effects of the

Hardtack II Shots. As a result of Rainier a settlement of a tenth of a foot and horizontal motion of approximately one and one half feet took place at one point atop the mesa. A thick bed of poorly cemented material above the WP and the highly fractured cap rock of the mesa apparently accounted for this displacement. To check the extent of such motions as a result of shocks in Hardtack II, pre-and post-shot surveys were planned for a network of stations on the surface of the mesa.

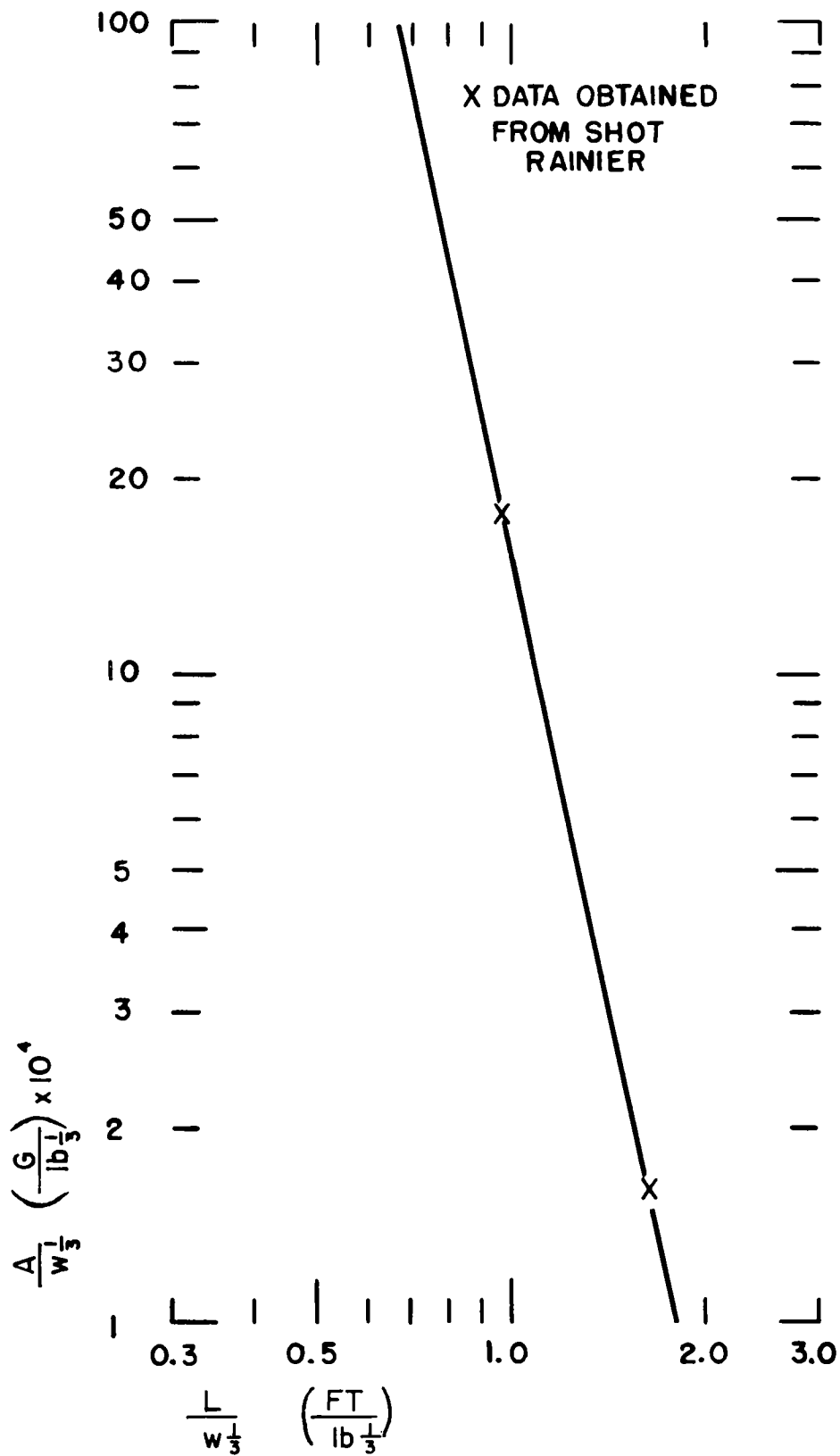


FIGURE I.1- PREDICTED ACCELERATION

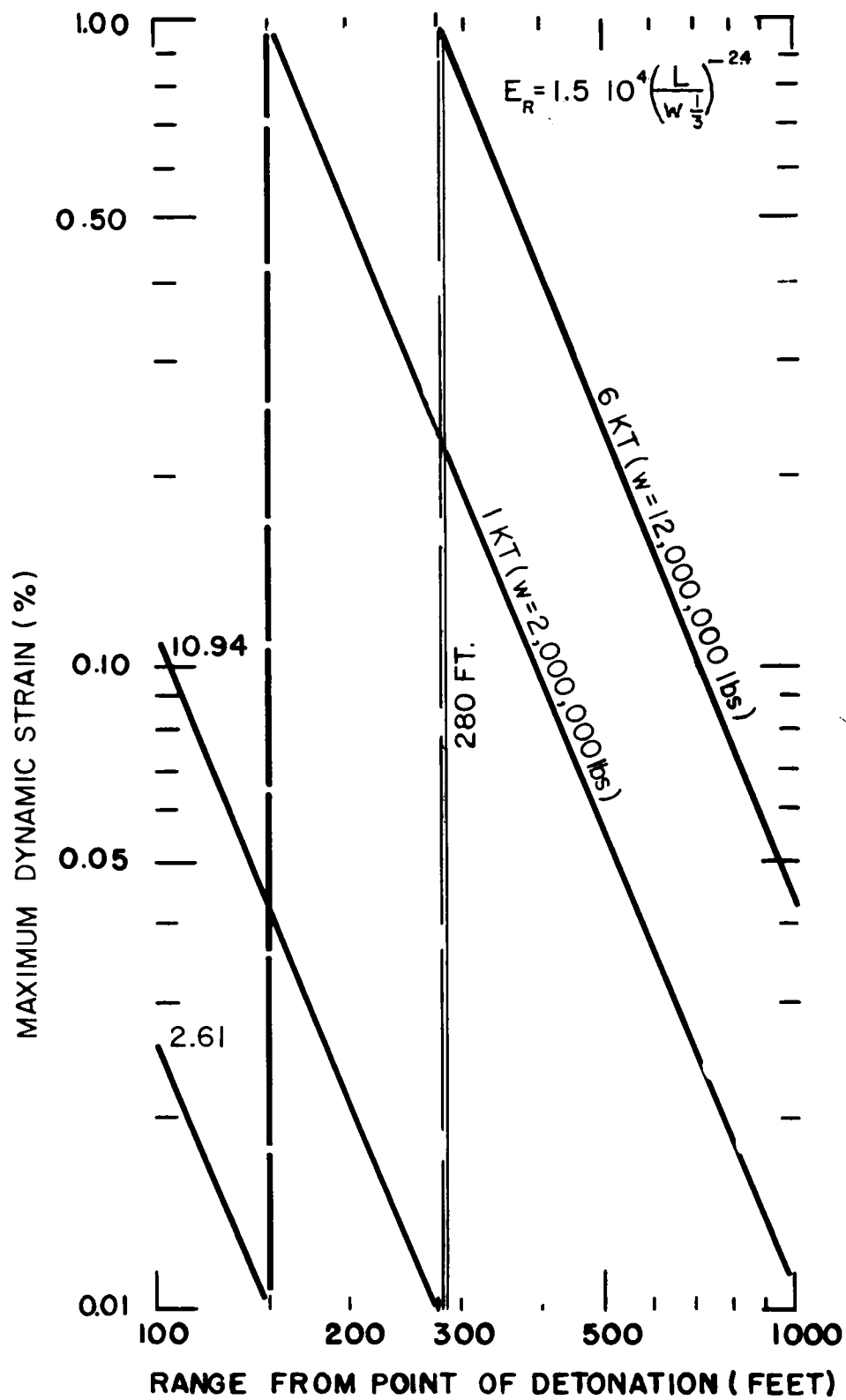


FIGURE 1.2 PREDICTED DYNAMIC RADIAL STRAINS

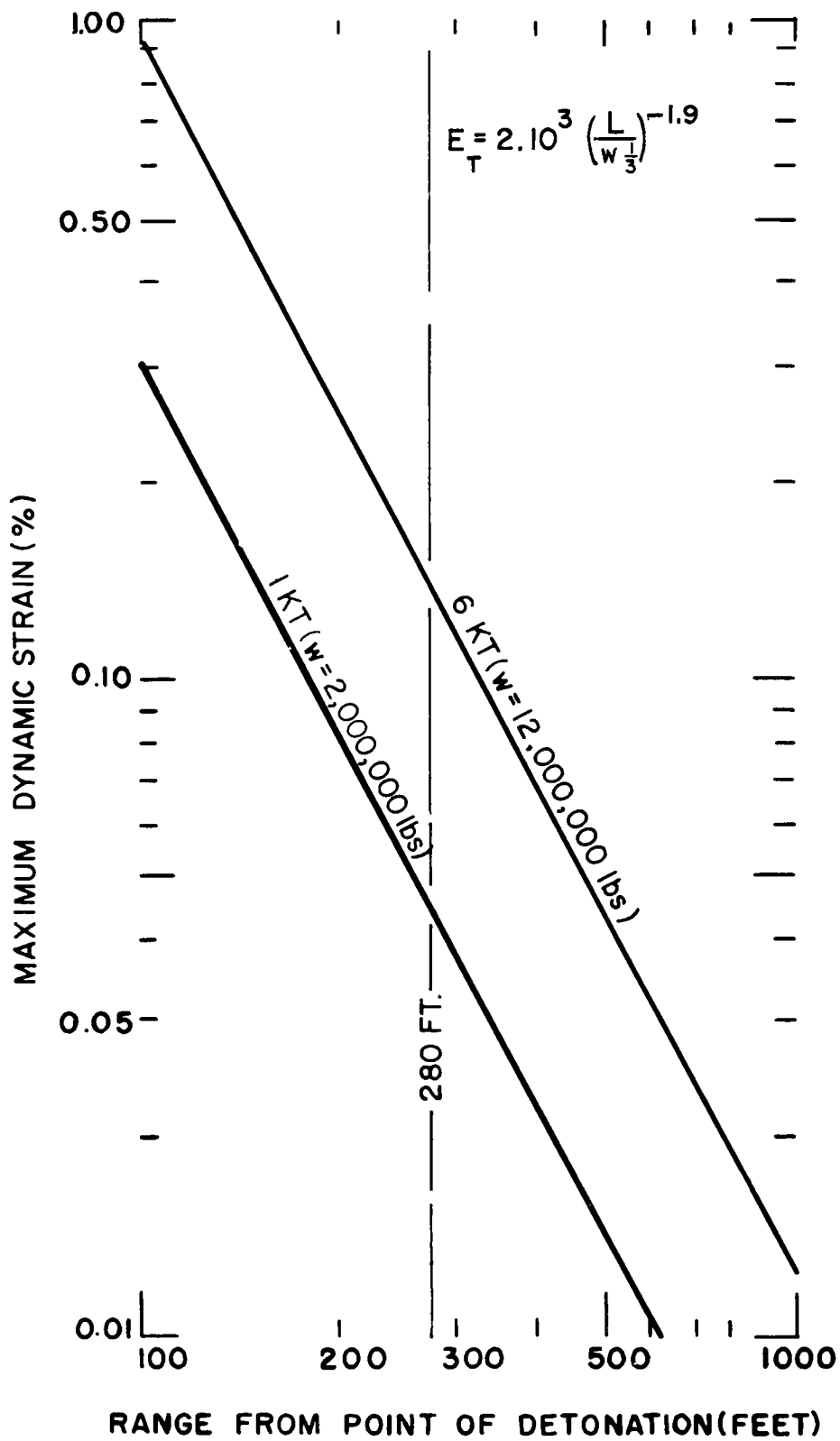
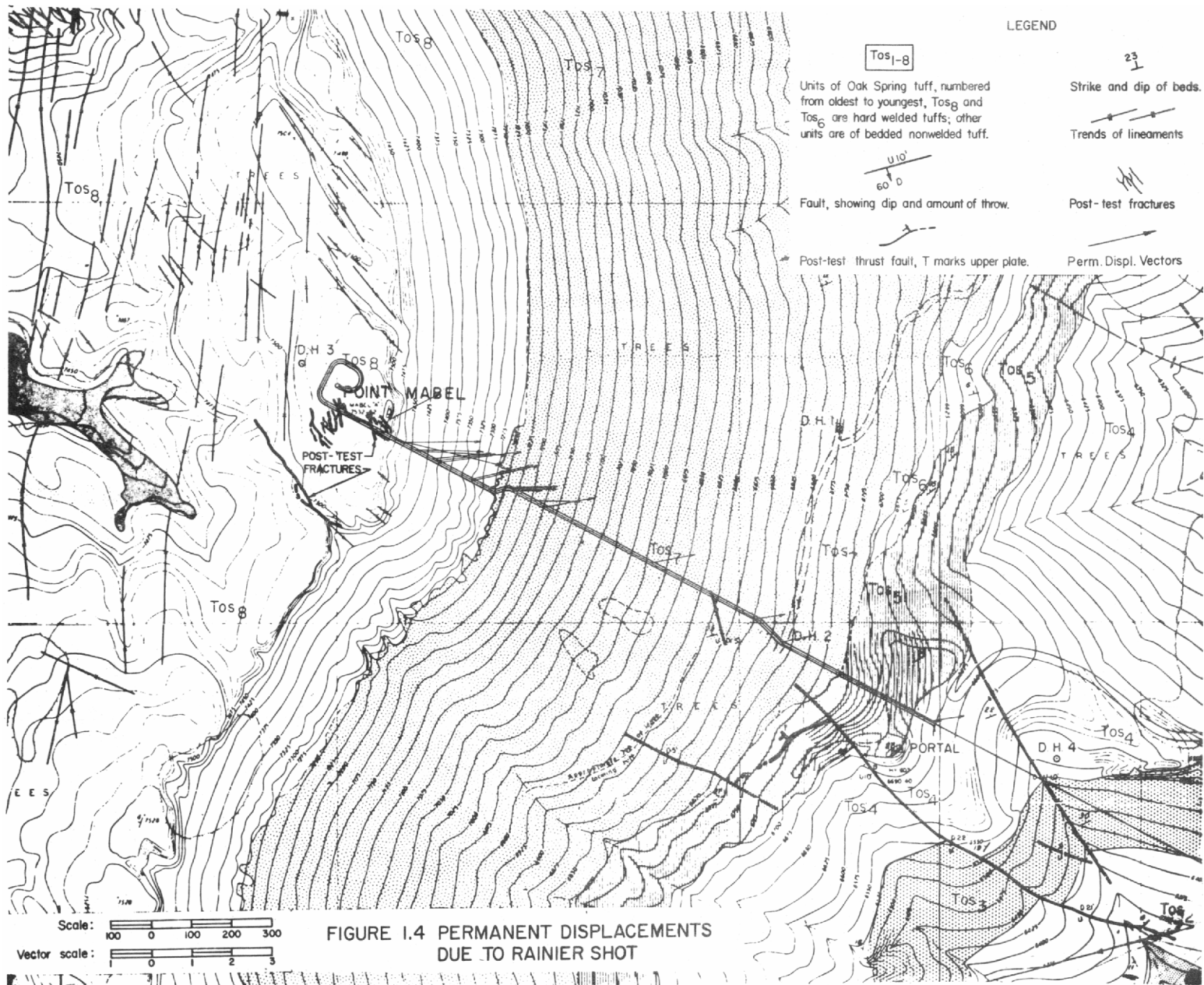


FIGURE 1.3 PREDICTED DYNAMIC TANGENTIAL STRAINS



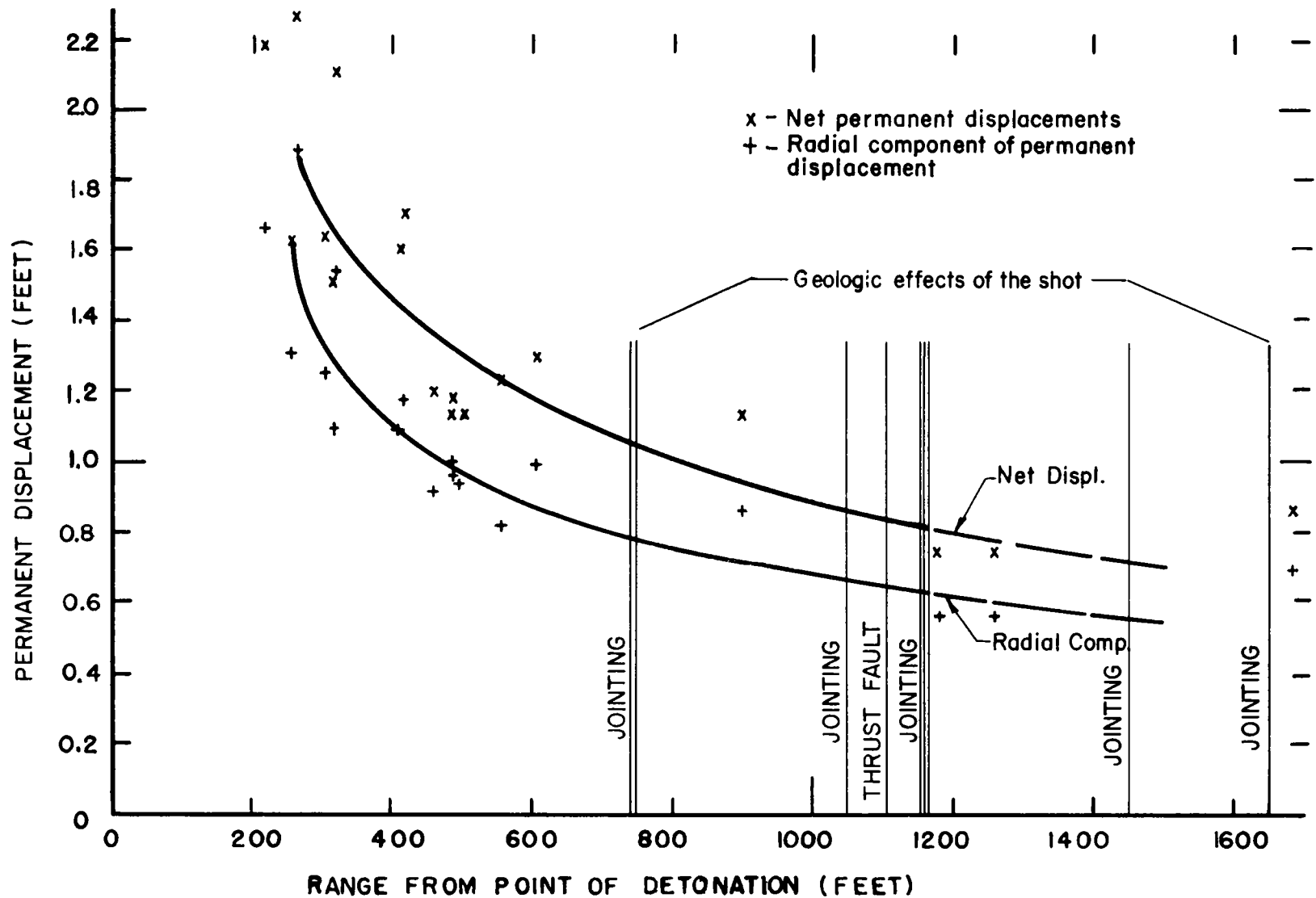


FIGURE 1.5 DISPLACEMENT WITHIN TUNNEL, SHOT RAINIER

CHAPTER 2

PROCEDURE

2.1 DESCRIPTION OF TESTS.

The Hardtack II series of underground tests as reported herein consisted of the detonation of five nuclear devices located as shown in Figure 2.1. The orientation and classification of the bedding in the vicinity of the tests are shown in Figure 2.1 and the bedding within the tunnels in Figures 2.2 and 2.3. Descriptions of the bedding are given in Table 2.1.

Points selected for measurement of permanent displacements on the surface are noted in Figure 2.1. Selected points for permanent displacement measurements within the tunnels are shown in Figures 2.2 and 2.3. The surface points were selected to give both overall area coverage and specific coverage at locations where differential movement appeared to be probable, as at the location shown in Figure 2.4.

The points within the tunnel complex were selected for coverage at locations of possible differential movement and to provide a broad coverage of the permanent effects of the shots. Criteria for the positioning of points to fulfill the latter requirement were the provision of sufficient points to cover the full range of motion from the recoverable point closest the WP out to the portal, and of points on the tunnel sides at those stations where occurrence of permanent measurable strain across the tunnel section was deemed possible.

Actual installation of the points selected for permanent displacement measurements within the tunnels was made by the use of one-inch reinforcing bars eighteen inches long sunk in drilled

holes. Brass benchmarks grouted into drilled holes were used for the points on the surface as illustrated in Figure 2.5. Permanent triangulation stations were placed at ranges of two to three miles from the site to insure that they would not be adversely affected by the shocks.

Dynamic measurements from force-beams were made for shot Evans. An alcove 280-feet from the WP contained three beams, emplaced as shown in Figure 2.6. The position of the alcove with respect to the WP, the geology, and other alcoves is shown in Figures 2.1 and 2.2. Though another alcove was in line to a radius from the WP, the shielding effect of the closer alcove was expected to be negligible due to the distance, dip of the bedding, and homogeneity of the rock.

The horizontal force-beams consisted of an approximately 21-foot long section of six-inch-diameter standard wall steel pipe adapted with a load cell and adjustable screw to make a measure of force exerted upon a structure within an alcove by the shock. A force-beam without the extension section is shown in Figure 2.7. The placement of the beams with the bearing plates and attachments were as shown in Figure 2.8. The capacity of the load cells used was 50,000 pounds and the allowable load on the column assembly was 56,000 pounds. Following installation of the force-beams, each beam was given a load of three thousand pounds by means of the screw adjustment. This loading was utilized to eliminate slack and to provide good bearing prior to the shock load of the

shot. The three thousand pound pre-loading did not change prior to the shot.

2.2 INSTRUMENTATION.

Pre-and post-shot surveys of the permanent displacement points were made for the Tamalpais, Logan, and Blanca shots of the series. Measurements by the load cells in the forcebeams were dynamically recorded under Project 26.3 for shot Evans.

Project 26.3 recorded, in addition to the load cells, strain and acceleration in the free field and strain across the alcove in which the forcebeams were placed.

TABLE 2.1 DESCRIPTION OF BEDDING

<u>Symbol on Dwgs.</u>	<u>Description</u>
Dn	Nevada Formation, limestone, about 1,380 feet thick. Chiefly limestone containing several quartzite interbeds. Medium to dark gray, hard, dense crystalline limestone.
Tos	Oak Springs Formation, Light gray, pink and red beds of Tuff. Miocene (?), Tertiary.
Tos-1 (Beds 1A- 1K)	Tuff, bedded; about 210 feet thick. Mostly purplish to pinkish red. Generally forms poor outcrop. Locally a basal conglomerate five feet thick.
1A	Red and white, bedded, fine to coarse, sandy tuff.
1B	Reddish-brown, pumiceous, sandy fine tuff, poorly bedded.
1C	Light gray, fine, massive tuff.
1D	Hard, red pumiceous fine tuff, bedded.
1E	Red and pink thin-bedded tuff.
1F	White micaceous tuff at base grades up to red pumiceous, fine tuff; evenly bedded.
1G	Red and white coarse tuff, some scour and fill structure, beds three to four feet thick.
1H	Dark brick red lithic tuff, moderately hard at top.
1J	Red friable well-bedded, fine to coarse tuff, white tuff bed about four feet thick at top; few porcellaneous beds less than one foot thick.
1K	Hard red and light gray fine to coarse tuff; some pumiceous red tuff beds with much hematite.
Tos-2 (Beds 2A- 2E)	Tuff, bedded; about 120 feet. Mostly light gray to buff but contains occasional thin pink, lavender, to brown beds. Forms fair outcrop.
2A	Generally white, fine to coarse tuff; reddish-brown and reddish-purple bands and mottling common.
2B	Red tuff with minor white fine tuff; reddish-purple bands and mottling common in white beds; reddish-purple and white very fine pisolitic tuff bed, four

<u>Symbol on Dwgs.</u>	<u>Description</u>
2B (cont'd)	feet thick, at base; useful as marker bed.
2C	Interbedded red and white fine to coarse tuff, some porcellaneous tuff in red beds; red fine tuff bed at base five feet thick.
2D	Greenish-gray, well-bedded, fine tuff; local channeling dark gray to black seams common.
2E	Pink and white pumiceous tuff.
Tos-3 (Beds 3A- 3D)	Tuff, bedded; about 100 feet thick; prominent red beds at top and base, pink to buff interbeds. Good ledge former. Contains welded tuff lense, white, in N.E. part of area.
3A	Hard to moderately hard structureless to indistinctly bedded coarse red tuff; thirty-nine feet thick.
3B	Moderately hard fairly well-bedded light gray coarse tuff, mottled and banded with red and purple; twenty-three feet thick.
3C	Soft to hard indistinctly to distinctly bedded light gray fine and coarse tuff, banded with pale yellow, red, and purple, contains common to abundant clastic grains of quartzite and volcanic (?) rocks; seventy-five feet thick.
3D	Hard distinctly to indistinctly bedded coarse medium-red tuff; at least thirty-three feet thick (top not exposed).
Tos-4 (includes Bed J)	Tuff, bedded; about 285 feet thick; light gray to buff, a few pink beds, especially towards top. Generally compact, and forms good outcrop.
J	Indistinctly-bedded variably soft tuffs, bonded and mottled in red and white. A few fine conglomerate layers contain one to two inch fragments of dark quartzite and dense lavas.
Tos-5 (Beds K,L)	Tuff, bedded; about 120 feet thick; light yellow green. Pumiceous and light-weight but forms good outcrop.

Symbol
on Dwg's.

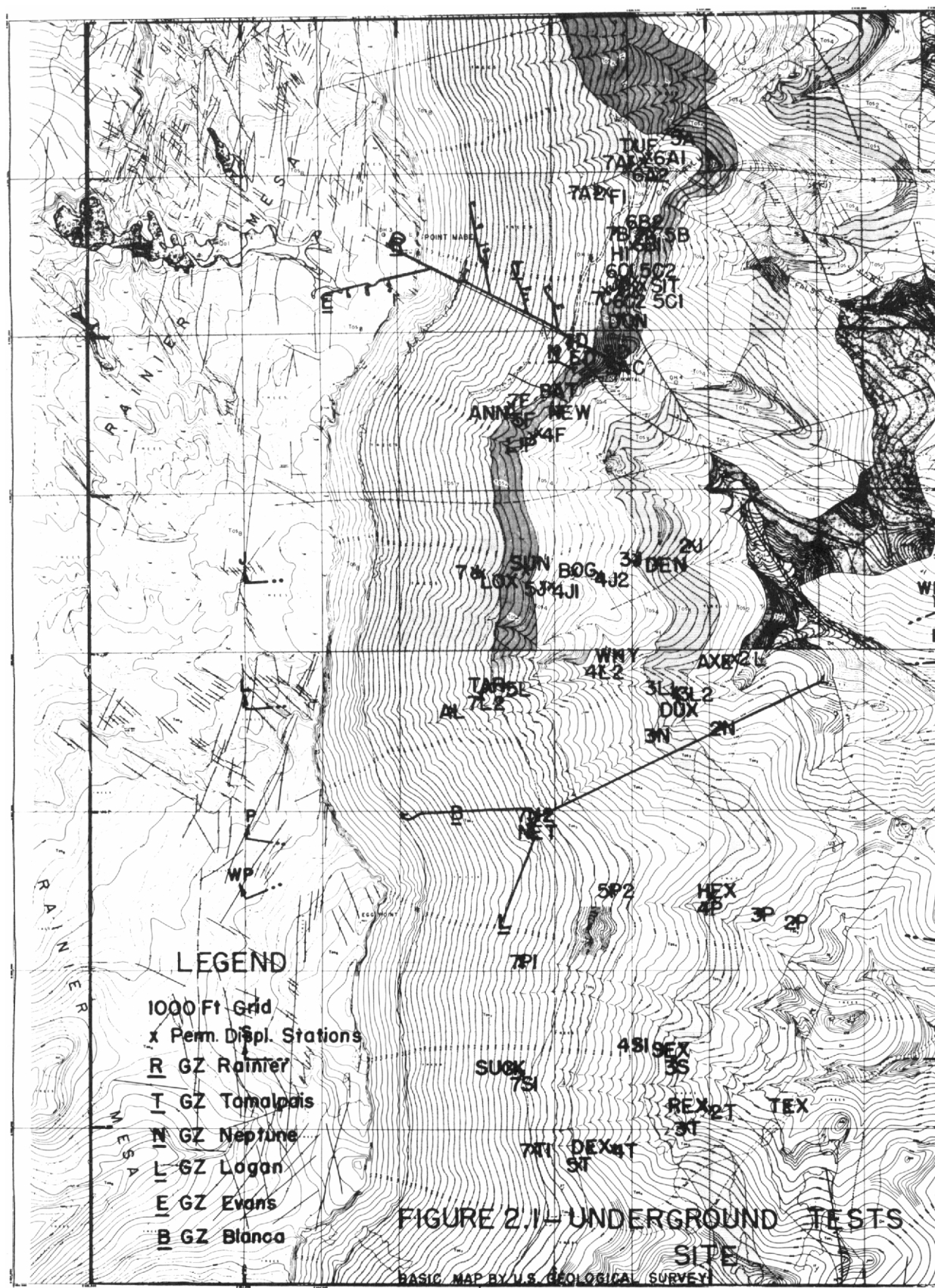
Description

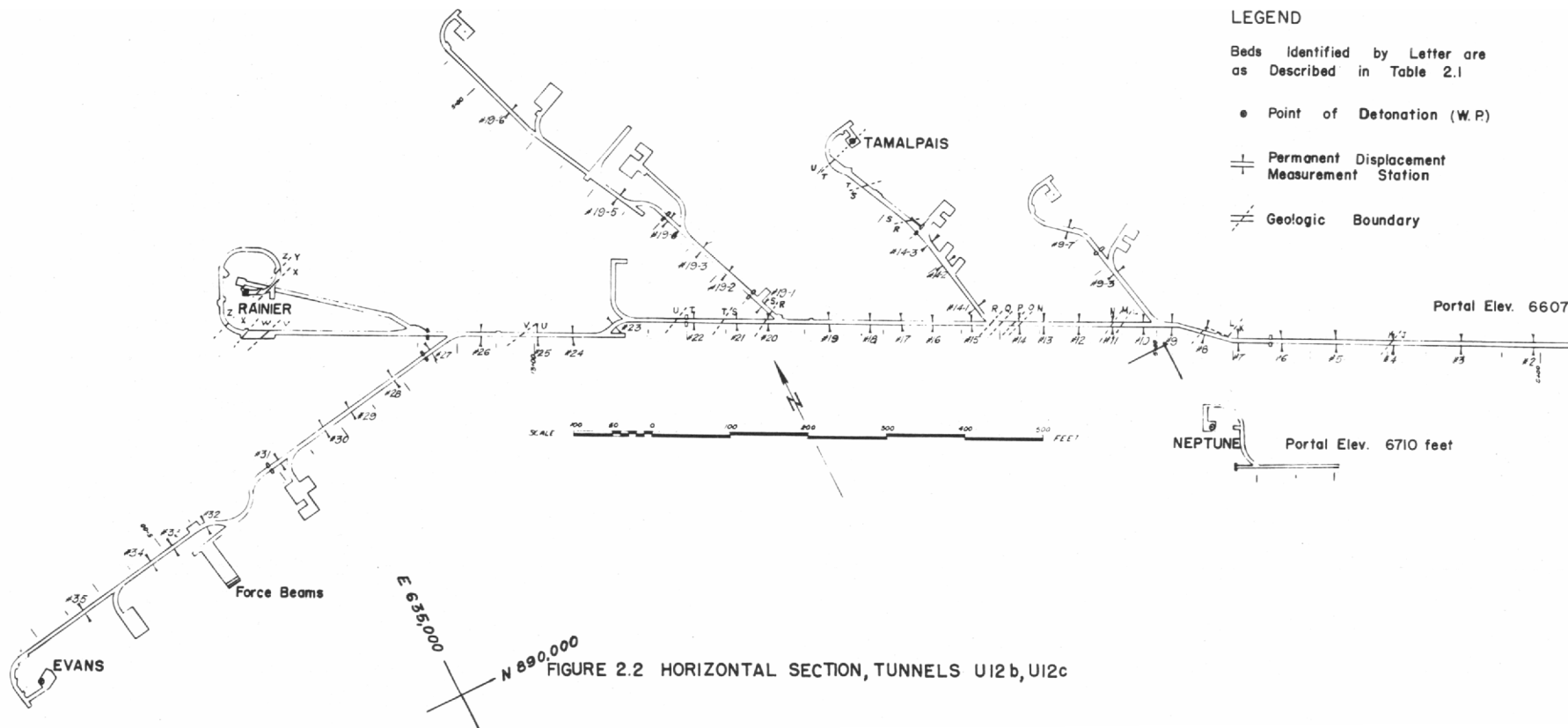
K	Pale buff, soft, fine-grained tuff, with dark quartzite fragments, little visible crystalline material. A few conglomeratic interbands are two to four inches thick, hard, reddish brown, with quartzite fragments up to two inches across.
L	Bedded tuff, gray, well bedded pumice at top, yellow soft granular to earthy tuff at base.
Tos-6 (Beds M, O)	Tuff, welded; \pm 75 feet thick but is lenticular and discontinuous. Probable unconformity at base. Forms good outcrop.
M	Conglomerate with roughly rounded boulders of volcanic rocks up to one and a half feet across, a two-foot bed of finer conglomerates at top of unit.
N	Hard dense rhyolitic welded tuff, red to gray, with flattened streaks of pumice up to three inches across. A perlite horizon three feet thick lies toward base of flow.
O	Soft medium-brown unbedded tuff with flattened pumice fragments and fragments of hard red and gray lavas up to two inches across. Erosional unconformity at top of unit.
Tos 7 (including Beds P-Z)	Tuff, bedded about 675 ft. thick; mostly loosely cemented and "sandy", but upper 35 ft. is moderately well cemented pumiceous tuff breccia. Lower 40 to 100 ft. forms prominent but discontinuous outcrop.
P	Fine-grained, reddish-brown, soft sandy tuff, whitish-pumice fragment, flattened, one-half inch long, two-inch spots of bright orange color.
Q	Medium-course soft gray pumice, reddish towards base.
R	Soft medium reddish brown earthy tuff, fine-grained matrix spotted by white pumice fragments up to one-half inch across. Bedding marked by fine rusty streaking.
S	Red-brown, modular and streaky-bedded variable tuff.
T	White, fine-grained, rather soft chalky tuff.

Symbol
on Dwg's.

Description

U	White, medium-course grained bedded tuff with abundant dark quartzite and pumice fragments. Individual beds are three to five feet thick, usually have base coarser than top. Interbands of greenish yellow hard conglomerate are three to six inches thick. A few beds are red.
V	Dark-red to brown massive tuff with white pumice fragments up to two inches across.
W	Soft, coarse-grained white tuff.
X	Red-brown coarse tuff with abundant half-inch white pumice fragments.
Y	White, soft, coarse-grained tuff, common biotite phenocrysts.
Z	Cross-bedded tuffaceous sandstone, reddish-brown, firm, medium coarse. A prominent erosional unconformity at base of unit.
Tos 8	Tuff, welded; about 270 ft. thick; rhyolite to quartz latite. Forms rim rock of mesa.





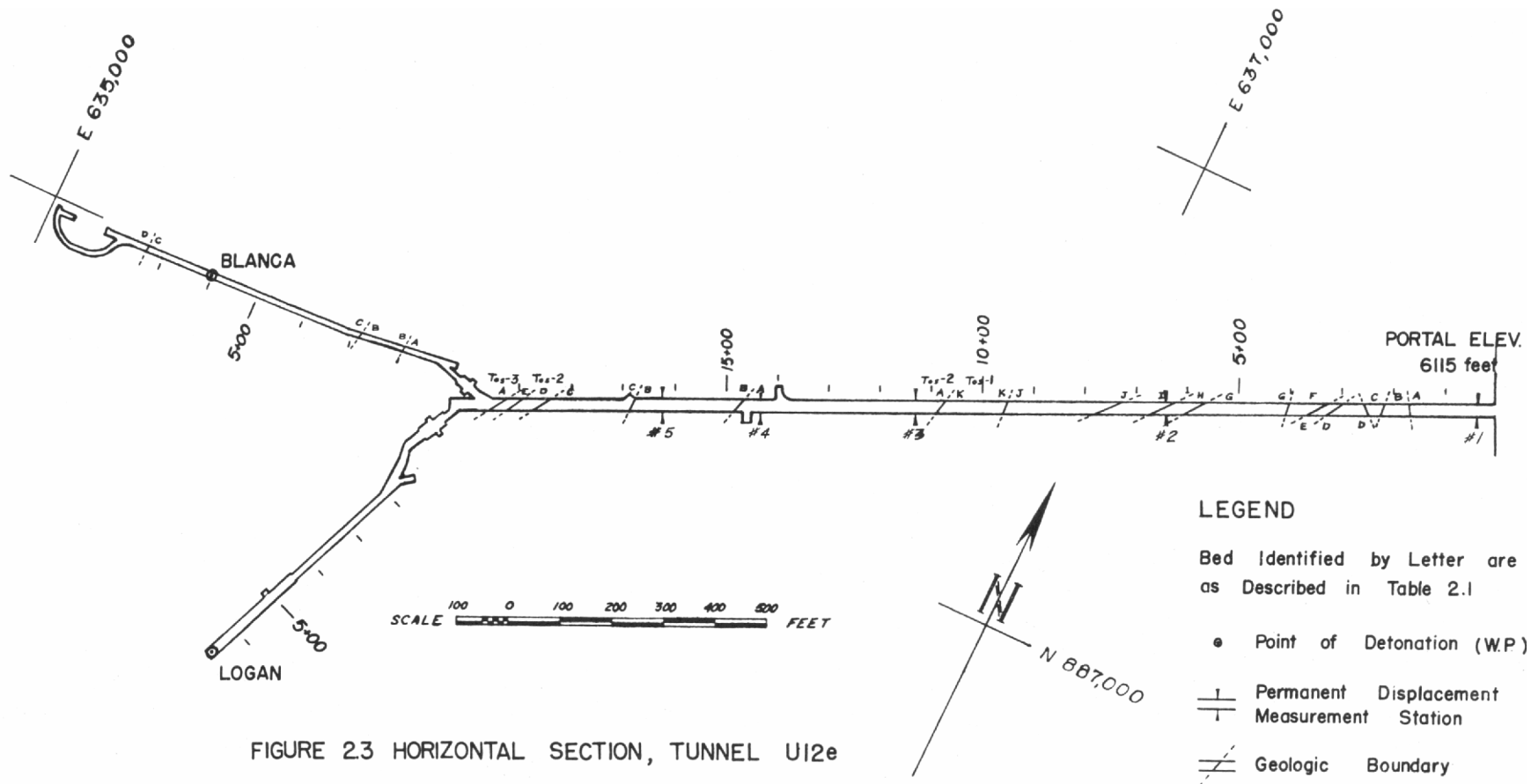




FIGURE 2.4 PERMANENT DISPLACEMENT STATIONS ON SURFACE.

Photograph shows location of stations 5C1 (foreground) and 5C2 (center extreme right) in the bedded tuff, Tos-5, and station 6C1 (upper left) in the welded tuff, Tos-6.



FIGURE 2.5A STATION ON SLOPE
Station 5-C-2 in Tuff, Tos-5.



FIGURE 2.5B STATION IN TUNNEL
Station #3, UL2e, at 11+34.

FIGURE 2.5 PERMANENT DISPLACEMENT STATIONING

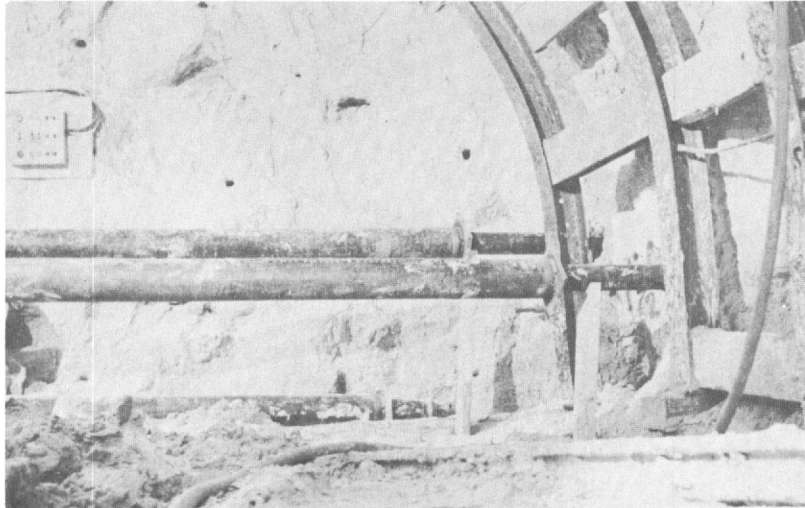


FIGURE 2.6A WEST SIDE OF ALCOVE
WP of Shot EVANS is approximately
280 feet to the right.



FIGURE 2.6B EAST SIDE OF ALCOVE

FIGURE 2.6 POSITION OF FORCE BEAMS IN ALCOVE

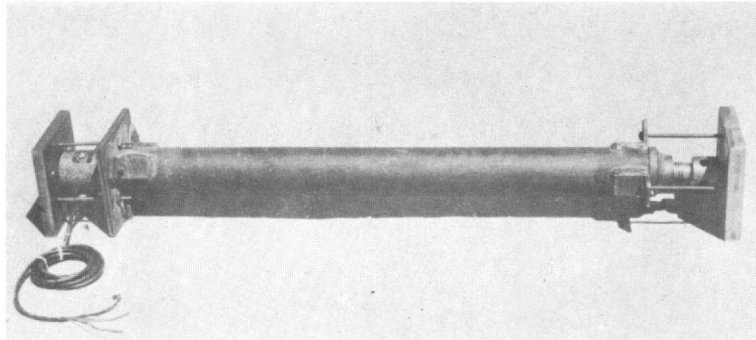


FIGURE 2.7A FORCE-BEAM BEFORE EXTENSION

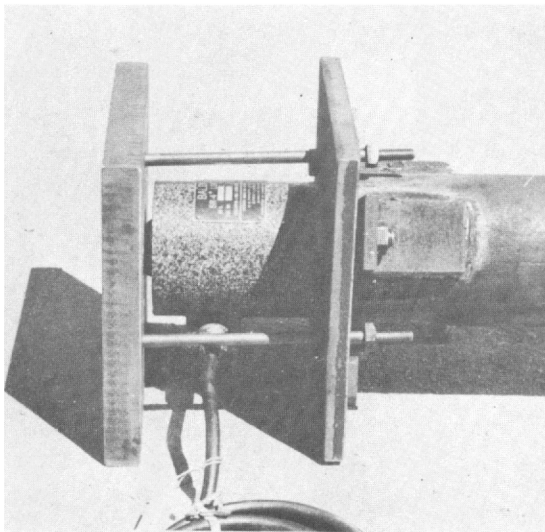


FIGURE 2.7 B LOAD CELL ASSEMBLY

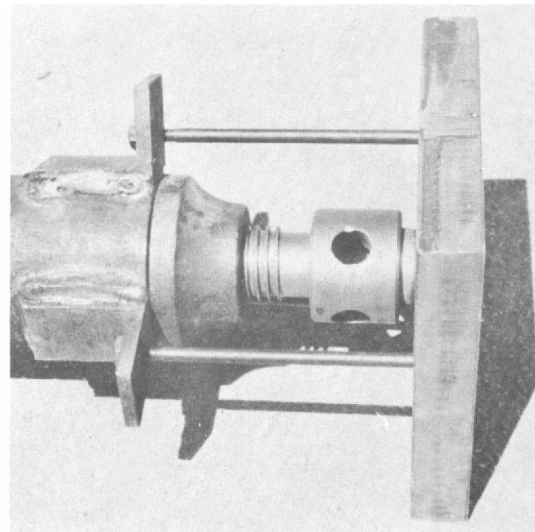


FIGURE 2.7 C ADJUSTABLE SCREW ASSEMBLY

FIGURE 2.7 BASIC FORCE-BEAM

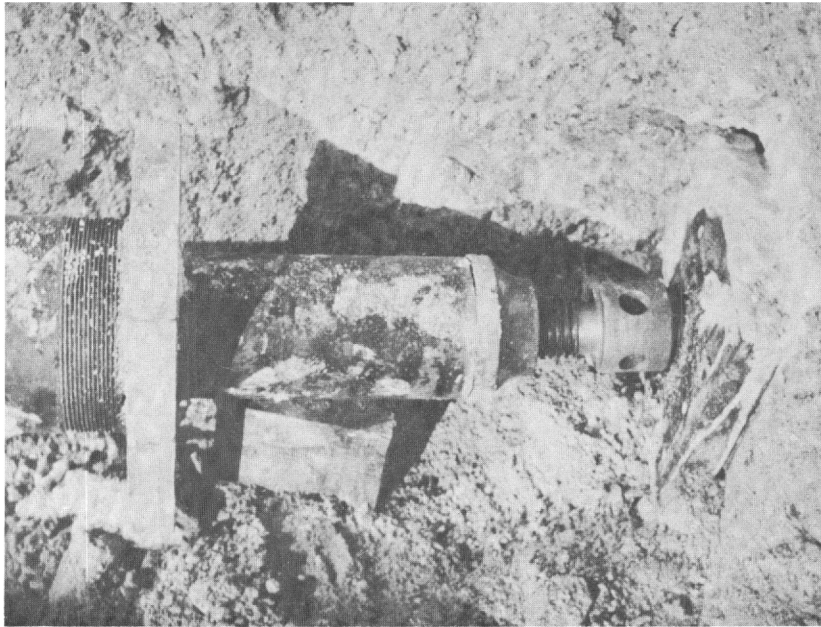


FIGURE 2.8A ADJUSTABLE SCREW ASSEMBLY



FIGURE 2.8B BEAM AND DISPLACEMENT
GAGE PLACEMENT

FIGURE 2.8 PLACEMENT OF FORCE-BEAMS

CHAPTER 3

RESULTS

3.1 GENERAL SUMMARY OF TESTS. The Hardtack II series as reported herein consisted of two shots, Tamalpais and Evans, in drifts off the U12b tunnel; two shots, Logan and Blanca, in drifts off the U12e tunnel; and shot Neptune in the U12c tunnel. Data on Shot Rainier is included in the report due to the similarity of that event to those of the Hardtack II series and to provide in one report results relating to structural effects and permanent displacement of all the below surface, in-rock, nuclear detonations.

3.1.1 TAMALPAIS CHARACTERISTICS.

Date: 8 October 1958

Approximate Radiochemical Yield: $72^{+} 10$ tons

Shot Chamber Dimension: 15 x 15 x 10 feet

Bedding at Shot Chamber: Beds T, U, V (Table 2.1)

Vertical Cover: 402 feet

Distance to Nearest Surface: 350 feet

Location: Tunnel U12b.02

Lat. N $37^{\circ}11'43.10''$ N 890,403.07 feet *

Long W $116^{\circ}12'01.65''$ E 635,789.38 feet *

Elevation 6616 feet Nevada State Grid (Ref 10) *

Form of Seal: Buttonhook tunnel with sandbag plug

Containment: Complete except for some gas leakage
into tunnel

Description: The detonation produced negligible

visible effect at the surface with the exception that a light dust was raised. Yield was roughly in the range of that predicted. Radioactivity in the tunnel was essentially all in gaseous form of relatively short duration. Spalling gradually increased from the junction of UL2b.02 with the main drift, where some utilities and cable trays were shaken down, to a region in which heavy damage occurred, within the blast door. Closure of the tunnel appeared to have been caused by a combination of spalling and block motion. Little disturbance from Tamalpais was noted in the UL2b.01 or UL2b.03 drifts on either side of UL2b.02.

3.1.2 NEPTUNE CHARACTERISTICS.

Date: 14 October 1958

Approximate Radiochemical Yield: 90⁺ 20 tons

Shot Chamber Dimensions: 17 x 12 x 10 feet

Bedding at Shot Chamber: Tos-7

Vertical Cover: 110 feet

Distance to Nearest Surface: 98 feet

Location: Tunnel UL2c

Lat. N 37° 11' 37.88" N. 889,876.56 feet

Long. W. 116° 11' 58.89" E. 636,015.34 feet

Elevation 6712 feet

Form of Seal: Buttonhook tunnel with sandbag plug.

Containment: Shot cratered, fireball appeared at surface.

Description: A crater of considerable extent was formed. The tunnel was sealed by shock across the buttonhook but there was very little damage done to tunnel in the initial straight portion from the portal. Some spalling was caused in the U12b tunnel in the vicinity of Permanent Displacement Station #8, located at a fault zone. Yield was an order of magnitude above that predicted. The crater and outthrow contained high residual alpha contamination.

3.1.3 LOGAN CHARACTERISTICS.

Date: 15 October 1959

Approximate Radiochemical Yield: $5 \begin{smallmatrix} + .02 \\ - .04 \end{smallmatrix}$ kt

Shot Chamber Dimensions: 31 x 9 x 9 feet

Bedding at Shot Chamber: Bed 3A (Table 2.1)

Vertical Cover: 932 feet

Distance to Nearest Surface: 800 feet

Location: Tunnel U12e.02

Lat. N. $37^{\circ} 11'03''$ N. 886,350.04 feet

Long. W. $116^{\circ} 12'04''$ E. 635,615.11 feet

Elevation 6136 feet

Form of Seal: Series of sandbag plugs.

Containment: Complete

Description: Logan produced major effects at the surface. Boulders were thrown from embedment in talus and large faults were formed, though no sink hole or depression due to collapse of the fireball cavity was evident. Yield was essentially

that predicted. The fused silica shell which forms by melting and condensation of the rock by the fireball was encountered at a range approximately 140 feet from the WP. Location of this fused silica was in the post-shot recovery drift adjacent and parallel the original drift. The great range to this shell as opposed to a shell radius of roughly fifty feet for Rainier is believed due to the shape of the detonation chamber and the possibility of large movement of some of the sandbag plugs in the straight-in tunnel. Lack of a noticeable sinkhole may also have been due to a fireball cavity in the form of an ellipsoid with axis along the tunnel, or more probably, a combination of spheroid at the WP with an elongation down the tunnel. In either case the lesser dimension of an enclosing rectangle would govern the height to which overbreakage would reach prior to formation of stable arching in the rock above the cavity.

The single-track drift, U12e.02, to the Logan WP was closed its entire length. Principal action in creation of tunnel closure at the closer ranges is difficult to determine. Inspection from the recovery drift revealed complete closure and firm remolding of the rock within the tunnel at a range of roughly 180 feet from the WP. At juncture with the double track, main U12e tunnel, closure appeared to have been mainly caused by heavy spalling due to action of the compression wave travelling roughly parallel the tunnel axis. Extensive photographic coverage of the effects of Logan at this point and outward are presented in the report of Project 26.14 (Ref. 11). Severe faulting and spalling occurred in the main tunnel and the U12e.05 drift, later

used for Blanca. Sections of these tunnels were essentially closed to use despite the presence of heavy and closely spaced rib reinforcement. Spalling occurred around the perimeter of sections of these tunnels but was heaviest at the back (term for roof of tunnel) and at the side closest the WP.

3.1.4 EVANS CHARACTERISTICS.

Date: 28 October 1958

Approximate Radiochemical Yield: 55^{+} 30 tons

Shot Chamber Dimensions: 20 x 17 x 10 feet

Bedding at Shot Chamber: Bed V (Table 2.1)

Vertical Cover: 850 feet

Location: Tunnel U12b.04

Lat. N $37^{\circ} 11' 41.47''$ N. 890,231.74 feet

Long. W $116^{\circ} 12' 17.03''$ E. 634,545.26 feet

Elevation 6620 feet

Form of Seal: Buttonhook tunnel with sandbag plug.

Containment: Vented into tunnel.

Description: Detonation produced no visible effects at surface with exception of small rock falls at the mesa rim and issuance of dust from the U12b portal. Yield was approximately one percent of that predicted. Venting of the shot created a level of high gaseous and particulate radiation in the tunnel with high residual alpha and beta contamination, particularly in the U12b.04 drift. This residual radiation has prevented observation of tunnel damage other than that caused by the air-pressure waves which resulted from the venting.

3.1.5 BLANCA CHARACTERISTICS.

Date: 30 October 1958

Approximate Radiochemical Yield: 19^{+} 1.5 kt

Shot Chamber Dimensions: 20 x 8 x 7 feet

Bedding at Shot Chamber: Bed 3C (Table 2.1)

Vertical Cover: 988 feet

Distance to Nearest Surface: 835 feet

Location: Tunnel U12e.05

Lat. N. $37^{\circ} 11' 09.37''$ N. 886,988.27 feet

Long. W. $116^{\circ} 12' 07.28''$ E. 635,352.96 feet

Form of Seal: Series of Sandbag plugs.

Containment: Vented to surface thru sinkhole formed by collapse of cavity formed by fireball, light gaseous leakage into tunnel.

Description: Detonation produced major earth tremor and serious faults and disturbance underground and at surface. Collapse of fireball cavity formed a large sinkhole with crater-like appearance but lacking throwout or pushout which characterize craters. A small residual radiation at the surface resulted from fallout of particulate matter carried aloft by the gas escaping past the falling rock in the sinkhole. Radiation of long duration was encountered within the mountain in a drift dug post-shot at the same elevation but closer to the surface than U12e.05. The radiation was in an approximately vertical fault with strike radial to the Blanca WP. Distance from the WP at this intersection

was roughly 600 feet. The U12e.05 drift was completely closed by the Blanca detonation even though it had continuous support from closely spaced sets. Damage to the main U12e tunnel was similar and on the same scale as that caused by Logan. At the intersection of the two tunnels, reopened after Blanca, utilities leading into U12e.05 had the appearance of being embedded in natural rock, remolding of the displaced material having been to the extent that its structural properties seemed to approximate that of the original rock. Logan created damage over the length of the U12e tunnel which was, on the average, as great as that which was caused by Blanca. The shape of the initial fireball cavity formed by either shot has not been determined from borings as of this writing. Possible shape of that of Logan was noted in Paragraph 3.1.3. The initial cavity of the Blanca fireball possibly had its shape strongly influenced by the lack of a solid plug between the WP and the unused inner section of the drift (refer to Fig. 2.3). Although heavy spalling caused by Logan had partially blocked this portion of the drift, a solid seal was not formed. The possibility that the fireball expanded much more rapidly in this direction and that a line source was consequently formed could provide the reason for failure of Blanca to give a scaled increase in damage within the tunnel, in rock whose structure and resistance to shock effects had been weakened by Logan.

3.1.6 RAINIER CHARACTERISTICS.

Date: 19 September 1957

Approximate Radiochemical Yield: 1.7 kilotons

Shot Chamber Dimensions: 6 x 6 x 7 feet

Bedding at Shot Chamber: Bed x (Table 2.1)

Vertical Cover: 905 feet

Distance to Nearest Surface: 800 feet

Location: Tunnel U12b

Lat. N. $37^{\circ} 11' 44.80''$ N. 890,570.94 feet

Long. W. $116^{\circ} 12' 11.35''$ E. 635,003.47 feet

Elevation 6611 feet

Form of Seal: Buttonhook tunnel with sandbag plug

Containment: Complete

Description: Detonation produced moderate surface effects consisting of fracturing and some rock fall at the rim of the cap rock (Tos-8) and a small thrust fault in the vicinity of the U12c tunnel. Collapse of fireball cavity did not produce a visible depression at the surface. Within the tunnel, closure of the drift was effected at a range of 200 feet from the WP principally by spalling accompanied by some block motion. Heavy spalling occurred beyond this range gradually decreasing with increasing range from GZ. This spalling was primarily on the tunnel side closest the WP and took the form of breaking along natural planes of weakness. One small fault within the tunnel was caused at range of over one thousand feet from the WP. Yield of Rainier was essentially that predicted. Radius to the initial fused silica shell formed by the fireball was approximately

fifty feet with the radiation generally contained within this shell.

3.2 FORCEBEAMS.

Load records obtained from the forcebeams tested in the Evans event showed oscillatory traces which were similar for the different beams. No buckling was apparent nor was there a detectable difference in loads experienced by beams in different orientations with respect to distance from the surfaces of the cavity. Long-base displacement gages across the alcove similarly indicated no difference due to orientation and were essentially of no value, due to the relatively long period of vibration of the stretched wire.

3.3 PERMANENT DISPLACEMENTS.

Detonation-produced displacements of selected stations in the U12 Area were measured by survey. The resultant permanent movements obtained by the surveys are presented graphically and tabulated in Appendix III. The time notations used refer only to the Hardtack II series. Displacements recorded within the U12b tunnel are the result of three surveys. The first, Pre-Events, was made prior to any of the reported Hardtack II shots; the second, Post-Tamalpais, was made during the interval between the Logan and Evans events and thus includes any effects of Tamalpais, Neptune, and Logan; and the third, Post-Events, was made following the test series and thereby includes the net displacement due to all shots. Two surveys were made of points on the surface in the vicinity of the U12b tunnel. The first

was made prior to any of the reported shots and the second, noted as Post-Tamalpais, followed Tamalpais, Neptune, and Logan shots and consequently includes any effects of these three shots.

Points within the U12e tunnel were surveyed prior to Logan and following Blanca. Due to the range from events in the U12b and U12c tunnels and the small yields of these events, the net displacements are labeled Pre- and Post-events with the assumption that all measurable movement resulted from the combined actions of Logan and Blanca. Points on the slopes, the "J" line of stations and those south of it (reference to Figure 2.1), were initially surveyed after Logan and then re-surveyed after Blanca, thereby reflecting primarily the action of the Blanca shot. Possible other factors which might have influenced the displacements were Shot Evans, which was of such a yield that creation of measurable effects was improbable, and settlement in the area disturbed by Logan. An estimate of the magnitude of possible settlements attributable to Logan is not feasible due to lack of data or theory of time-lapse settlement from underground detonations.

CHAPTER 4

DISCUSSION

4.1 ACCURACY OF MEASUREMENT.

Permanent Displacement measurements were made to an accuracy selected on basis of the magnitude of effects anticipated, the time available between events, and the capabilities of modern geodetic instruments and procedures. First-order triangulation including use of electronic ranging equipment was employed for establishment and recovery or reestablishment of the main triangulation stations, which included the U12b and U12e portals. Within the tunnels horizontal control was done in accordance with second-order procedures, but without closure of traverse. Leveling was by second-order procedures using first-order benchmarks. Permanent displacement points on the slopes were recovered by traverse from a control station. These control stations were surveyed by triangulation and leveling. Accuracy of surveying by the means outlined provided a rough maximum error for points on the slopes of ± 0.02 feet vertical control and ± 0.20 feet horizontal control, with a significantly less average error.

Within the tunnels the lack of closure would cause the work to approximate third order, which would provide maximum error of one in five thousand in distance and \pm five seconds in angle. Maximum accumulated error under these circumstances would be approximately 0.3 feet at the innermost station in the U12b tunnel and 0.4 feet at the innermost station of the U12e tunnel. These errors are very significant, particularly in

connection with the U12b results with the absence of more than fractional kt events within the tunnel. The tunnel surveys have accuracy sufficient for measurement of relative displacements between adjacent stations and between points comprising a station. Distances between adjacent stations in U12b are accurate to within one to two hundredths of a foot, depending on distance. Locations of points comprising a station are accurate to the order of thousandths of a foot relative to each other.

Lack of a closed traverse within the tunnels would cause any error or mistakes made in angle measurements of the outer stations to be greatly magnified at the innermost points, though would not affect strain calculations based on adjacent stations. Magnitudes of displacements created by Rainier in U12b, and Logan and Blanca in U12e overshadow the effects that errors may have created. However, there is no correction for mistakes that might have occurred in reading or recording.

4.2 INTERPRETATION OF RESULTS.

Direct application of measurements made in the Hardtack II series to design of protective installations may not be made. The detonations took place at a scaled depth below the surface that would not be obtainable by an attack weapon such as a missile or bomb. In the case of a placed device, as for purpose of demolition, sabotage, or weapons testing, some direct correlation is possible. The results may be of some direct connection with studies of surface effects which relate to the detection of nuclear detonations by post-shot

investigation.

The results obtained from Hardtack II and Rainier were influenced in varying degrees by factors which would cause them to require considerable adjustment for use in situations of structural design:

(1) The test shots, including Neptune, were at depths at which the free field conditions within the rock were as though there were complete containment,

(2) The rock in which the detonations occurred varied considerably in structural integrity between the U12e site and the U12b and U12c sites,

(3) Shot chamber effects on the formation of the fireball caused indeterminable variation between actual and symmetrical conditions and consequently between the various shots themselves, and

(4) The nature of the rock, tuff, is such that extension of results to situations in other rock requires extrapolation for which data of adequate scope is not available.

A detailed theoretical study based in part on dynamic measurements of Rainier effects was made under ERDL sponsorship (Reference 12). This study provides indications of some of the effects that chamber size, stemming, depth of burial, and other factors might have on the results of this project. Some correlation of shock effects between types of rocks may be based on results of the Underground Explosions Test Program (References 9 and 13), though that program did not include rock

similar to the tuffs of the nuclear tests. Partitioning of blast energy at an interface, as might occur from military employment of nuclear weapons against underground structures, was investigated and reported by ERDL (Reference 14). This investigation was primarily concerned with cratering in soil. Additional study would be required for transfer of data to the case of a rock, with its tensile strength, structure, and other characteristics which set rock apart from soil.

Effects were caused by the nuclear detonations studied which would probably not occur with a surface burst or which can not be scaled by partitioning, rock strength analysis, or other means to the practical structural design case. Principal of these effects is faulting. Observation of faulting in the free-field of rock, which for the shots reported would be in the direction toward the center of the mesa or below the WP, was only possible for two shots, Neptune and Tamalpais. No conclusive data was obtained, the yields of both shots being small and the range from the Neptune WP to the U12b tunnel where free field conditions were approximated was large in relation to the yield. All faulting observed was thus at the surface or in a direction, from the WP concerned, that had a large surfaceward component. A detonation at or near the surface should produce no faults on the scale of those created by Logan and a minimum of faulting beyond the zone in which block motion takes place.

The WP of the shots of the Hardtack II series and

the rock surrounding them generally experienced net displacement towards the surface. The results observed and surveyed of these nuclear detonations indicate that the nearness of the surface allowed a general expansion to occur. This expansion occurs in rock loosened by the shock and is exaggerated surfaceward by the essential incompressibility of the medium below and into the mountain from the WP. Displacement of the WP is hypothetical in that a cavity was formed at that point, but the net displacement surfaceward of essentially all disturbed material has application to a tactical situation. Points within bedrock below a surface burst would be expected to experience net displacement upward, or towards the surface, the magnitude of which would increase with decreasing distance from the WP. Such points located near an escarpment or face of a mountain may have the magnitude of the motion additionally increased if marked bedding exists and the plane of this bedding is sloped up into the face.

The effects of Logan and Blanca on the steel sets and blocking used to reinforce the tunnel cavities indicate desirable features for protective construction. The steel sets, in the form of legged 180° arches allowed considerable spalling and constriction of the tunnel opening to occur while retaining a passageway traversable on foot. Closure of the tunnel at ranges greater than that at which complete failure of the sets occurred was caused by failure of the wood lagging between adjacent sets and by separation of adjacent sets by uneven yielding. Either of these actions permitted wood blocking, lagging, and spalled rock to close the cavity.

The ability of the steel arch to hold open a cavity while undergoing extensive general or local yielding seemed to be confirmed by the results of the post-test observations. Weakness of the support system used in the tunnels was due to lack of continuity of longitudinal beam action. A remedy would be structurally continuous steel liner braced by arching ribs. Blocking between the liner and the rock as used in the U12e tunnels appeared to be satisfactory. This blocking applied point loading on the liner, which in U12e was the wood lagging between the steel sets. This may not be desirable, but it had compensation in that it left considerable void between the liner and rock, and thereby allowed some room for decrease in cross section of the cavity to occur without excessive contraction of the liner.

Compared with arched steel sets, posts and cap wood supports used in sections of the U12e tunnel provided reduced resistance to failure in the zone of heavy spalling. Comparison of concrete and steel construction is not feasible in that reinforced concrete was only used in the very massive construction of the frames for blast doors. Such concrete sections had strengths out of proportion to that of adjacent lining. Damage to the frames occurred but comparison with that to the lining was not practical.

4.3 RELATED WORK

4.3.1 HIGH EXPLOSIVE TESTS.

Prior to and in preparation for the Rainier event the USGS exploded ten tons and fifty tons of dynamite in a tunnel in Oak Springs tuff approximately two miles from the portal of U12b.

This USGS tunnel had maximum cover of roughly 175 feet, was at the end of ridge off the main "Rainier" Mesa (term now applied to the mesa, a section of Belted Range, under which Rainier and subsequent nuclear detonations took place). The rock in which the USGS HE shots were located had less water content and more fracturing than that in which the large nuclear shots took place.

Qualitative results of the HE shots indicated that the major actions which took place were: (1) Shattering of the rock in the vicinity of the detonation, without detectable plastic flow and with minimal remolding, (2) Block motion and minor faulting at a greater range developing out of the shattering, and (3) Spalling, overshadowed by block motion and shattering at the closer ranges but constituting the major cause of tunnel cavity blockage beyond these ranges. Extensive coverage of these tests and the geology of the USGS and Rainier tunnels are reported in References 6 and 7.

Subsequent to the Rainier shot, in material very similar to that in which it took place and less than 500 feet from its WP, ERDL exploded one ton of HE for a study of possible scaling values (Reference 10). Actions on the tuff by this detonation affecting the cavity of the drift were primarily block motion of large sections of the side of the drift closest the WP; shattering, in the vicinity of the WP causing the reexcavated tunnel to have a considerably enlarged section; and spalling, primarily of the side of the drift closest the WP creating considerable blockage of the drift. Plastic motion essentially was not detected,

though some remolding of the shattered material was noted.

A detailed study including certain effects of HE detonation in rock was made by Engineering Research Associates, Inc. for the Office, Chief of Engineers (References 9 and 13). HE charges of various weights, depth of burial, and means of tamping were exploded in granite, limestone, and sandstone. No plastic deformation was reported. Major effects of the shots in all of the rock types were shattering and some block motion, with action beyond the range of severe overbreakage in the nature of spalling. Variations due to strength of rock and geologic structure were considerable, range of spalling and block motion having been greater in the sandstone than in the limestone and still greater than in the granite. Spalling in these tunnels was caused primarily from travel of the shock wave parallel to the axis of the tunnel, as opposed to that due to shock reflection, the case in the HE tests previously noted.

4.3.2 NUCLEAR DETONATIONS.

Studies, related to this project, made during the Plumbbob Operation on shot Rainier and during the Hardtack II series were conducted under Program 26. Projects were included which made detailed investigations of transient motions, geologic effects, and visual interpretations. Results have been published in the Weapons Test series, as USGS Trace Elements Investigations or Memorandum Reports, and as Laboratory Reports published by the project agencies. Those reports which most directly relate to this project have been referenced.

CHAPTER 5

CONCLUSIONS AND RECOMMENDATIONS

5.1 DISPLACEMENTS.

Accurate quantitative prediction of permanent displacement at surface or underground due to nuclear shock is not made from the data obtained. However, interpretations of results as appear to be justified by the nature of the data collected are presented.

Effects to be anticipated from in-rock detonations vary from craters and localized geologic effects with shallow depth of burial, to widespread faulting and movement with fully contained detonations.

Dimensions and orientation of the detonation chamber measurably influence the magnitude and direction of mass movement of the rock.

Bedding and the planes of weakness which are formed thereby have a large influence on the magnitude of surface displacements due to contained detonations. Bedding itself directs the shock by reflection of the strain waves while planes of weakness create conditions favorable to faulting. Effects underground are similarly influenced by bedding and planes of weakness due to faulting or jointing. Greatest effect is upon spalling, which is the principal problem in tunnel protection as it causes closure of cavities in the rock at greater ranges from the WP than block motion or plastic flow.

Greatest spalling will occur on the side of the tunnel closest the WP, varying in degree and orientation with the

geologic structure. With the rock in which the reported detonations took place, minimum spalling along a tunnel cavity would be to expected with a plane of bedding normal to the axis of the tunnel. Maximum effect would be achieved with plane of bedding parallel the tunnel axis. Most serious dip of the bedding for spalling effects would depend on the orientation and elevation of the tunnel with respect to the WP. Based on observation of effects of the shots reported, strain waves which traveled to the tunnel perpendicular or parallel to the bedding would be expected to be more destructive than those whose travel was across the bedding at some other angle. Basis for this is that the greatest amount of energy available for destruction should be transmitted to the cavity by travel parallel to the bedding and greatest destruction occurs from a given amount of energy at the cavity when applied perpendicular to the bedding. Bedding at an angle to the direction of travel would cause the strain energy to arrive by a partially deflected path and with a tendency to parallel the bedding.

Application of results to the placement of underground cavities subject to shock from surface or near-surface nuclear detonations indicate the following:

5.1.1 Any permanent displacement experienced is expected to have a large surfaceward component, the size of which would increase with nearness of the cavity to the surface and with decreasing range from the WP.

5.1.2 Beyond the region of true crater, spalling is the most probable cause of closure of the cavity. Such spalling

would be at a minimum in rock lacking definite bedding and planes of weakness due to bedding or fractures. In a rock having the adverse geologic structure, spalling is reduced when the plane of the bedding is perpendicular to the axis of the tunnel.

5.1.3 Faulting or block motion should not be a problem for cavities subjected to shocks from surface or near surface bursts. Possible exceptions would be in cases of cavities near the surface slope of an escarpment, and then likelihood of faulting would depend on geologic structure of the rock and the position of detonation.

5.2 PROTECTIVE LINING FOR CAVITIES.

Spalling has been indicated as the principle effect which lining for cavities must withstand to resist closure by nuclear shock. Steel arch ribs can provide the required strength and in addition possess the desirable ability to undergo large plastic deformation without complete failure.

Most effective tunnel lining to provide passage for foot traffic would have inverted "U" sets with bare floor. Heave of the floor or inward movement of the legs of sets would not create additional material to be removed, which would be the case with concrete or wood flooring. A tunnel which contains tracks for train or monorail would require full circle ribs or structurally floored section to provide protection from floor and inward movement. Track in such a tunnel would still be liable to require some realignment in any yielded section. Provision

for such realignment could readily be made by use of a sand or gravel ballast.

Wood lagging proved to be poor in preventing partial closure of the tunnel cavity in regions of severe spalling, due to breaking of the wood or slipping of the ends of the lagging from positions on the wideflange steel sets when adjacent sets suffered different deflections. Steel lagging would be expected to suffer similar failures, either slipping from position or excessive yield of the lagging causing pulling away from end anchorages. Such failures could be avoided in large measure by the use of a structurally continuous steel liner braced by steel sets. Appropriate liners would be plates bolted to adjacent plates both longitudinally and tangentially or curved corrugated steel sheets lapped and bolted to adjacent sheets. Corrugations could run longitudinally or tangentially, the important feature being the creation of a solid liner which could yield with point loading and deflect with yielding sets without causing a serious rupture in the lining of the tunnel.

The tests reported herein had effects which indicate that blocking between the liner and rock would be preferable to packing, for increasing protection under heavy spalling. Blocking, in which scattered point loadings are applied to the rock and the liner by use of wood spacer blocks is preferred since it leaves considerable void between the liner and rock, as opposed to packing, in which the void is filled with scraps, rubble, concrete, or other material. The voids left by blocking allow some constriction of the cavity cross section to occur without an equal reduction

in the area within the lining. The point loading applied caused some local buckling under heavy spalling, but the buckling was not greater than that which would have been expected under uneven loading of spalled material had packing been used instead of blocking.

Theoretical analysis of the relative merits of blocking and packing under normal, static conditions is available in Reference 16. Evaluation of concrete tunnel lining is not attempted due to lack of appropriate evidence of the effects on such linings in regions of heavy spalling.

5.3 CONFIRMATION AND CONTINUATION.

Permanent displacement and strain measurements should be made in connection with any surface or buried detonations in or on rock. With shots in material similar to that in which the detonations reported took place it would be of value to confirm the probable effects predicted in this study. Detonation in other rock media would be of value in comparing displacement and spalling effects in such other rock to those effects which were observed in the Hardtack II series conducted in tuff.

Test of the conclusions set forth for design of tunnel lining could be made without requiring nuclear detonations. Linings emplaced in the manner recommended and in other ways, as with packing, or without longitudinal continuity, could be tested by use of high explosive detonations. Similarly, concrete linings could be tested, preferably in sections adjacent to steel linings. The use of small detonations, the availability of abandoned mines

on military proving grounds, and the location of such mines in widely varying rock types should enable considerable information on rock behavior to be obtained at relatively small expenditure for use in the design of underground installations.

PART II. STRUCTURAL RESPONSE MEASUREMENTS

CHAPTER 6

INTRODUCTION

6.1 OBJECTIVES.

Project 26.7 was continued beyond the conclusion of the Hardtack II Series to investigate those original objectives for which information was not obtained during the nuclear tests. Additional objectives which were by-products of the methods used to continue the investigation were: (1) to provide data on structures subjected to nuclear shock in prior test series which would enable a better understanding of the results obtained in those tests, and (2) to provide experimental field data on effective mass of earth cover to permit verification or revision of theoretical design formulae currently in use.

6.2 BACKGROUND.

Basic objectives of the continued Project 26.7 were to have been achieved by investigations conducted during the nuclear series. Data that was obtained from Hardtack II through measurement or observation of effects provided some of the required information. No direct data on use of cushioning material such as light-weight plastic foam or on the use of concrete construction in rock was obtained. Structural shapes similar to those which would be used in practice for lining rock cavities had been tested buried in soil. Further analysis of these shapes and of the materials of which they were constructed was chosen as the most promising approach to the unfulfilled initial objectives.

6.3 THEORY-SHOCK ISOLATION ANALYSIS.

Theoretical approach to analysis of benefit of foam plastic shock isolation was by vibration analogy. The simplest case, that of a rigid flat-roofed structure at shallow depth of burial was selected for initial study. With such a structure an analagous single-degree-of-freedom system was used having a mass equal to that of the soil above the structure and a spring with variable stiffness equivalent to the reaction of the plastic foam supporting the earth cover. The theoretical analysis of foam protection for a flat-roofed rigid structure is presented as Appendix II.

6.4 THEORY-VIBRATION TESTING.

The approach used to study underground structures without nuclear testing was to seek in a common parameter a factor which would assist prediction of full-scale response. With a soil medium the stiffness of the structure and the interaction of the structure with the medium encompassing it combine to determine a dependent function, the period of vibration. The factors which determine this period in large measure are those which determine the response of the structure under shock loading. The period is consequently used in most theoretical approaches to the prediction of blast response. Determination of vibration characteristics of main structural elements would be useful not only in prediction of response to blast and shock loadings and design for resistance to such effects, but would also have certain non-defense application such as analysis of

response to bridge loadings or the vibrations of heavy machinery.

Vibration characteristics were useful although oscillatory motion is not the prime concern in the case of structures subject to loads varying similar to the typical blast overpressure decay curves. Under such blast loading the maximum response to the positive phase is generally the critical condition, with subsequent decaying vibration not apt to cause failure if the structure should withstand the initial displacement. Amplitude of response to blast loading is dependent on the mass of the structural elements, the nature in which the soil acts in conjunction with the structure, the nature of the structure's resistance to increasing load, and other factors such as the yield and ultimate strength of the material. As blast overpressure on the surface has in itself no momentum, energy is absorbed into the structural system by work of the pressure acting over a distance. The mass and the stiffness of the structure are the principal factors determining the acceleration and, consequently, the distance over which the overpressure acts as it decays.

The effective mass concerned and to a lesser extent the stiffness are difficult to measure on an in-place structure, particularly if the structure is buried. Theoretical approaches have been presented for making approximations of the fundamental periods of response for various types of structures and structural elements (References 17 and 18). These theories have had a

minimum of confirmation by tests on existing structures. Tests that have been made have generally involved response to rotation of an eccentric mass or to natural forces of wind or wave.

An initial assumption was made in this investigation that the natural modes of vibration of a structure or structural element are independent of the means of excitation or amplitude of vibration if the mass remains unchanged and the structural elements remain elastic. It was further assumed that initial response to the shock loading due to nuclear detonation would correspond closely to response of a single-degree-of-freedom system, in that vibration would be predominantly in one mode. Feasibility of measuring natural periods of existing structures with simple means of excitation was studied in preparation for the non-destructive vibration testing. This feasibility study, the report of which is Appendix I, indicated that the desired vibration characteristics could be readily induced and measured.

Structures were selected for study from among those tested during past nuclear test series conducted at the Nevada Test Site. Among the essentially undamaged structures remaining from past series suitable for vibration testing were the following:

- Buried rectangular reinforced concrete shelters of varying dimensions including a massive underground garage;

- Small buried precast concrete domes;

- Buried reinforced concrete 180° arch structures;

- Large buried culvert sections of circular reinforced concrete, circular corrugated steel, and cattlepass corrugated steel;

Large 180° arch buried corrugated steel;
Vertical axis cylindrical buried precast concrete;
Above-ground reinforced concrete dome.

Circular corrugated steel and concrete culverts were selected for study in that they represented typical materials of construction in a basic shape. Cattlepass corrugated steel culverts were selected as they were available at three different depths of burial. The massive underground concrete garage was used in the study as being a representative of common blast resistant design. The above-ground dome was tested to give correlation with nuclear test results and to investigate the nature of the modes induced by eccentric loadings. All of the structures chosen for the testing had been tested during the Priscilla Event of Operation Plumbbob.

6.5 THEORETICAL PERIODS - STEEL ARCH STRUCTURES.

The corrugated steel arch structures tested were two of those built under Project 3.3, Operation Plumbbob (Reference 19). The steel plate used in these structures and in the cattlepass and circular steel culverts was ten gage, thickness 0.1345 inches, with six-inch pitch, two-inch depth corrugation. The following properties of the corrugated plates, in terms of per foot of horizontal projection, were also common to all of the steel structures tested: moment of inertia, 0.937 in.⁴; area of section, 2.003 in.²; section modulus, 0.878 in.³; and radius of gyration, 0.684 inches.

The ribbed arch structure had radii of 12 ft 7-1/2 in. to

centroid of the corrugated plate and 12 ft 4-1/4 in. to the centroid of the steel ribs. The ribs were 6" x 3.33" I 12.5 lbs. per lineal foot and were spaced at four-foot intervals. Effective radius, to the centroid of the combined rib-plate system, was twelve feet six inches. Radius to the centroid of the corrugated plate of the unreinforced arch structure was approximately twelve feet seven inches, essentially the same as effective radius of the ribbed structure.

6.5.1 COMPRESSIVE MODE.

The expression used for computation of the compressive mode was that presented in Reference 17, which relates the period of the compressive mode, T_c ; the radius of the curved structure, r ; the mass per unit area, m ; the modulus of elasticity, E ; and the thickness of the arch, D :

$$T_c = 2\pi r' \sqrt{\frac{m}{ED}} \quad (6.5.1.1)$$

Simplification of this expression was made: since m is equal to the mass density, ρ , times the thickness, the expression under the radical becomes $\sqrt{\frac{\rho}{E}}$, which is equal to $1/c_v$ where c_v = velocity of sound in the material. Computation for intermediate grade steel yields a $c_v = 16,500$ feet per second (fps). With this c_v used, the period of the compressive mode for both the ribbed and unreinforced steel arch structures when not covered by earth was computed to be 4.68 milliseconds. When soil is placed above the structural elements, a modified period, T , is used.

The theoretical approaches referenced call for this modification to the period to be made by relating the combined mass of the soil acting with the structural element and the mass of the structural element itself (m' , the combined masses) to the mass of the structural element alone, m .

$$T' = T \sqrt{\frac{m'}{m}} \quad (6.5.1.2)$$

A limit to the application of Formula 6.5.1.2 is given in Reference 19 which states that a depth of soil cover greater than the span length should not be considered.

The steel arch structures had five-foot depth of cover at the vertex. In accordance with the referenced procedures, the mass of earth vertically above the structure was assumed to act with the structural elements. With an assumed unit weight of 115 pounds per cubic foot of soil based on soil samples taken during construction, the m'/m ratio for the unreinforced structure was computed to be 77.5. Owing to the greater mass of the structural elements, the m'/m ratio for the ribbed arch was computed as 54.8. By multiplying the period found for the uncovered situation by the square root of these ratios, the theoretical compressive mode periods were computed to be 42 milliseconds for the unreinforced steel arch structure and 35 milliseconds for the ribbed arch structure.

6.5.2 FLEXURAL MODE.

The flexural, or deflection mode of vibration as described in References 17 and 18c is asymmetric about the vertex,

with the result that the simplifying equivalent may be assumed to have a pin connection at the vertex. The end connections for the arches tested were essentially the equivalent of pin connections. For an uncovered arch the expression for the period of the deflection mode, T_{nd} , as given by Reference 18c is:

$$T_{nd} = \frac{2\pi L^2}{C_3} \sqrt{\frac{m}{EI}} \quad (6.5.2.1)$$

where L is the span of the arch
 m is the mass per unit area of the arch surface
 I is the moment of inertia of the arch cross section per unit width
 E is the modulus of elasticity
 C_3 is a dimensionless variable, dependent on the central angle of the arch, equal to 8.8 for central angle 180° .

A similar expression for the period of the deflection mode of an arch is given in Reference 17:

$$T = R_o L^2 \sqrt{\frac{m}{EI}} \quad (6.5.2.2)$$

where T is the period of the deflection mode
 L is equal to the developed length (arc length) of half the arch
 R_o is a factor dependent on support conditions, 0.636 for simple support.

The above formulas provide a period for the deflection mode of the unreinforced arch structure in the uncovered situation

of approximately 0.49 seconds (Formula 6.5.2.1) and 0.27 seconds (Formula 6.5.2.2). The ribbed arch has a moment of inertia roughly sixteen times that of the unreinforced arch and thus has corresponding periods in the uncovered situation of 0.12 seconds (6.5.2.1) and 0.067 seconds (6.5.2.2). When the mass of the earth cover is considered as recommended in Reference 17 and as used in the theoretical determination of the compressive mode (Formula 6.5.1.2), the periods of the deflection modes in the covered case become:

Unreinforced arch	(Formula 6.5.2.1):	4.3 seconds
	(Formula 6.5.2.2):	2.4 seconds
Ribbed Arch	(Formula 6.5.2.1):	0.89 seconds
	(Formula 6.5.2.2):	0.50 seconds

6.6 THEORETICAL PERIODS - BURIED CULVERTS.

Buried culvert sections tested were seven of those built under Project 3.2, Operation Plumbbob (Reference 20). The corrugated steel of the cattlepass and circular steel sections had properties as were noted in paragraph 6.5. The cattlepass sections had shape and dimensions as illustrated in Figure 6.1. The circular steel structure had a radius of 96 inches. The circular concrete pipe had internal diameter of 96 inches, shell thickness of nine inches, specified concrete compressive strength of 3000 psi, and two lines of circumferential reinforcing steel, which had a cross section area which totaled 0.75 square inches per linear foot. Moment of inertia of the concrete section computed from the above values was 17 inches⁴ per inch width. Soil tests made during emplacement of the culverts provided measure-

ment of an approximate soil density of 115 pcf.

The circular steel and circular concrete culvert sections, which had a nominal depth of cover 7-1/2 feet at vertex, had average cover over the structure approximately the same as the structural diameter of the sections. The actual average depth of cover over the circular steel culverts, which varied slightly from the design and which is based on measurements made after the nuclear test, was 102 inches for structure F3.2-9018.01 and 90-1/2 inches for structure F3.2-9018.02. Both had a measured average depth of cover of approximately 96 inches, compared with a structural diameter of 105 inches.

6.6.1 COMPRESSIVE MODE.

The depth of cover over the circular steel and concrete sections was at the limit of permissible application of the expression for the compressive mode presented in Reference 17 and used in Section 6.5.1. The uncovered period of the compressive mode of the steel and concrete sections was computed from this expression, as simplified by use of the sound velocity in the material, c_v :

$$T_c = \frac{2 \pi r'}{c_v} \quad (6.6.1)$$

A c_v equal to 9600 fps was used for the concrete and c_v equal to 16,500 fps was used for the steel. Theoretical uncovered compressive periods of the circular structures were computed as: 2.86 milliseconds for the reinforced concrete and 1.52 milliseconds for the steel structure.

Modification to account for the soil overburden was made in accordance with Reference 17 and Formula 6.5.1.2. The ratio of effective mass of covered case to the uncovered case was computed as 43.3 for structure F3.2-9018.01, 38.2 for structure F3.2-9018.02, and 6.64 for the circular concrete structures. The mass of the entire circular section was used for computation of the above ratios. The square root of these ratios times the uncovered periods provide the following theoretical periods for the compressive mode of vibration:

Circular Steel Structure F3.2-9018.01: 10 milliseconds
Structure F3.2-9018.02: 9.4 milliseconds
Circular Reinforced Concrete Culvert: 7.4 milliseconds

Due to the complex geometry and greater depth-span ratios of the cattlepass sections, no theoretical analysis of natural periods of vibration has been attempted in this report for either compressive or flexural modes of those structures.

6.6.2 FLEXURAL MODE.

The theoretical approaches to computation of the periods previously referenced do not specifically include the case of an integral circular structure. Fundamental mode for flexural vibration of such a structure has an approximately elliptical modal shape. Nodes located at quarter points are taken as a reasonable approximation. An equivalent beam having length one fourth the circumference is assumed, which allows use of the expression given in Reference 17 (Formula 6.5.2.2). L is taken to be one fourth the circumference and R_0 as 0.636, as the nodal points approximate simple supports.

The above analogy and formula were used to find the following periods for the uncovered case:

Circular Steel Culvert: 27 milliseconds

Circular Reinforced Concrete: 27 milliseconds

If the ratio of masses of the covered and uncovered situations are taken as those used for the compressive mode, the computed periods for the covered case of the fundamental flexural mode are:

Circular Steel Structure F3.2-9018.01:	178 milliseconds
Structure F3.2-9018.02:	167 milliseconds
Circular Reinforced Concrete:	70 milliseconds

6.7 THEORETICAL PERIOD - CONCRETE DOME.

The only aboveground structure tested in this investigation was the intact responding reinforced concrete dome originally built and tested under Projects 3.6, 3.7, and 30.5a, Operation Plumbbob (References 21, 22, and 23 respectively). The dome has a structural radius of thirty six feet, thickness of six inches, and incloses an angle of ninety degrees. Average 28-day concrete cylinder compressive strength was 4125 psi (Reference 21). The theoretical analysis of the structure presented in Reference 21 used a value of 3670 psi for the compressive strength to make allowance for heat, low humidity, and methods of construction at the test site.

The period of the compressive mode may be computed for the dome by dividing the spherical circumference by the sound velocity in the material which is essentially the expression used for the arch structures (Formula 6.6.1). If a modulus

of elasticity of 3.67×10^6 psi and a concrete density of 150 pcf are used, the resultant computed period is 22 milliseconds. The flexural mode period for a dome is taken as equal to the period for the compression mode (Reference 17), which is based on the nature of a dome to carry point loadings as well as uniform loadings by membrane action.

6.8 THEORETICAL PERIOD - UNDERGROUND GARAGE.

Current design practice for massive concrete underground shelters was represented in the program by vibration testing of a reinforced concrete dual-purpose garage. This structure was originally built and tested under Projects 3.7 and 30.2 (References 22 and 24 respectively), during Operation Plumbbob. Detailed structural drawings and design criteria of the garage are contained in Reference 24. The condition of the garage was essentially unchanged by the nuclear shot and was not affected by the flooding which took place during the nondestructive test program.

The fundamental period of the reinforced concrete garage roof slab was calculated using the methods set forth in EM 1110-345-416 (Reference 18b). All numbers in parentheses refer to the pages in that document where the various formulas can be found. Most of the expressions used are empirical and are based upon experimental work in flat slab construction. In most cases the definitions presented here are the same as those listed on pages V-XXIII of the manual mentioned above. Any additional references will be made clear when used.

First, the fundamental period, T_n (seconds), is found to be

$$T_n = 2\pi \sqrt{m_{te}/k_e} \quad (\text{p. 27})$$

where

m_{te} = total mass of the equivalent system (kip-sec²/ft.)

(1 kip = 1000 pounds);

k_e = equivalent spring constant (kips/ft.).

The mass, m_{te} , is expressed as

$$m_{te} = K_M m_t \quad (\text{p. 4})$$

where

m_t = total mass of the element or structural system under consideration (kip-sec²/ft.);

K_M = mass factor.

From an examination of the garage drawings the total mass of one panel and its earth cover is 17.6 kip-sec²/ft. With $K_M = 0.35$ (p. 68) the equivalent mass, m_{te} , is 6.16 kip-sec²/ft.

Next, the expression for the equivalent spring constant is

$$k_e = K_L k \quad (\text{p. 7})$$

where

K_L = load factor;

k = spring constant, force required

to cause unit deflection of spring (kips/ft.).

This spring constant is written

$$k = \frac{189 (a^2 - d^2) EI_a}{(a - \frac{d}{2})^4} \quad (\text{p. 69})$$

where

a = column spacing in flat slab construction (feet),

d = diameter or width of column capital in flat slab construction (feet),

E = compressive modulus of elasticity of concrete (kip/in.²),

I_a = average of the gross, I_g (in.⁴/ft.), and transformed, I_t (in.⁴/ft.), moments of inertia of a strip of slab one-foot wide (in.⁴/ft.);

Units of 189 are ft.²/in.².

In this case a = 29 feet and d = 14 feet.

Using these values it is possible to convert the expression for the spring constant into the form shown on page 20 of the reference. It will be

$$k = 3.02 \frac{EI_a}{a^2}$$

where the units of 3.02 are ft.²/in.².

The modulus of elasticity of concrete in compression, E, is found by dividing the modulus of elasticity of steel, E_{steel} (30×10^6 psi), by a ratio, n, which is expressed

$$n = \frac{30,000}{f'_c} \quad (\text{Reference 25})$$

where f'_c is the compressive strength of the concrete in psi, in this case 4,000 psi. Using this value $n = 7.5$, and $E = 4 \times 10^6$ psi.

By use of conventional methods the gross moment of inertia, I_g , is found to be 27,000 in.⁴/ft. and the transformed

moment of inertia, I_t , 6,810 in.⁴/ft. The average of these values, I_a , is 16,900 in.⁴/ft.

From these values the spring constant, k , is 2.43×10^5 kips/ft.

Using this value and the load factor, $K_L = 8/15$ (p. 67), the equivalent spring constant is 1.30×10^5 kips/ft.

The result of this is that the fundamental period of vibration for the slab is computed to be 43.3 msec.

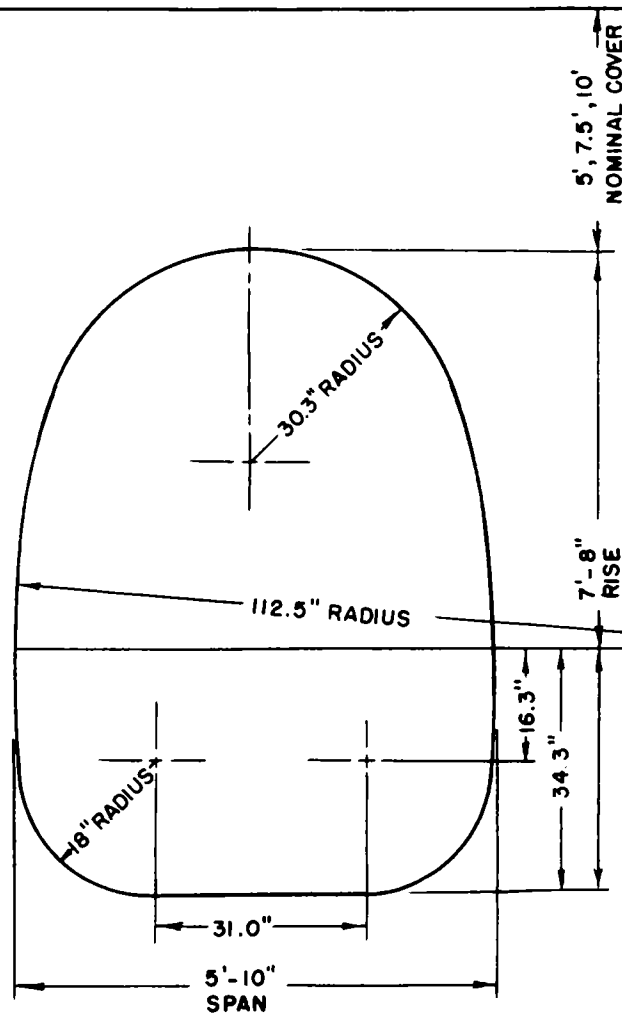


FIGURE 6.1- CATTLEPASS SECTION

CHAPTER 7

PROCEDURE

7.1 FIELD OPERATIONS.

The non-destructive vibration test program was conducted during a two week period in the summer of 1959 at the Nevada Test Site. Some hindrance was experienced due to flooding of Frenchman Dry Lake by heavy rain. All direct and incidental work pertaining to the program was performed by the three project personnel at the site.

7.2 INSTRUMENTATION.

All vibration measurements were made by use of accelerometers with output recorded dynamically on film and magnetic tape. Instruments used were Statham Laboratories model C, ± 1 g range accelerometers, Consolidated Electrodynamics three-kilocycle carrier recording equipment for galvanometer records on film, and Ampex magnetic tape recording equipment for back-up of the film records. A load cell was used with certain installations of the force beam to statically measure the pre-and post-release forces applied to the structure and thereby to confirm adequacy of the load release.

7.2.1 ACCELEROMETER TESTING

Various calibration and natural frequency tests were made on the accelerometers employed in the testing. The accelerometers were calibrated by recording accelerometer output on the Consolidated equipment at the sensitivity settings used in the field tests. The one component of acceleration accelerometers used have output variation equivalent to the force of gravity (1 g) when the axis

corresponding to the component of sensitivity is rotated 90° from a horizontal or vertical orientation. The accelerometers were calibrated through their usable range by varying and accurately measuring the angle of orientation. With the component of sensitivity vertical the equivalent acceleration output was assumed to vary as the cosine of the variation from vertical.

The Statham Model C,[†] 1 g accelerometers have a stated natural frequency of 40 cycles per second and a damping factor whose value is approximately seven-tenths of critical damping. As a result of this damping characteristic, the gage responds approximately linearly to accelerations occurring with frequencies less than forty cps. At forty cps the signal amplitude indicates approximately seven-tenths of acceleration actually being experienced by the gage. At frequency above this value the amplitude ratio of signal to actual accelerations decreases rapidly. At these higher frequencies, however, the accelerometer acts as a seismograph in that it provides a signal that varies approximately linearly with a displacement having a frequency greater than forty cps. The decay in vibration associated with the damping factor of the gage is such that the amplitude of each cycle is approximately five hundred times that of the succeeding cycle.

The damping is sufficient to prevent any resonant behavior of the accelerometer and consequently no harmonic vibrations measured in the test program are considered to have been that of the gage itself.

7.2.2 GAGE MOUNT TESTS.

The accelerometers were used in mounts composed of three rectangular plastic sheets bolted together to firmly clamp the lips of the accelerometer. Attachment to the structure was by one bolt through the mount, close to the accelerometer. Expansion plugs with bolts were used to fasten the assembly to the concrete structures. The corrugated steel structures were prepared for gage mounting by a hole drilled into the flat section midway between a concave and convex corrugation. A hook formed from the cut eye of a turnbuckle was inserted into the hole, the gage mount assembly was placed on this eyebolt, and held in place by the turnbuckle used as a nut. The resulting installation created a beam of the plastic mount which spanned the six-inch corrugation pitch and which was held in place by a bolt, approximately one inch from one of the supports. A gage mounted as described and a turnbuckle attachment are shown in Figure 7.1.

The means of installation of the gage mounts on the concrete structures resulted in a mount which was flush with the structure surface in the case of the underground garage and edge supported in the case of circular concrete culvert. The concrete dome had radius sufficiently large that edge support conditions were approximated. The equivalent beam width of three inches with the installations on the curved concrete structures was assumed to create a mount of natural frequency sufficiently high that any mount vibration would be too small to influence the records obtained in the testing.

The period of vibration of the gage mount assembly when installed on six-inch-pitch corrugated pipe was made the object of a laboratory investigation. The corrugated pipe was simulated by the following test procedure: (1) The accelerometer was placed in a plastic mount identical to those used in the field tests, (2) The gage mount assembly was placed on parallel round bars at six inch spacing atop a two-hundred-pound plate of 1-3/4-inch thick steel, (3) The resultant beam was held in place as in the field by a 5/16-inch hooked turnbuckle, except that it was inserted through a slit in the steel plate, and (4) The accelerometer was excited by striking the plastic mount or the accelerometer a single sharp, rebounding tap with a light steel rod. Induced vibrations were recorded on a Memoscope with permanent records obtained by photograph of the scope traces. Confirmation that the beam period was that being measured and not the natural frequency of the gage was obtained by use of two other support conditions: with one, the supporting bars were placed parallel but at the ends of the plastic mount thus forming a beam of eight-inch span with the turnbuckle in the location described above, and with the other, one bar was placed adjacent and inside to the turnbuckle and the other bar was placed at the same end of the plastic mount forming a cantilever beam with supports three inches apart and with a five-inch cantilever section. As with the six-inch span installation, excitation was by means of single sharp taps by a steel rod at various locations on the assembly.

Repeated testing gave results which indicated that a good reproducibility of data was being obtained from the test procedures

employed. The approximate period of the gage mount assembly installed to simulate mounting on corrugated steel was 3.6 milliseconds. With end support forming an eight-inch beam the mount assembly had a period of 4.4 milliseconds and when installed as a cantilever it had a period of eleven milliseconds. As expected from gage damping, natural frequency of the accelerometer was not noted, while the variation of the period with support conditions confirmed that the vibrations measured were those of the mount assembly acting as a beam.

7.3 STRUCTURAL VIBRATION INDUCTION.

Means employed to induce vibrations in the test structures were those developed in the feasibility study, Appendix I, and by the use of small high explosive detonations. A load column, capable of exerting a static thrust of over two tons was used on the underground concrete and the steel arch structures. Wire rope was used to create a static deflection in the remaining steel structures. The wire rope was attached to the structure by turnbuckles with the eyes cut to form hooks which would slip into holes drilled in the corrugated steel. The wire was tensioned by the turnbuckles and released by means of a manually operated quick release device. Wire rope was used for a few runs on one of the steel arch structures where an existing attachment to the concrete floor made such an installation feasible.

Explosive detonations were used to permit interpretation of the results obtained from the mechanical means of vibration by providing, for comparison, results from excitation caused by sharp overpressure rise at the ground surface. Detonation of explosives

was the sole means employed to cause vibration of the aboveground concrete dome. Flooding of the dome interior by heavy rain which occurred during the test program created conditions which made use of the load column impractical. The rain caused a flooding in the vicinity of the test structures which hampered operations and which may have affected some of the test results.

The recording runs made of the various testing schemes on the test structures are listed in Table 7.1. The test structures used in the program are shown in the plot plan, Figure 7.2. The flooding mentioned above occurred during a time interval between Runs 45 and 46. Test runs were numbered chronologically.

TABLE 7.1 - TESTING SCHEMES

<u>Structure</u>	<u>Excitation</u>	<u>Runs</u>
180° Corrugated Stl Arch Reinf. with Stl Ribs 5-ft Earth Cover	Load Column, Vertical	1,2,3,
	Load Column, 60° fr Horiz	6,7
	Wire Rope, 2-point 60° and 120° from Horiz	4,5
	Explosive, 5 lb @ 8 ft above Ground Surface	116
180° Corrugated Stl Arch 5-ft Earth Cover	Load Column, Vertical	88,89,90
	Load Column, 60° fr Horiz to GZ	95,96,97
	Load Column, 120° fr Horiz to GZ	91-94
	Explosive, 5 lb @ 5 ft above Ground Surface	99
360° Corrugated Stl Culvert 7-1/2-ft Earth Cover	Wire Rope, 2-Point, Vertical	12-14,55,56
	Wire Rope, 2-Point. Horiz	15,20-25,52-54
	Wire Rope, 3-Point, incl Vertex	26-30
	Wire Rope, 4-Point	31-34,49-51
	Explosive, 1 lb @ 9 ft above Ground Surface	76
	Explosive, 2-1/2 lb. 7-1/2 ft above Ground Surface	113
	Explosive, 2-1/2 lb. 4 ft above Ground Surface	114
	Explosive, 5 lb. 4 ft above Ground Surface	115
	Explosive 10 lb. 9 ft above Ground Surface, 100 ft to side of Structure	118
Corrugated Stl Cattlepass 5-ft Earth Cover	Wire Rope, 2-Point Horiz	78-81
	Wire Rope, 2-Point Vert	82,83,84
	Wire Rope, 4-Point	85,86,87
Corrugated Stl Cattlepass 7-1/2-ft Earth Cover	Wire Rope, 2-Point Vert	57,58,59
	Wire Rope, 2-Point Horiz	60,61,62
	Wire Rope, 4-Point	64,65,66
	Explosive, 2-1/2 lb. 9 ft above Ground Surface	117
	Explosive, 10 lb. 9 ft above Ground Surface, 100 ft to Side of Structure	118
Corrugated Stl Cattlepass 10-ft Earth Cover	Wire Rope, 4-Point	67,68,69
	Wire Rope, 2-Point Vert	70,71,72
	Wire Rope, 2-Point Horiz	73,74,75
	Explosive, 1 lb. 9 ft above Ground Surface	77
	Explosive, 2-1/2 lb. 8ft above Ground Surface	112

TABLE 7.1 (CONTINUED) - TESTING SCHEMES

Circular Reinf Conc Culvert 7-1/2-ft. Earth Cover	Load Column, Vertical	35-39,46-48
	Load Column, Horizontal	40,41,42
	Load Column 45° towards GZ	43,44,45
	Explosive 2-1/2 lb. 9 ft above Ground Surface	100
	Explosive 10 lb. 9 ft above Ground Surface, 100 ft to side of Structure	118
90° Reinf Conc Dome above Ground	Explosive 5 lb. 9 ft above Ground Surface 100 ft fr Vertex	119
	Explosive, 5 lb. 9 ft above Ground Surface, 90 ft fr Vertex	120
	Explosive 6-1/2 lb. 9 ft above Ground Surface, 90 ft fr Vertex	121
Concrete Garage 3-ft Earth Cover	Load Column mid span	101-103,108,109
	Load Column mid span of Column Strip	104-107
	Load Column Quarter Span of Middle Strip	110

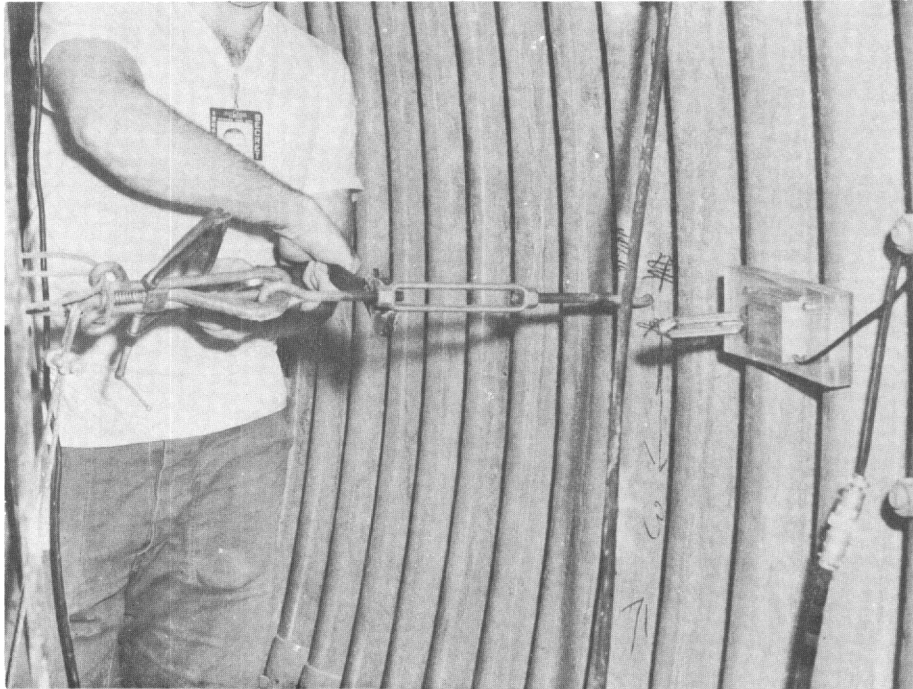
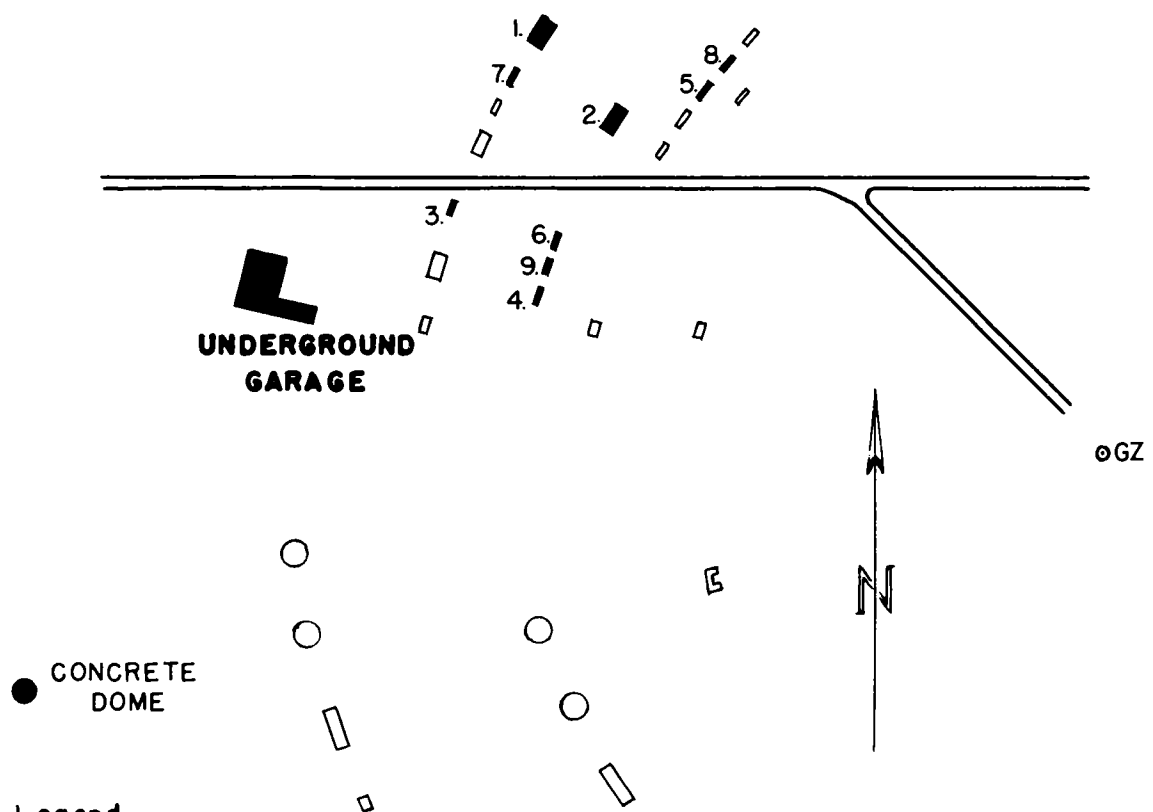


FIGURE 7.1 - ACCELEROMETER AND TURNBUCKLE ATTACHMENT.
Tensioning wire rope for two-point loading scheme in a cattlepass.



Legend

NOT TO SCALE

1. UNREINFORCED STEEL ARCH

2. RIBBED STEEL ARCH

3. CATTLEPASS, 5' COVER

4. CATTLEPASS, 7 1/2' COVER

5. CATTLEPASS, 10' COVER

6. CONCRETE CULVERT F3.2-9017.02

7. CONCRETE CULVERT F3.2-9017.03

8. CIRCULAR STEEL F3.2-9018.01

9. CIRCULAR STEEL F3.2-9018.02

OTHER STRUCTURES NOT USED

FIGURE 7.2 - PLOT PLAN, TESTED STRUCTURES

CHAPTER 8

RESULTS

8.1 GENERAL.

During the two week test program eleven structures were tested, under thirty-one different mechanical excitation setups or variations in structural conditions, and under fourteen explosive detonations. A total of one-hundred-eleven runs were put on record (Table 7.1). In addition, four accelerometer calibration records were made with the accelerometers located within one of the test structures. Three accelerometers were used on each run to make measurements at different locations within the structure being tested. Film records were developed and given preliminary examination at the test site so that sufficient data could be obtained prior to departure. As a result of these preliminary examinations, some of the initial tests made on the circular concrete and circular steel structures were repeated.

The results obtained are presented in detail, to provide basis for evaluation of the vibration test procedures and of the conclusions presented. Various periods measured by each accelerometer are tabulated. Only those runs from which apparently usable traces were obtained are listed. The period of any harmonic noise in the accelerometer trace was determined by measurement on that part of the trace made prior to the excitation of the structure. Frequently, that same period was measured immediately after excitation, and as a consequence

certain of the periods tabulated are suspect. Due to the nature of the traces it was occasionally possible to measure the period of the same mode at different times on the same record. Galvanometers and amplifiers used for recording the accelerometer signals were varied occasionally to prevent a continual interference of a trace by any defects in the amplifying and recording equipment.

8.2 STEEL ARCH STRUCTURES.

The steel arch structures, which essentially differed only in that one was reinforced by steel ribs, were tested under similar loading schemes. The results obtained from the various test runs on the two structures are presented in Table 8.1. The accelerometer positions and loading schemes employed for the testing are listed in Table 8.2. The interior of the unreinforced structure with the load column and accelerometers in position for Runs 91 through 94 is illustrated in Figure 8.1. Placement of five pounds of forty percent straight dynamite for Run 99 is shown in Figure 8.2. This type high explosive and the method of positioning shown in the figure were used for all of the explosive runs of the non-destructive test series. The amount of explosive and the height above the ground surface was varied but with the exception of Runs 118 through 121, the position was always over the vertex of the structure at midlength. Similarly, the accelerometers and loading schemes were employed at approximately the midlength of all the underground structures.

The period of the fundamental mode as obtained from the mechanically excited vibrations and from the explosive run

was in close agreement for each structure. The reinforced arch structure had an average period of 62 ms obtained from mechanical excitation and 66 ms from the explosive run. The unreinforced arch structure had an average period of 69 ms obtained separately from both the explosive and mechanical means of excitation.

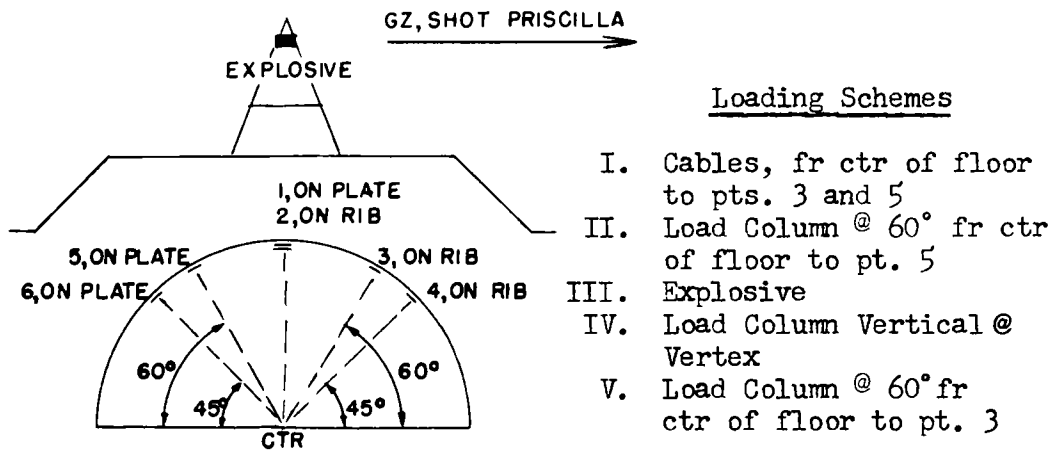
TABLE 8.1 MEASURED PERIODS - STEEL ARCH STRUCTURES.

<u>Run No.</u>	Accel No:	Periods (Milliseconds)		
		<u>102</u>	<u>103</u>	<u>104</u>
<u>Reinforced Arch</u>				
5		4.7	61, 8.3 N-1.4 ²	NR ¹
7		NR	62, 2.6 N-1.4	2.6
116 (Explosive)		64, 67 13.6, 13.7	66	66, 5.5 5.9
<u>Unreinforced Arch</u>				
88		68, 2.1 2.3, N-2.4	NR	67
89		67, 2.4 N-2.4	68, 6	68
90		67, 2.4 N-2.4	NR	69, 4
91		2.4, N-2.4	2.3	69, 2.0
93		N-2.4	NR	2.1
94		2.4, N-2.4	1.9	1.9
95		70, 3.5 2.4, N-2.4	NR	NR
96		70 (Approx) 2.4	70	NR
97		69, 6.4 2.4, N-2.4	71, 6.5	71, 6.4
99 (Explosive)		70, 2.5 N-2.4	69	68

1. NR: Negligible Response or not measurable

2. N-: Period of harmonic noise

TABLE 8.2 ACCELEROMETER AND LOADING POSITIONS-STEEL ARCH STRUCTURES



<u>Run No.</u>	<u>Accelerometer Positions</u>			<u>Loading Scheme</u>
	<u>102</u>	<u>103</u>	<u>104</u>	
<u>Reinforced Arch</u>				
5	5	1	2	I
7	5	1	2	II
116	2	4	3	III
<u>Unreinforced Arch</u>				
88-90	1	6	5	IV
91-94	1	6	5	II
95-97	1	6	5	V
99	1	6	5	III

8.3 CIRCULAR STEEL CULVERT.

The flooding of the site of the test structures during the test program necessitated the use of two similar circular steel culverts. The mobile blast laboratory used for recording the accelerometer signals was temporarily stranded in a position adjacent to structure F3.2-9018.02, used for the mechanical excitation tests. As a result, runs 76, 113, 114, and 115 were made on structure F3.2-9018.01. The other runs were made on the former structure, including explosive run 118, which was made after the truck was moved from the stranded position. Run 49 and those following were made with the surface above F3.2-9018.02 flooded by a few inches of water. The nature of the flooding, the truck and generator in the stranded position, and the surface above structure F3.2-9018.02 are shown in Figure 8.3. The surface above F3.2-9018.01 was not flooded at any time during the test program.

Periods measured from the test records are presented in Table 8.3. In the case of some of the traces it was possible to measure the logarithmic decrement, δ , of the decaying vibration. Those that were measured are included in Table 8.3. The position of the accelerometers in the various runs is given in Table 8.4.

The high explosive detonations induced vibration in at least one mode which did not appear to have been excited on the records made with the mechanical excitation means. Maximum response to the explosions apparently did not always occur in the same mode, as may be observed in the record from Run 113,

Figure 8.4. Maximum recorded response to the explosions took place in either of the modes with average periods of 9.4 ms or 55 ms. A period similar to 55 ms was not measured from the mechanically induced vibrations. Some of the approximate periods relatively well established by the mechanical vibration testing were 8.0 ms, 5.4 ms, and 2.1 ms. Variation in periods measured seemed to have had some relationship to accelerometer location and water on the surface above the structure.

TABLE 8.3 MEASURED PERIODS - CIRCULAR STEEL CULVERT.

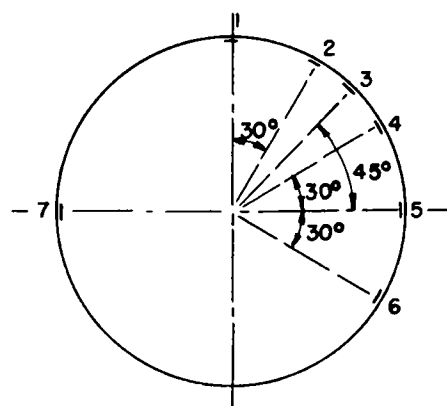
Run No. (F3.2-9018.02)	Acce1 No.	Periods (Milliseconds)			Logarithmic Decrement, δ
		<u>102</u>	<u>103</u>	<u>104</u>	
12		NR ^{1.}	8.7(approx) 2.5, N-1.4 ^{2.}	NR	NR
13		NR	2.2, N-1.4	NR	NR
14		NR	2.1, N-1.4	NR	NR
20		4.8	2.3, N-1.4	4.8	NR
21		5,N-2.4	2.4, N-1.4	4.8	Ln 1.31 (103) ³
22		5.0 N-2.4	2.4, N-1.4	4.8	Ln 1.26 (102)
23		2.4	2.5, N-1.4	4.4	Ln 1.30 (102)
24		2.4	N-1.4	4.3	Ln 1.29 (102)
25		2.4	8, N-1.4	4.0	Ln 1.25 (102)
26		NR	4.0, 2.4 N-1.4	NR	Ln 1.31 (103)
28		NR	2.4, N-1.4	5.1	Ln 1.32 (103)
29		5.6	2.4, N-1.4	5.1	Ln 1.27 (103)
31		2.0, 2.0	2.3, N-1.4	4.0	Ln 1.31 (102)
32		2.0	2.3, N-1.4	4.0	NR
33		2.0, 2.0	2.4, N-1.4	4.0	Ln 1.26 (102) Ln 1.25 (103)
(Following runs on F3.2-9018.02 were made with the ground surface flooded)					
49		5.4	1.9, N-1.9	2.04,2.0 2.0, N-1.9	Ln 1.22 (102)
51		5.5	NR	8.0,2.1,2.1 2.1,2.1,2.06 Ln 1.26 (104)	Ln 1.23 (102) Ln 1.12 (104)

1. NR: Negligible trace or not measurable.
2. N-: Period of harmonic noise
3. Ln: Log_e; (103): δ computed from trace 103.

TABLE 8.3 (Continued)

Run No.	Accel No:	Periods (Milliseconds)			Logarithmic Decrement, δ
		<u>102</u>	<u>103</u>	<u>104</u>	
52	5.2, 5.4	4.6	8.0,8.0,8.1 8.0,8.1,2.0 2.0,2.0,2.05 2.02, 2.06	Ln 1.20 (104) Ln 1.61 (104) Ln 1.29 (104) Ln 1.21 (104)	
53	NR	N-1.9	2.0	NR	
54	5.4, 5.0	2.3,N-1.6	7.9,2.0,2.0 2.0,2.0,2.0 2.0,2.0,2.0 2.1, 2.1	Ln 1.25 (102) Ln 1.78 (104)	
55	5.4	N-1.7	NR	Ln 1.21 (102)	
56	5.4	N-1.7	NR	Ln 1.16 (102)	
118 (Expl)	51	Not Used	Not Used	NR	
(F3.2-9018.01)					
76 (Expl)	2.4	1.86,N-8.4	5.4,5.2	NR	
113 (Expl)	12.9,2.4	42,13.3 4.6	65,9.3	NR	
114 (Expl)	2.6	57, 41	58,9.5,9.3	Ln 1.45 (104)	
115 (Expl)	43,2.6	58, 42	59,9.4,9.3	NR	

TABLE 8.4 ACCELEROMETER AND LOADING POSITIONS-CIRCULAR STEEL CULVERT.



GZ, SHOT PRISCILLA →

Loading Schemes

- I. 2 pt. Vertical
- II. 2 pt. Horiz.
- III. 3 pt., 1 @ vertex
- IV. 4 pt., 1 @ vertex
- V. Explosive

Run No.	Accelerometer Positions			Loading Scheme
	<u>102</u>	<u>103</u>	<u>104</u>	
(F3.2-9018.02)				
12-14, 20-22	7	1	2	I
15, 23-25	6	1	4	II
26-30	5	1	4	III
31-34	6	1	4	IV
49-51	1	4	6	IV
52-54	1	4	6	II
55, 56	1	4	5	I
118	1	(103, 104 Not Used)		V
(F3.2-9018.01)				
76	3	1	5	V
113-115	5	3	1	V

8.4 CATTLEPASS STRUCTURES.

Three corrugated steel cattlepass structures at different depths were tested. Two of these with nominal 7-1/2-foot and 10-foot depth of cover (F3.2-9016.05 and F3.2-9016.04 respectively) were subjected to high explosive testing in addition to the mechanical means of vibration excitation. The structure at nominal depth of cover of five feet (F3.2-9016.06) was vibrated only by the use of the wire rope assemblies. The ground surface over the structures with 5- and 7-1/2-foot depth of cover was flooded by a few inches of water during the period of the testing while the surface over the one with 10 feet of cover remained dry.

The results obtained from the testing are tabulated in Table 8.5. Where feasible, rate of decay of the vibrations was computed and is listed with the trace from which computed. Positions of the accelerometers and loading schemes employed were as noted in Table 8.6. The interior of a cattlepass with accelerometers and four-point loading scheme in position is shown in Figure 8.6.

With the exception of the results obtained from the explosive runs, little difference was noted in the periods due to various types of mechanical loading. No general trends appear to have been established for variation of the measured period due to depth of cover, position of accelerometer, or presence or absence of water. Some vibrations occurred in the structures due to explosive loadings which did not appear with mechanical vibration induction. Prime response to the explosion appeared to take place in such a mode of vibration.

TABLE 8.5 - MEASURED PERIODS-CATTLEPASS STRUCTURES.

Run No.	Accel No:	Periods (Milliseconds)			Logarithmic Decrement, δ (Trace Used For δ)
		<u>102</u>	<u>103</u>	<u>104</u>	
Structure with 7-1/2-foot cover					
57	2.3, 2.3	2.3, N-1.7 ^{1.}	1.9	Ln 1.14 (102) ^{2.} Ln 1.25 (103)	
58	2.4, 2.4	2.3, N-2.7	2.9, 3.3	Ln 1.25 (102)	
59	2.3, 3.7 2.4	2.3, N-1.7 N-3.4	3.1	Ln 1.25 (102)	
60	2.3, 2.4	2.4, N-2.1	2.0, 1.8 1.9	Ln 1.25 (103) Ln 1.25 (104)	
61	2.4, 2.4	2.4, N-1.9	1.9	NR ³	
62	2.3	2.3, N-1.9	1.9	Ln 1.41 (103)	
64	2.4, 2.4	2.4, N-2.0	1.8, 1.8	Ln 1.25 (104)	
65	2.4, 2.4	2.4, N-1.8	1.8, 1.9, 2.0, 1.9, 1.8	Ln 1.23 (102) Ln 1.20 (104)	
66	2.3, 2.3	2.3, N-3.2	1.8, 1.8 1.8	Ln 1.30 (104)	
117 (Expl)	17	31, 20, 2.3	36, 27, 3.2	NR	
118 (Expl)	(102, 103 Not Used)			46	NR
Structure with 10-foot cover					
67	1.7, 2.4	2.6	2.4, 2.4	Ln 1.23 (104)	
68	2.7, 2.4 N-2.4	2.7	2.3, 2.5	Ln 1.35 (103) Ln 1.43 (104)	

1. N-: Period of Harmonic Noise

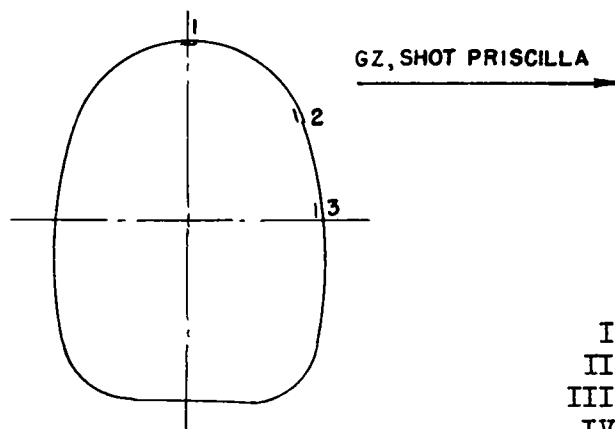
2. Ln: Log_e

3. NR: Negligible trace or not measurable

TABLE 8.5 (Continued) - MEASURED PERIODS-CATTLEPASS STRUCTURES.

<u>Run No.</u>	<u>Accel No:</u>	<u>Periods (Milliseconds)</u>			<u>Logarithmic Decrement, δ (Trace Used For δ)</u>
		<u>102</u>	<u>103</u>	<u>104</u>	
69		2.7, 2.4 N-2.4	2.6	2.4, 2.4	Ln 1.15 (104)
70		2.7, N-2.4	2.6	2.3	Ln 1.22 (102)
71		2.7, N-2.4	2.6	NR	Ln 1.20 (102)
72		2.7, 2.4 N-2.3	2.6, N-1.8	NR	Ln 1.22 (102)
73		2.7, N-2.3	2.6	2.4, 2.3	Ln 1.19 (104)
74		2.7, N-2.4	2.6, 2.5	2.3, 2.1, 2.4	NR
75		2.7, N-2.3	2.7	2.4, 2.3 2.4	Ln 1.28 (104)
77 (Expl)		15, 18, 1.7 1.8, 1.8, 1.8	2.8, 11 12	25, 9.3 1.8	Ln 2.15 (102) Ln 1.70 (103)
112 (Expl)		32, 17, 1.9, 2.0	33, 22 2.1	34, 19 3.0	NR
Structure with 5-foot cover					
78		2.4	3.9	1.8, 1.8	Ln 1.27 (104)
79		2.3	3.9	1.8, 1.7 1.8, N-2.1	Ln 1.22 (104)
80		2.3	4.0	1.8, 1.8	Ln 1.33 (104)
81		2.4	4.0	1.8, 1.8	Ln 1.41 (104)
82		2.3, N-2.4	NR	1.8	NR
83		2.3	NR	2.7, 9.5 N-1.8	NR
84		2.4, N-2.4	1.8, 2.6	1.8, 9.4	NR
85		2.3, 2.4 N-2.4	1.8, 1.8	1.8, 1.7	Ln 1.25 (104)
86		2.3, N-2.5	1.8, 1.8	1.8, 1.8	Ln 1.20 (104)
87		2.3, 2.4	1.8, N-1.8	1.8, N-1.8	Ln 1.19 (104)

TABLE 8.6 ACCELEROMETER AND LOADING POSITIONS-CATTLEPASS STRUCTURE.



Loading Schemes

- I. 2 pt. Vertical
- II. 2 pt. Horizontal
- III. 4 pt., 1 @ Vertex
- IV. Explosive

Run No.	Accelerometer Positions			Loading Scheme
	<u>102</u>	<u>103</u>	<u>104</u>	
Structure with 7-1/2-foot cover				
57-59	1	2	3	I
60-62	1	2	3	II
64-66	1	2	3	III
117	3	2	1	IV
118	(102, 103 Not Used)		1	IV
Structure with 10-foot cover				
67-69	1	2	3	III
70-72	1	2	3	I
73-75	1	2	3	II
77	1	2	3	IV
112	3	2	1	IV
Structure with 5-foot cover				
78-81	1	2	3	II
82-84	1	2	3	I
85-87	1	2	3	III

8.5 CIRCULAR REINFORCED CONCRETE CULVERT.

Two similar circular concrete culvert sections were used for the vibration testing. One of these (F3.2-9017.03) was used for one explosive test (Run 100) due to temporary stranding of the recording truck near the concrete culvert used for the remainder of the tests (F3.2-9017.02). The results obtained from examination of the test records are presented in Table 8.7. Accelerometer positions and loading schemes are given in Table 8.8.

Principal period measured from mechanically induced vibrations was approximately 7.2 ms. This was approximated by some periods measured from an explosive run, but was apparently not the period of the mode in which principal response to the explosions took place. The results do not appear to confirm what this period of the principal response was, but two readings of 28 ms were recorded. The records were not such as to justify computation of the damping coefficient. A portion of the trace on one of the explosives runs is reproduced as Figure 8.6.

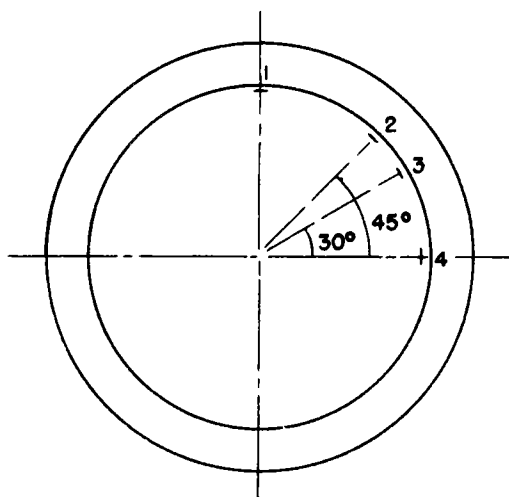
TABLE 8.7 - MEASURED PERIODS-CIRCULAR CONCRETE CULVERT.

<u>Run No.</u>	<u>Accel No:</u>	<u>102</u>	<u>103</u>	<u>104</u>
F3.2-9017.02				
38		7.0	NR ^{1.}	NR
39		7.2	NR	NR
40		7.3	NR	NR
41		7.3, 7.2 (14, Rough)	2.1, 2.1 2.1, N-1.4 ²	NR NR
42		7.1 (18, Rough)	NR	4.4
43		NR	2.0, 2.0 N-1.4	NR
44		NR	2.1, N-1.4	NR
45		6.6	NR	NR
46		7.9	NR	NR
48		8.4	NR	NR
118 (Expl)		Not Used	63	Not Used
F3.2-9017.03				
100 (Expl)		44, 9.0 8.3, N-2.4	28, 4.8	28, 7.1

1. NR: Negligible trace or not measurable

2. N-: Period of harmonic noise

TABLE 8.8 - ACCELEROMETER AND LOADING POSITIONS-CIRCULAR CONCRETE CULVERT.



GZ Shot Priscilla →

Loading Schemes

- I. Load Column Vertical
- II. Load Column Horizontal
- III. Load Column @ 45° clockwise from Vertical
- IV. Explosive

Run <u>No.</u>	Accelerometer Positions			Loading <u>Scheme</u>
	<u>102</u>	<u>103</u>	<u>104</u>	
F3.2-9017.02				
35-39	1	3	4	I
40-42	1	3	4	II
43-45	1	3	4	III
46-48	1	3	4	I
118	Not Used	1	Not Used	IV
F3.2-9017.03				
100	1	4	2	IV

8.6 CONCRETE DOME.

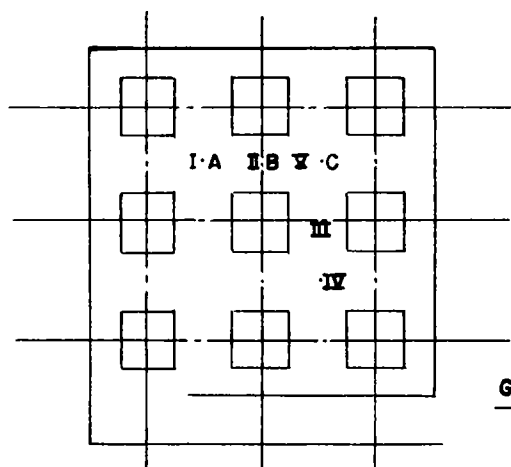
The concrete dome was tested for three runs, with high explosive used as the means of exciting vibrations in the structure. The position of the explosive charges, the accelerometers, and orientation with respect to GZ, Shot Priscilla are shown in Figure 8.7.

Similar results were obtained from each test and from each of the accelerometer traces. Two distinct and concurrent modes of the same order of magnitude appeared. Very little damping was present, as can be noted from the trace from Run 119, Figure 8.8. The periods of the two modes were approximately twenty-one and twenty-three milliseconds. Gage characteristics are such that both modes should be assumed to have been present in the structure. Of the two modes, that with the period of twenty-one milliseconds was apparently that in which the principal initial response took place.

8.7 UNDERGROUND GARAGE.

The massive dual-purpose reinforced concrete underground garage-mass shelter was tested by application of the steel load column to the bottom of the roof slab (Figure 8.9). The results of the analysis of the traces (Table 8.9) show good repetition of results and provide a period for the fundamental mode of approximately sixty milliseconds. This same period was measured for the principal mode excited in runs made with the load column in a variety of positions. Measurement of the damping was not feasible due to the low amplitude of the signal and the recorded traces.

TABLE 8.9 MEASURED PERIODS - UNDERGROUND GARAGE.



Run No.	Loading Pt.	Accel:	Periods (Milliseconds)		
			<u>102</u>	<u>103</u>	<u>104</u>
102	I		60	60	NR ^{1.}
103	I		43,11	60A ^{2.}	NR
104	II		60A	60A	59
106	III		59	NR	59
107	III		61	NR	60
108	IV		60	60	NR
109	IV		60	61	NR
110	V		60	60	60,3.9
111	V		61	61	60,3.9

1. NR: Negligible trace or not measurable
2. A-: Approximate, within 5 ms

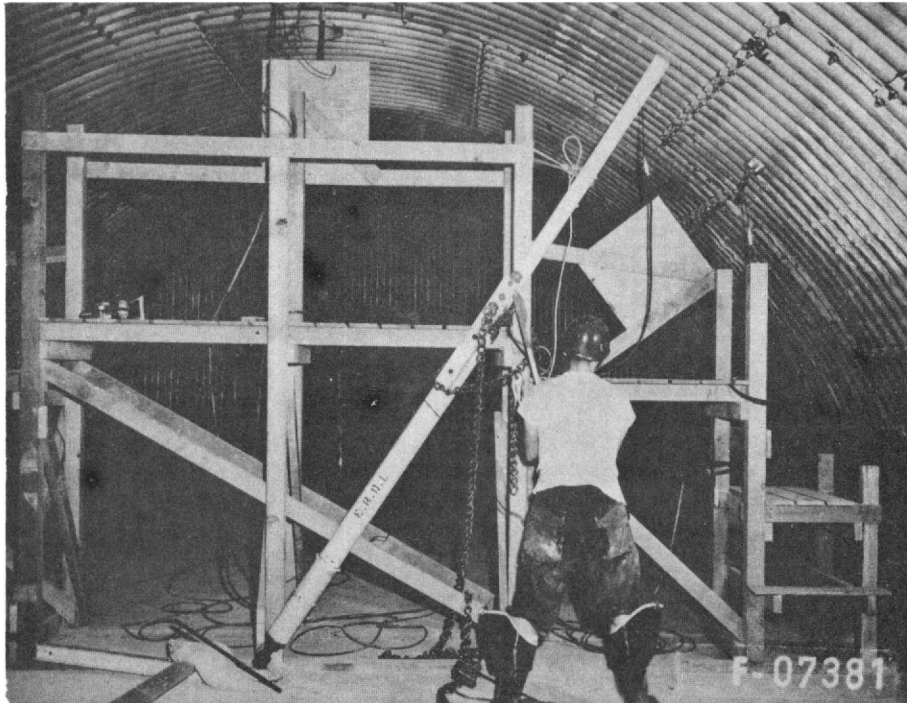


FIGURE 8.1 - UNREINFORCED STEEL ARCH STRUCTURE.
Load column and accelerometers in position for Run 91.



FIGURE 8.2 - TYPICAL HIGH EXPLOSIVE PLACEMENT.
 Five pounds of dynamite centered over unreinforced steel arch structure for Run 99.

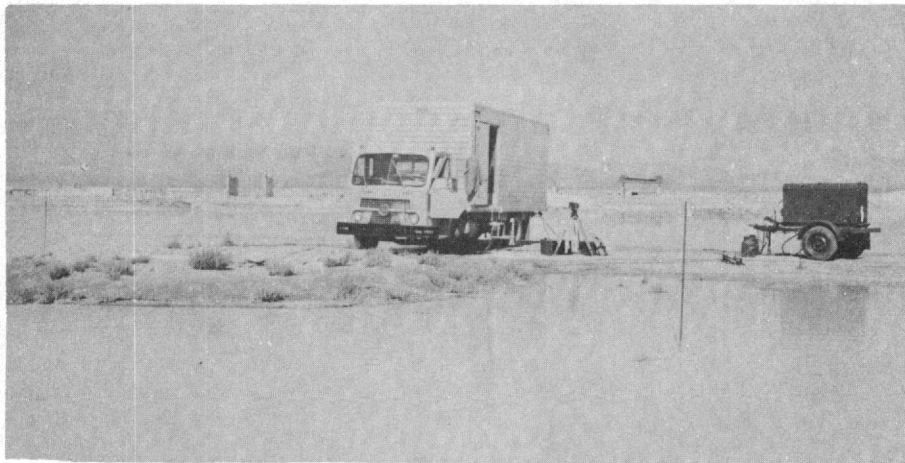


FIGURE 8.3 - TEMPORARY FLOODING AT PROJECT SITE.
 Photograph shows Mobile Blast Laboratory in stranded position, the entrance to the steel culvert F3.2-9017.02 (left foreground), and the surface condition above the structure (center and right foreground).

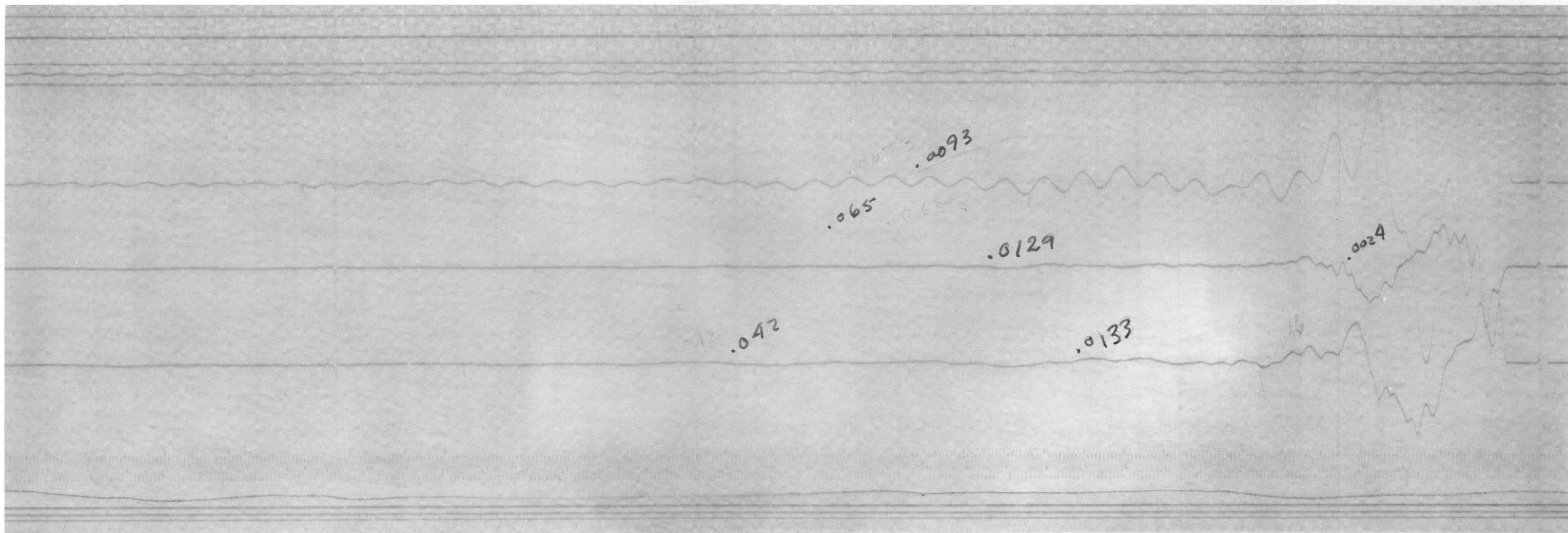


FIGURE 8.4 - RECORD OF RUN 113, CIRCULAR STEEL CULVERT

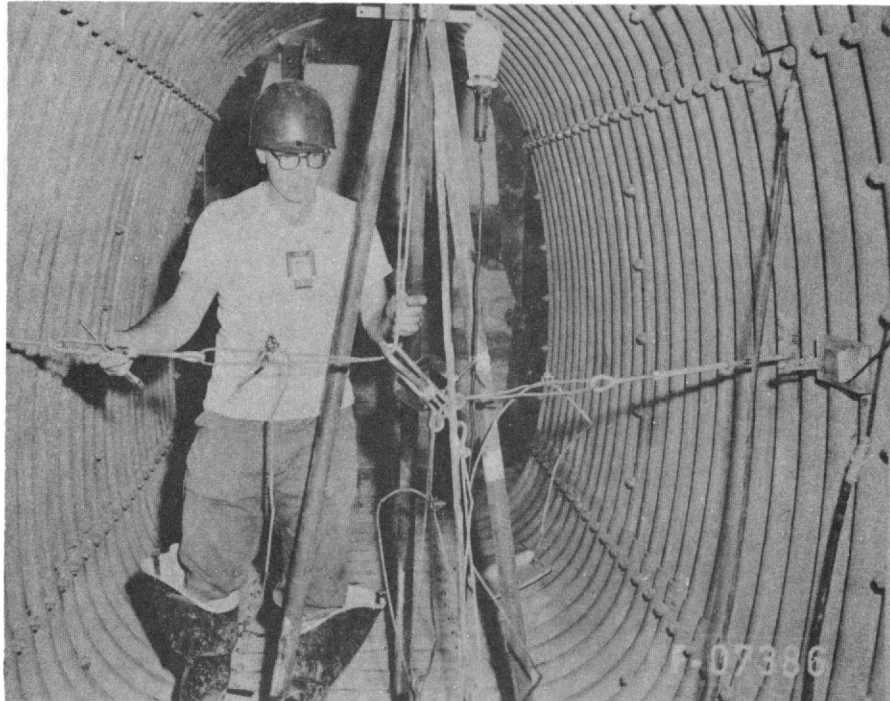


FIGURE 8.5 - FOUR-POINT LOADING IN CATTLEPASS.

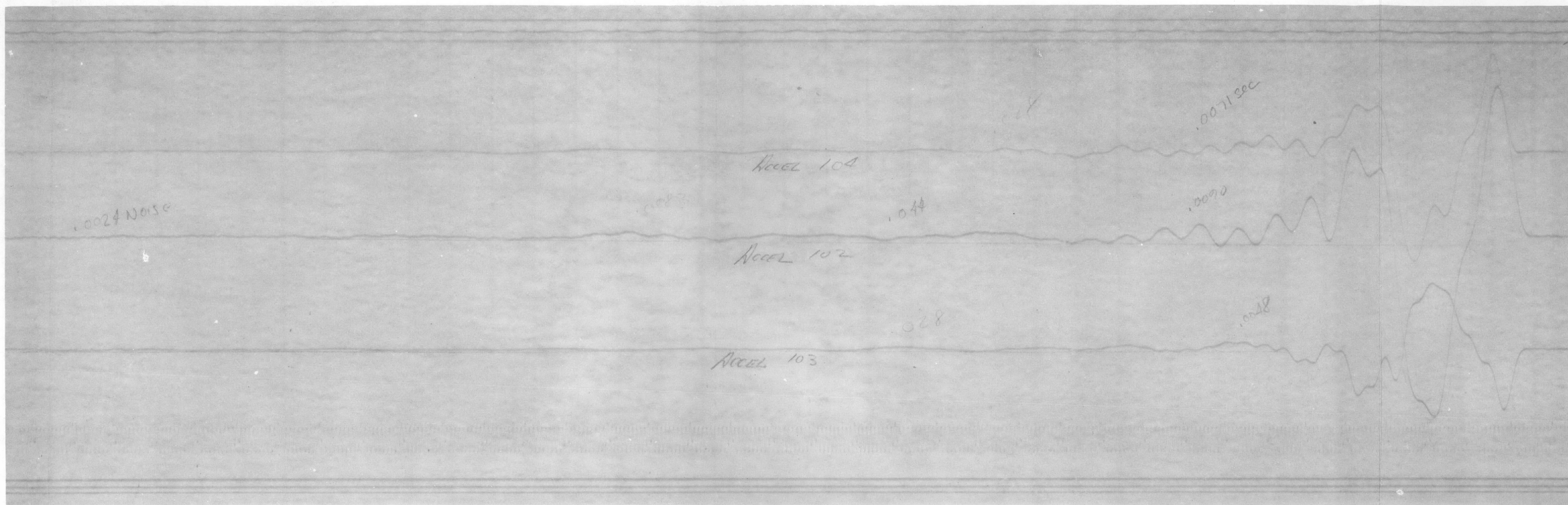


FIGURE 8.6 - RECORD OF RUN 100, CIRCULAR CONCRETE CULVERT

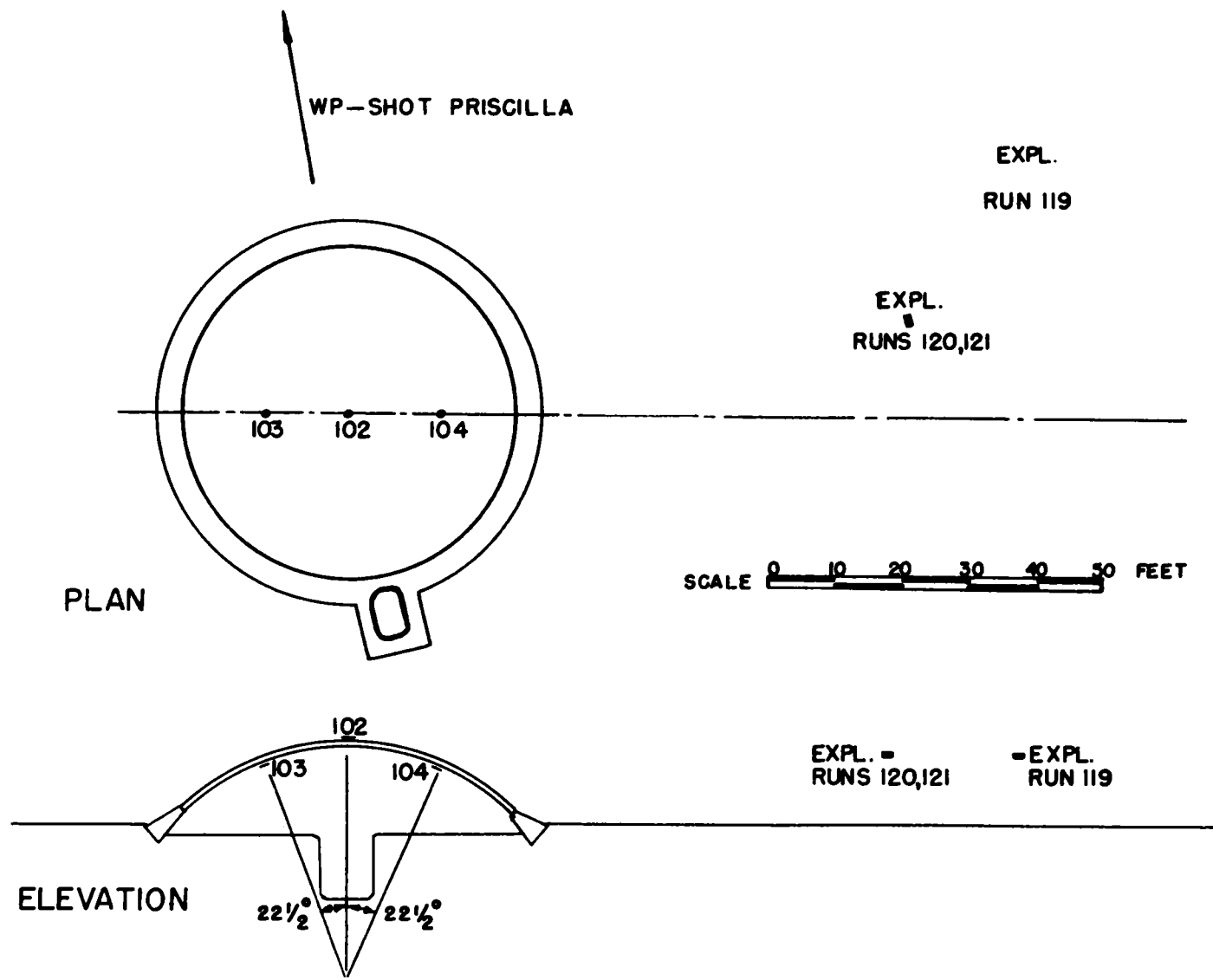


FIGURE 8.7—ACCELEROMETERS AND LOADING, CONCRETE DOME

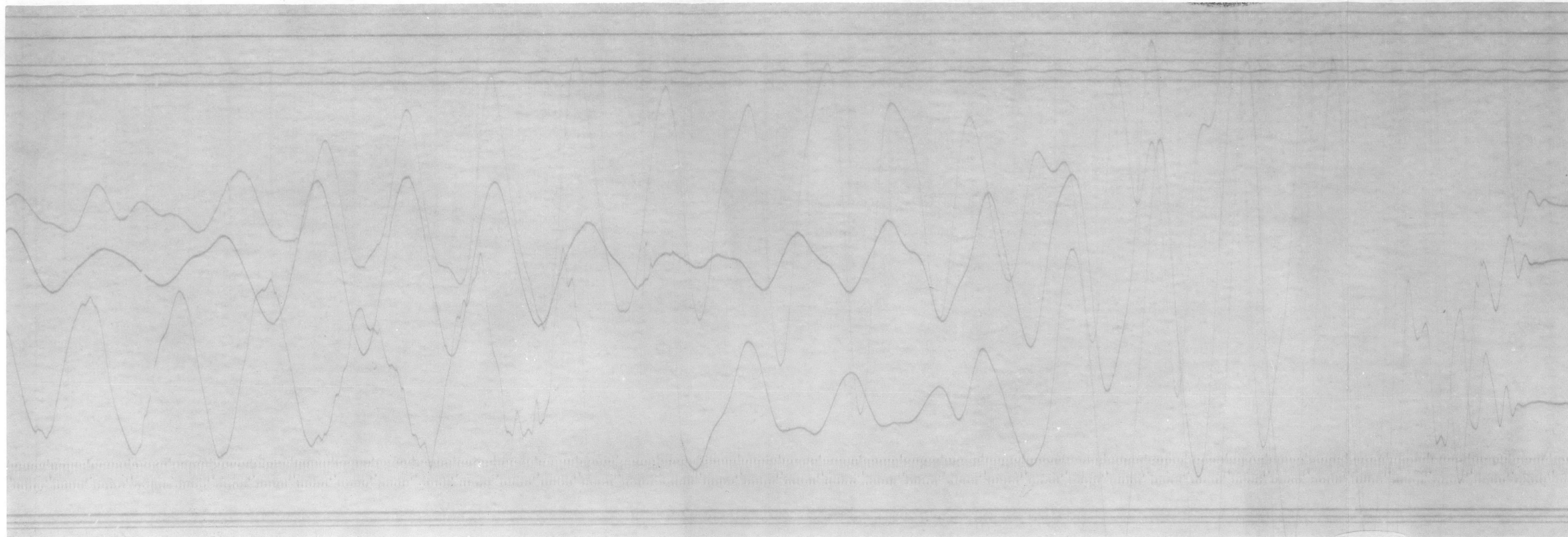


FIGURE 8.8 - RECORD OF RUN 119, CONCRETE DOME

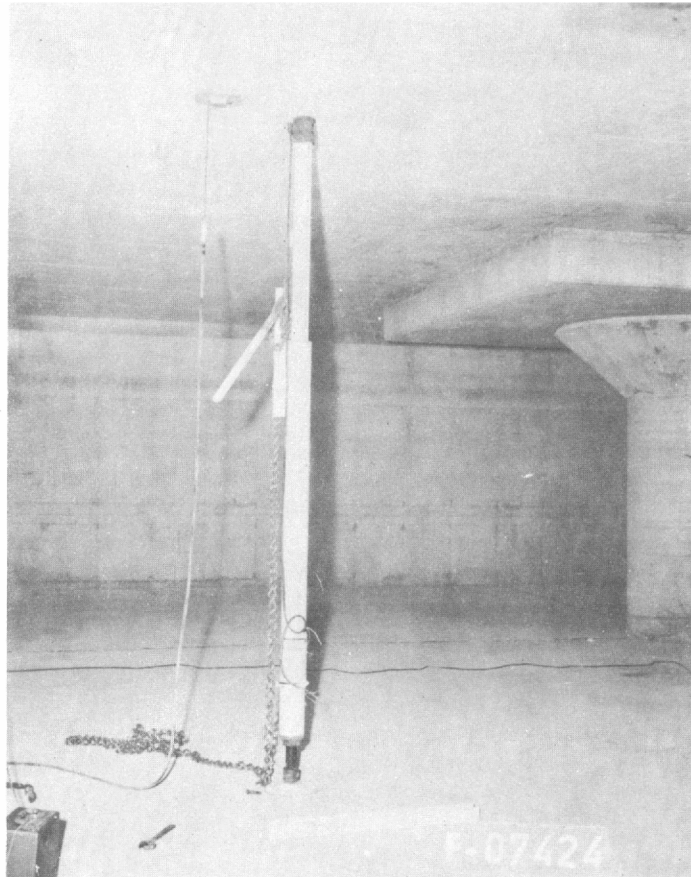


FIGURE 8.9 - UNDERGROUND GARAGE INTERIOR.
Load column and accelerometer in place for Run 102.

CHAPTER 9

DISCUSSION

9.1 ACCURACY OF MEASUREMENT.

The absolute magnitude of the acceleration or displacement that occurred during the vibration of a structure was not made a subject of study. Relative amplitude of vibrations in different modes was observed for the purpose of identifying the mode in which the maximum response to shock overpressure occurred. The characteristics of the gage used are presented in Chapter 7. These characteristics were such that measurements required to satisfy the above objective could be satisfactorily made.

Accuracy of the measurement of the period was dependent upon both the accuracy of the time standard and the duration and clarity of the vibrations in the mode under examination. The time standard had a rated accuracy of + 0.001% and consequently was not a source of measurable error. Gage response was such that the trace that appeared on film did not contain resonant vibration of the gage. For vibrations at the higher frequencies, the accelerometer was actually acting as a seismograph in that the output varied directly with the displacement. At frequencies slower than the natural frequency of the gage (approximately forty cycles per second) the gage had an essentially linear response to acceleration. Damping of the gage was such (δ roughly equal to $\ln 500$) that for any vibration induced in the natural mode of the gage by a sharp blow or sudden movement, the second cycle would have an amplitude of about one-fifth of one percent that of the preceding cycle. The result of the above

is such that it may be assumed the signal as put forth by the gage provided an accurate record of the accelerations or displacements that were experienced by the gage.

The amplifying and recording equipment was used at maximum amplification, with a consequence that some noise was present on some of the signals. The noise that occurred on the recording traces was generally of an harmonic nature with a small amplitude and with a very short period. The period of this harmonic noise was usually between 1.5 and 3 milliseconds and was such as to cause some difficulty in reading and interpretation of gage signals with periods in the same range. The fundamental periods of the structure were generally larger, usually so by at least an order of magnitude, than that of noise however, and consequently their measurement should not have been affected by the noise in the signal.

Major source of inaccuracy in the measurement of the periods originates in the visual interpretation of the trace. When more than one mode was present at the same time, considerable interpretation was required in order to follow the vibration of the mode under study through beats and along other vibrations which might have been of larger amplitude. The number of cycles which could be used for the measurements determined the amount of error that was introduced in the selection of the limits of sample. Low amplitude vibrations with a long period were particularly difficult to interpret in regards to selection of a similar phase point for both limits of the sample.

Calculation of the damping coefficients were generally made by plotting total width of the vibrating trace on a semi-logarithmic graph and then measuring the slope of the best representative straight line through the points representing the peaks of the decaying vibrations. Other means of calculation employed similarly used the measurement of the amplitude at peaks of the vibrations and then averaged the ratios of the heights of adjacent peaks.

9.2 CONDITION OF THE STRUCTURES.

All of the structures tested were in excellent condition. Variations from the structural conditions which had existed prior to the nuclear test were apparent only in the concrete culvert F3.2-9017.02 and the concrete dome. These structures had undergone some cracking, not to an extent that would materially effect the structural resistance, but which might have had an effect on the nature of response to very light loadings, as were used for the non-destructive tests.

The concrete culvert had suffered light longitudinal cracking at the vertex and invert, observable from within the structures. From this it may be inferred that additional longitudinal cracking had occurred to some extent at the outside of the culvert at approximately midheight. Such cracking may have affected the vibration in the flexural mode as the cracks would create points in the cross section at which pin connection would be approximated or would be partially in evidence. A reduced stiffness in the flexural mode would be the result.

Cracking in the concrete culvert and dome would be expected to have little effect on the compressive mode of vibration in so far as the cracks were not of a size that would permit increased inward or outward displacement under vibration in that mode. The cracks observed in these structures did not appear to have been of such magnitude as to affect the amplitude of the compressive mode vibrations. As stated in Chapter 6, the flexural mode for a dome is taken to have the same period as the compressive mode, due to the resistance by membrane stresses of uneven loading upon the dome. Hairline cracks of random pattern as occurred in the dome should have had a minimal effect on the membrane stresses, and consequently on the period of the dome, so long as the dead weight of the structure prevented any tensile stresses from developing. The loads applied to the dome by the high explosive detonations used in the testing should not have been of a size that would have counteracted the compressive stresses created by the dead weight of the dome to the extent of permitting tension.

The structural condition of the underground garage was essentially not changed by the nuclear test. The visible portion of the roof slab had the appearance of other concrete slabs as used in buildings or bridges, in which the presence of hairline tension or shrinkage cracks is normal. Such cracks existed in the roof slab of the garage and most of these had been initiated or had been lengthened during response of that structure to the nuclear shock. They were not of a nature that would affect the characteristics of the response to nuclear or lesser shocks.

Results of the nuclear test effects on the corrugated steel structures indicate that slippage at the riveted or bolted joints probably took place during the blast overpressure loading on the structures. Such slippage would lengthen response time and provide some energy absorption. The slippage that did occur was not of a damaging nature and the main geometry and structural characteristics of the structure were apparently unchanged by the slippage, or any other effects. Slight permanent dimension changes occurred as a result of the nuclear shot but not to a scale that would have any significance to the accuracy of the theoretical or measured periods.

9.3 INTERPRETATION OF RESULTS - BY STRUCTURES.

9.3.1 STEEL ARCH STRUCTURES

Response to blast overpressures was in the compressive mode of vibration for the two steel arch structures. This assumption is based on the response of these structures to the high explosive detonations used in this test program, the theoretically predicted period for the compressive mode, the good repetition of results achieved with a variety of test loadings, and the measurement of similar periods with varied emplacement of the accelerometers. A deflection mode would have had a minimum of radial displacement or acceleration at the vertex while the compressive mode should have had roughly the same amplitude over the extent of the structural element.

The slight difference between the fundamental periods measured for the ribbed arch as compared to that for the unreinforced arch is another strong indication that the

compressive mode is that in which fundamental response was taking place. The theoretical variations in periods for the compressive mode of the two types of structures is due to the difference in the ratios between the mass of the effective soil plus the mass of the structural elements and the mass of the structural elements alone. As computed, using only the soil above the structure combined with the structure, the ratio for the unreinforced arch was 77.5, while that for the reinforced arch was 54.8. As the period varies with the square root of mass the variation that would be anticipated between the compressive periods for two structures would be 1.19 to 1, with the unreinforced structure having the slightly longer period.

In the flexural mode the period theoretically varies as the square root of the inverse of the moment of inertia. The ratio of the moment of inertia of the ribbed arch to that of the unreinforced arch was sixteen to one. The resultant ratio for the periods would be one to four, or one for the ribbed structure to 4.75, for the unreinforced structure, when the effective mass is taken into account in the manner done for the compressive mode. The measured periods varied by roughly 1.1 to 1, the unreinforced structure having the longer period, very close to the predicted variation for the compressive mode.

The theoretically computed periods were considerably shorter than those measured. It is believed that the major source of this difference is due to inaccuracy in the estimate of the amount of earth that should be assumed to act in conjunction with the structure vibrating in the compressive mode.

If it is assumed that the difference between theoretically computed and measured periods for the compressive mode is due to the amount of earth cover acting on the structure, that amount of earth which acted with the structure may be computed. A further assumption, that discontinuity at the ends of the structure may be neglected, is necessary for this analysis. The computation is made for the unreinforced structure, which had a measured period of sixty-nine milliseconds and a computed period for the compressive mode of forty-two milliseconds. A constant mass for the structural element is used. Initial theoretical computations (Paragraph 6.5) based on the mass of soil vertically above the structure provided an effective mass of soil to mass of structural elements ratio of 77.5 to 1. The theoretical period varies as the square root of this ratio and consequently a ratio, R, which would correspond to the measured period may be found by the expression:

$$\sqrt{R} = \frac{69}{42}$$

The resultant R is 2.7 to 1, which would indicate that a mass of soil acted with the structural element in the compressive mode that was 2.7 times the mass of the soil vertically above the structure.

A similar factor may be computed by use of the theoretical (35 ms) and measured (64 ms average) periods of the ribbed arch structure. With computations made as with the unreinforced structure a value of 3.34 to 1 is obtained for the ratio of the mass of soil that acted with the structural element in the compressive mode to the mass of soil vertically above the structure.

The above computations, for semi-circular structures at shallow depth of burial indicate that the assumptions made by theoretical approaches made use of an average of only thirty percent of the effective soil mass actually acting with the structures. In that the longer period that was actually measured should improve resistance to nuclear blast overpressures, any error in the theoretical assumption would be in the form of providing for overdesign rather than of a nature that would allow unsafe assumptions.

The absence of measured response in the much-longer-period, deflection mode is of special significance. Mode of failure of the arch structures as indicated by the results of this study would appear to be most probably buckling of the corrugated plates in compression. In such a situation the arch rib reinforcement would provide considerable additional strength to the structure even though it has but a nominal effect on the period in the compressive mode. Most economical use of materials would call for a deep corrugation in the curved plate and closely spaced arch supports with continuous or frequent attachment to the arch. An all welded structure with continuous welds between rib and plate and between lapped plates would be expected to be the most resistant to buckling. In a bolted or riveted structure some space between the rib and plate would allow for slippage in the plate connections, but would reduce the rigidity of the rib-plate connection. In any of the installations the foundation for the arch should be separate from the floor and should be designed to allow some yield under

the design overpressure, in effect increasing the amount of energy absorption and the response time of the structural system. The floor itself, if of concrete, should be scored to control and direct cracking which might occur with differential settlement or heave.

9.3.2 CIRCULAR STEEL CULVERT.

A conclusive interpretation of the results obtained by the testing on the circular steel structures does not appear to be justified. Comparison of the results with the theoretically computed periods, however, does provide some basis of analysis. Theoretical computations yielded periods of 9.4 ms and 10 ms for the compressive modes of the two structures tested. Average periods of 8.0 ms and 9.4 ms were measured for respective structures. A variation in depth of cover above the structures accounted for the difference in the theoretically computed periods. The structure with theoretical period of 9.4 ms was tested before and after flooding of the ground surface. With the exception of two rough measurements of 8 ms and 8.7 ms from runs made prior to flooding, the average period of 8.0 ms was measured from runs made while the ground surface was under a couple inches of water. All of the measurements of this period on this structure were made by the mechanically induced vibrations. The other structure, with 10 ms as the computed period of the compressive mode was only tested by explosive means. Principal structural response to the detonation was in some instances in a mode having an average period of 9.4 ms, in other runs in a mode having an average period of roughly 58 ms (Table 8.3). The

principal explosive response of the other culvert, based on one accelerometer trace from one run, was in a mode with period of 51 ms. Other modes measured by mechanical excitation of this other structure had periods of roughly five and two milliseconds. Rough approximations of these periods were measured from results of some of the explosive runs.

The compressive mode of vibration appears to have been excited by the mechanically induced vibrations. Results of the explosive detonations indicate that the same mode is one of the principal modes in which response to the blast overpressure took place. Comparison with theoretically predicted periods for the compressive mode indicate that little modification of the theoretical assumptions are justified. The theoretically computed periods for the flexural mode for the two circular steel structures (paragraph 6.6.2) were 167 and 178 ms. For similar but uncovered circular steel culvert the flexural period was computed as 27 ms. These theoretical periods indicate, but do not prove, that a flexural mode was excited and that the effective mass of the soil acting with the structure vibrating in this mode was less than the amount of soil vertically above the structure.

The other periods measured, on the order of five milliseconds and two milliseconds are of the order of magnitude of the compressive mode for the uncovered case. The period of this mode was computed (Paragraph 6.6.1) to be 1.5 ms. Results do not provide sufficient information to confirm the nature of the modes whose periods were measured, whether flexural,

compressive, or a longitudinal flexural action.

Interpretation for the purpose of improvement of structural design practice is similarly not furnished adequate results. In that principal response can occur in the compressive mode appears to have been confirmed. Strengthening of a circular steel structure for increased resistance to failure in such a mode would be of the nature described in Paragraph 9.3.1 for the steel arch structure.

Additional testing would be required to confirm that response did occur in a flexural mode. Resistance to failure in such a mode, however, would be increased by the same measures set forth for resistance to failure in the compressive mode. With the arch structures, failure in either the compressive mode or due to flexure tangential to the curved section occurs as buckling or failure of the joints between the plates. Failure due to flexure which is longitudinal, which might be the result of end effects, uneven loading, foundation failure, or some other cause would be most apt to occur as failure of the plates or joints between the plates. Ability to withstand longitudinal flexure without failure may be increased by either designing the structure for increased longitudinal flexibility or by providing longitudinal reinforcing structural members.

9.3.3 CATTLEPASS STRUCTURES.

The corrugated steel cattlepass structures were not analyzed theoretically due to the irregular shape, the variation in the radii of the segments of the structure, and the depth-to-span ratio, which was greater than one to one (Paragraph 6.5.1).

The results obtained from the testing reflect the irregularity of the shape and structural behavior in that definite modes were not obtained or separable, the nature of the action taking place was not discernible, and variation due to depth of cover or saturation of soil was not measurable.

The principal responses to the explosive detonations were in vibrations with periods in the range of twenty to thirty milliseconds. The response to the nuclear detonation, Priscilla, as determined from the records of Project 3.7, Plumbbob (Reference 22) was in one structure in a mode with a period of roughly twenty milliseconds, while in another, in modes with periods roughly twenty-four and five milliseconds.

The nuclear test records are from accelerometers mounted at mid height on the side of the structure. The sides of the cattlepass had a radius of curvature of nine feet four inches. A compressive mode based on this radius of curvature and on the rough approximation that the earth cover to structure mass ratio used for the circular steel structures could be used, would be in the range of twenty milliseconds. Establishment of the mode in which principal response does take place might be of assistance in designing increased resistance to overpressures. The singular geometry of the structure would require considerable planned use of the shape however, to justify additional testing of the structure. A significant factor though, is the approximation of the nuclear test response by the response to a couple pounds of dynamite placed so as to be entirely non-destructive.

9.3.4 CIRCULAR REINFORCED CONCRETE PIPE.

Some of the results obtained from the tests on the

circular concrete pipe were in close agreement with the theoretically computed period for the compressive mode. The principal period measured from records of mechanically induced vibrations was approximately 7.2 ms, compared to a period of 7.4 ms predicted by theory (Paragraph 6.6.1).

The principal response to the dynamite-produced overpressures appeared to have been in a mode of roughly twenty-eight milliseconds. The theoretical period for the flexural mode of the concrete culvert, without any effect of cover considered, was twenty-seven milliseconds (Paragraph 6.6.2). When the mass of earth vertically above the structure was assumed to act with the structure, a period of seventy milliseconds was computed.

A period of sixty-three milliseconds for the response to the explosive detonation was found for the structure which had undergone some cracking during the nuclear test. A principal period of forty-four milliseconds and two of twenty-eight milliseconds were measured from the traces of the three accelerometers employed in the structure which had undergone virtually no cracking.

These results indicate that the compressive mode was excited and measured, but that a flexural mode was predominant in the response of the structure to the blast overpressures. A circular reinforced concrete section is one of the most economical for providing great resistance to failure in a compressive mode. The predominance of a flexural mode in this structure as opposed to the apparent predominance of the compressive mode in the

circular steel structure seems incongruous. The value of using circular concrete sections would be considerably diminished if this is the usual situation for such structures. A more thorough study of the nature of response would thus be of value for design purposes.

9.3.5 CONCRETE DOME.

The reinforced concrete dome responded to the small high explosive detonations in periods which approximated those which were measured during the nuclear tests. Two distinct modes with periods approximately twenty-one and twenty-three milliseconds were measured from records of each run. Theoretical analysis (Paragraph 6.7) provided a period of twenty-two milliseconds. Method of selection of a value for the critical, modulus of elasticity however was not adequately set forth in the original report. As the period varies as the square root of the inverse of this modulus, and consequently is not sensitive to minor changes in elasticity, the value used was acceptable for the confirmation of the theory. Response measured during the nuclear test provided measurements of a time interval of forty-one milliseconds for two cycles of vibration obtained from two records. A third, poorer trace from the nuclear test indicated a time of fifty-seven milliseconds for three cycles. These records would indicate the presence of a mode with a period of roughly twenty milliseconds.

Theory is consequently substantiated by the test results of both the nuclear and high explosive detonations. An explanation in this report for the presence of two distinct

modes would be based on conjecture. The effect that the compressive mode of vibration of the ring foundation of the dome might have had is for a similar reason not determined. A rough approximation based on the mean radius and modulus of elasticity of the ring provide a period of approximately 0.015 seconds, without any effect of earth cover considered. Simple tests with dynamic measurements made on the dome and on the foundation might distinguish the source of the two modes measured in the run made for this report, which could be of value in furthering dome action theory.

9.3.6 UNDERGROUND GARAGE.

A theoretical approach was used to compute the fundamental period of the garage. The corresponding mode of vibration was assumed to be that which would occur when a uniform downward load was applied suddenly over the horizontal area of the structure. The period of vibration computed for this mode was forty-three milliseconds. The average of the measured periods of vibration produced by mechanical excitation was sixty milliseconds, while the principal nuclear detonation response had periods of seventy-five to eighty milliseconds.

These results are not in serious disagreement. Physical changes caused by the passage of time and erroneous assumptions would have been sufficient to cause these differences. Factors which may have added inaccuracy to the computation of the theoretical period were: failure to take into consideration an "elastic" response of the foundation acting upon the soil or the elasticity of the columns, inaccurate approximations

used in stiffness computations, variations of concrete elasticity from that assumed, and vibration in a mode other than that corresponding to an overall uniform downward loading.

Variation between the periods measured from the nuclear test records and those excited by use of the load column may have been due to some of the following factors: change in concrete elasticity and response characteristics of the soil in the two-year time interval, change in structural continuity from cracking or aging effects, and vibration in different modes due to the differences in excitation. A rough approximation may be readily made of the effect that just one factor might have had upon the computed period by use of single-degree-of-freedom analogy. A single-degree-of-freedom system has a period which is proportional to the square root of the static deflection of the mass when acted upon by a force equal to the weight of that mass. If the roof system is assumed to have a fundamental mode analogous to a single-degree-of-freedom case in that a static deflection which would correspond to the period of the fundamental may be used, an effect for the elasticity of the column may be included by using the additional deflection the columns allow under the weight of the roof system mass. The inclusions of the columns in the theoretical computation by this method resulted in a calculated period of forty-nine milliseconds.

It is reasonable to assume that the fundamental mode of shock response (the shock-induced mode of vibration having the largest amplitude) is that in which the displacement of the entire roof at any time during vibration in that mode is

simultaneously above or below the static configuration. Such a mode would be excited by a uniform, unidirectional load suddenly applied to (or released from) the slab. There are other possible modes of vibration having periods of the same order of magnitude as the one described above. One of these is of such a form that it could have been the principal mode initially excited by the passing shock wave. In this mode, vibration in adjacent rows of panels is in opposite directions at any one time. A loading which typifies this mode would be that of a uniform load applied downward on the first row of panels, upward on the second row, downward of third row, and so on. Another possible mode of vibration would be that in which vertical vibrations in adjacent panels are in opposite directions, in checkerboard fashion. If a uniform forcing load were applied, one color on the checkerboard would represent a downward application, while the other color an upward application of the load.

The nuclear test possibly induced vibration in a horizontal mode. With such a mode, vibration of the earth and roof slab mass would be resisted by the side walls, the columns and end walls acting as beams, and the surrounding soil. This mode would be in the form of horizontal vibration of the roof system, forced by ground shock or the transmitted air-shock pressure acting on a wall of the structure, with some additional lateral forcing caused by drag of the shock front passing over the structure.

The deflection records made during the nuclear test

were all of a long base displacement type which employed wires which ran diagonally from the base of columns to the roof slab. The wires were all at an angle of less than forty-five degrees from horizontal, and consequently those which had a component in the direction of a radius from Ground Zero would produce records seriously affected by any horizontal mode of vibration. This horizontal mode should not have been induced by the load column excitation used in the non-destructive test program, however. Similarly, the accelerometers were used at such an orientation that any horizontal vibration would not have been measured.

The modes in which the structure vibrated were to have been determined in the nuclear test (Shot Priscilla). Deflection gages were placed in one bay to provide the required measurements. The gages were mounted in groups of three at the base of the four columns. The pickup wires were attached to the roof slab at the center of the bay and at midpoints between the four columns. These hookups together with a reference gage would have been sufficient to determine the horizontal and vertical motion of all these points (Reference 24). Unfortunately this array made each record dependent upon at least two others. If strategic records were lost, others would become essentially useless for positive identification of the actions which took place. This is what occurred. The use of independently acting accelerometers or seismographs apparently would have been desirable.

The period measured by the non-destructive testing,

approximately sixty milliseconds, would have a quarter wave length approximately equal to the time required for the shock wave of the nuclear detonation to traverse the distance between column lines (29 feet). A period of similar magnitude for the mode of vibration in which adjacent rows of panels move in opposite directions might permit a large response in that mode. It would be conceivable that potential energy due to an induced upward motion of the slab prior to the arrival of the shock wave at that slab would create a potential energy which would add to the maximum downward deflection of the slab under the advancing shock overpressure. This response was not observed in the dynamic deflection records of the nuclear detonation, however. The principal vibrations measured in the non-destructive testing were the same for point load release at the center of the slab, at the midpoint of the slab between columns in one row, and at a point midway between these two. These results would indicate that the fundamental mode is that in which the vibratory motion is in the same direction at any given time over the entire roof slab.

The design procedures for predicting the flat slab response appear to have been confirmed. This was done by calculating a reasonable period using currently accepted methods. Although this period was conservative by being shorter than those measured, the difference was not significant. The only disadvantages encountered were cumbersome calculations. A value equally as accurate may have been obtainable from simplified expressions. These observations suggest that the current

theoretical approach could be changed to provide closer agreement of experiment and theory. Another possibility would be the use of shorter calculations to provide a theoretical period as realistic as that obtained from present theory.

9.4 INTERPRETATION OF DAMPING MEASUREMENTS.

It was practical to measure vibration damping from some of the traces of the cattlepass and circular steel culverts. The vibration traces of the other underground structures were for the most part of too small an amplitude or of such irregularity that a reasonable determination of the rate of decay was impractical. In the records made from runs on the aboveground dome, the presence of two modes of the same magnitude and with closely similar frequencies resulted in a beat, which made separation of modes difficult and measurement of damping practically impossible.

The effect of damping on traces from the steel structures was measured by plotting on semi-logarithmic graphs the amplitudes of the decaying vibrations. The slope of the most representative line provided the means of computing the logarithmic decrement, δ . The value of δ is that of the natural logarithm of the ratio in amplitude of successive vibrations. As an example, a mode with $\delta = \ln 1.25$ has the amplitude of each cycle approximately 1.25 times the amplitude of the successive cycle. The value is only approximate for the peaks of the vibrations as the actual measurement is to the point of tangency of the trace with the envelope of the decaying vibration, a close approximation to the peak for situations in which damping

is much less than critical.

Measurements made from different traces showed a generally close agreement in the amount of damping. Significant exceptions to this were the damping measurements made on the explosive runs, in which the decay occurred at a greater rate. The average results from the mechanical excitation runs were $\delta_{\text{equal}} \ln 1.25$ for the circular steel culvert and $\delta_{\text{equal}} \ln 1.26$ for the cattlepass structures. One measurement of $\delta_{\text{equal}} \ln 1.45$ was made from an explosive run on the circular steel and measurements of $\delta_{\text{equal}} \ln 1.70$ and $\ln 2.15$ were made from one explosive run on a cattlepass culvert.

No significant variation in δ was noted between runs made on the cattlepass structures at different depths of burial, between the traces from accelerometers at different positions, or between runs made with different mechanical excitation schemes. This lack of variation in δ , the similarity between the damping of the circular steel culvert and cattlepass, and the lack of confirmation from the explosive tests cause the measured damping results to appear more as an effect peculiar to the corrugated steel plate than as a characteristic of the soil cover. A more comprehensive study of the damping could be made by the use of more explosive runs per structure, allowing a closer identification and consequently a better separation of the modes of vibration. Thus, no conclusions based on the damping measurements made appear to be justified.

9.5 DISCUSSION OF TEST PROCEDURES.

A review of the results obtained from each of the two

principal means of exciting the vibrations reveals that the use of small explosive charges provided consistently usable traces while the value of the mechanical excitation varied with the stiffness of the structure. Mechanical excitation proved quite usable with the larger structures, as the steel arches and the concrete garage. With the smaller and stiffer structures mechanical excitation provided traces which generally did not give a good correlation with the results obtained from the explosive runs.

The procedures used proved to be satisfactory for obtaining the majority of the information sought. The mechanical means of excitation for purpose of vibration measurement was suitable for use on above ground and the large underground structures. If necessary much larger forces than those used in this project could be employed in creating an initial deflection and still not exceed the elastic limits of the structural members. The use of explosives is not always practical for vibration of existing structures, but it did provide the most worthwhile results on the buried culverts and a close approximation of the nature of the nuclear blast overpressure on the structures with which used. The explosive results thus are more readily accepted for making estimates of the nature of nuclear blast response, and should be obtained when practical.

9.6 DISCUSSION OF FOAM CUSHIONING.

Increased ability to withstand nuclear shock overpressures by use of a plastic foam cushioning was not proved feasible for flat roofed structures (Appendix II). The opposite effect,

that of causing structures to fail under overpressures which might be withstood without the presence of shock isolation was indicated as being a probability. The blast overpressure acting on the mass of earth supported by the foam could transmit considerable energy into the system with the foam acting as spring, and then have this energy applied to the structure as a sharp impact when the compression of the foam reached the limiting thickness. The use of foam plastic to increase the period of response of the structural system was consequently discarded as a means of increasing the ability of a flat-roofed buried structure to resist blast overpressures.

The use of plastic foam to achieve such increased resistance to damage does appear to have potential for arch-type structures, through a detailed theoretical analysis of such use was not made a portion of this project. The action by which a foam plastic layer over an arch structure may provide increased ability to withstand shock overpressure is of a different nature than that for a flat-roofed structure. The foam plastic upon which the theoretical work has been based is the family of polyurethane rigid and flexible foams. The resistance of certain of these foams is such that a relatively large load may be supported with a deflection of ten to fifteen percent of the thickness. Little increase in load is then required to cause a deflection of sixty to seventy percent of the original thickness. Beyond this the rate of increased load per increased deflection rises rapidly, as the voids in the material are closed. With such action, a blanket of the

foam could be designed such that the dead weight of the soil would cause deflection to approximately the "yield" point. The foam would then permit a relatively large strain to take place in the soil without a large increase in load upon the structure. By permitting motion inward of the soil cover of the arch a large tangential stress could be developed in the soil. This arching action would be much greater than in the case of a structure without isolation where the reduction of the perimeter and consequently the development of a large tangential stress adjacent the structure is severely limited. Radial strain in the soil and yielding of such a structure do permit some arching in the soil not in contact with the structure but not to the extent that the use of foam apparently would allow.

The stress-strain characteristics of open cell polyurethane foam as described were for static loading conditions. Under impact, as from nuclear shock overpressures, the static characteristics of the foam would be augmented principally by the characteristics of compressed gas, due to the air trapped within the cells of the foam. The use of holes bored into the foam at an adequate spacing to provide a short mean path for gas escape might allow the static characteristics to be approximated under sudden loading conditions. With such application the gas would have to evacuate into the structure or at least to a dead space within the structure. The foam would require an impermeable membrane between it and the soil, which would however be necessary for weathering protection in any case.

The above discussion is based upon a brief examination of

probable action of soil and the plastic foam and has not been analyzed in detail by theoretical or experimental means. The potential of foam protection of buried arches is possibly quite large. A theoretical study to determine the amount of increased ability to withstand shock overpressure that could be achieved might be based on ideal characteristics of the foam (as was used in the study of the flat-roofed situation, Appendix II), and idealized backfill and structural response. Experimental work in approximating ideal foam characteristics under dynamic loads and measurement of load relief by arching on models under static uniform loading might justify full-scale work. Existing underground structures at the Nevada Test Site could be exposed to large overpressures from aboveground high explosive detonations in their present condition and then tested again with the structure modified by a foam cover and vents, and the soil replaced.

Tests with a blast simulator or with shock transmitted directly from a buried detonation might provide similar experimental verification of the ability of plastic foam to provide an increase in an arch structure of its shock overpressure capacity.

CHAPTER 10

CONCLUSIONS AND RECOMMENDATIONS

10.1 BASIS.

The conclusions presented are based on the results of many similar tests made on a limited number of structures. The structures did not provide a spectrum of the variations of stiffness, material, shape, and depth of burial that occur with underground construction. Instead, results are concentrated on specific shapes and construction materials, and with certain depths of cover. However, the results are primarily for structures in basic geometric shapes, constructed of materials representative of underground construction, and covered by backfill placed under highly controlled conditions.

10.2 APPLICATION OF UNDERGROUND VIBRATION THEORY.

Results partly verified certain of the underground vibration theories used for prediction of period. Revision of theory, or more extensive tests on the structures, was suggested by other results, depending on the structure or the construction material.

The theory for estimating the fundamental period of a circular section buried at a depth approximately equal the diameter gave periods which were very close to those measured in the sections of both concrete and steel construction. The compressive mode was apparently the principal mode excited by the high explosive overpressure in the circular steel structure and it was one of the principal modes so excited in the concrete

culvert in the high explosive tests. The presence of a flexural mode of large amplitude was indicated by the high explosive tests on the concrete culvert. The effectiveness of earth cover in increasing the responding mass as assumed by the theory, that the soil vertically above the structure could be assumed to act with the structure, was apparently confirmed as valid for the compressive mode computation of the structures as situated.

Theory was not readily adaptable to the cattlepass culverts nor were clear results obtained from the tests on these structures. Of significance was the absence of any variation in results from structures with 5, 7-1/2, and 10 feet of cover. A rough correlation between the period measured and that recorded from the nuclear test was obtained. The data was not sufficient to permit identification of the mode of the response.

Measured periods of the steel arch structures were for the compressive mode and indicated that a mass of soil acted with the structure that was three or more times the mass of soil assumed to be effective by the theory. A mass equal to that of the soil vertically above the structure was that used by the theory. Though the span of the structures were over twenty-four feet and there was only five feet of soil cover above the vertex, no flexural modes were apparently excited by either explosive or mechanical means. Mechanical excitations were such that initial deflections were imposed in the structures

which should have closely approximated the deflection configuration of the fundamental flexural modes.

Adaptation of the theories presented was required for analysis of the underground garage. A theoretically derived fundamental period of forty-three milliseconds was roughly approximated by the average measured period of sixty milliseconds, and the average period of roughly seventy-five milliseconds computed from records of the nuclear test. The theoretically assumed modal shape for blast response was apparently verified by nuclear and mechanically excited vibrations. Though not accurate, the period derived from theory would have the effect of providing only a slight additional factor of safety in design.

10.3 DOME RESPONSE.

The three high explosive tests run on the aboveground concrete dome provided little additional information for supplementing the original nuclear test reports (References 21 and 23). Periods of vibration were measured which closely corresponded to harmonic portions of the nuclear test records and to the theoretically predicted period of response. Significant but not lending to ready interpretation was the presence of two modes of the same order magnitude and of only slightly different frequency. This condition would present a possibility that the two modes might permit a greatly increased response to sudden application of overpressure than would be the case with a single dominant principal mode. The source of two modes might have been due to vibration of the circular foundation, discontinuities in the structure, or other causes not discussed; but the possible

effect on response would indicate that a good reason exists for a determination of the cause.

10.4 STEEL VERSUS CONCRETE FOR UNDERGROUND STRUCTURES.

The results obtained in both the non-destructive testing and from the Hardtack II nuclear series indicated that steel plate rather than the reinforced concrete was more apt to provide a usable structure following a nuclear shock. The continuity of structure provided by connected corrugated or stamped steel plates allows large deflection or yielding to occur without destroying the usefulness of the structure. Principal response of the concrete culvert was in either a flexural or a compressive mode. Increased reinforcement for a flexural mode would be principally in the form of increasing the steel in the inner and outer cages, and for the compressive mode of increasing the thickness of the concrete. As all the principal vibrations of the steel structures measured by the non-destructive testing appeared to have been in the compressive mode, the form of response and failure from nuclear shock could be more readily predicted. As a result, reinforcement for increased protection could be more efficiently designed than for a similar concrete structure. These conclusions would combine with the advantages of transportability and construction of steel shapes to indicate that they form the optimum arch shelter material. Two factors, not evaluated but of considerable importance in the selection of material are: one, that a concrete arch section is at its greatest efficiency when under compressive loading and two, that the effect upon the concrete

section of a tensile rebound in the compressive mode is not known nor has the possible magnitude of such rebound been discussed. The existence of these factors indicate a possible direction of study for future theoretical or test projects.

10.5 USE OF NON-DESTRUCTIVE TESTING.

Tests of structures to determine the principal mode of response and the effect of earth cover may be readily performed by non-destructive means. With structures of smaller span (ten feet) and earth cover, small high explosive charges (one pound) above the surface provide measurable vibration. Larger structures may be adequately vibrated by simple mechanical means. Such testing is of value principally to determine the mode in which principal response takes place and consequently the form in which failure would be most apt to occur. Determination of the period of vibration allows the use of theoretical response prediction procedures and provides an evaluation of the benefits to be obtained from increased depth of cover.

10.6 PLASTIC FOAM CUSHIONING.

Underground arch structures in soil may be provided a considerable increase in ability to withstand nuclear shock by use of a plastic foam cushioning. Such an increase would be principally due to an increased arching effect in the soil. Neither tests nor theory have been conducted to an extent that would allow evaluation of magnitude of possible increased resistance.

Flat-roofed structures at shallow depth of burial are likely to have their ability to withstand shock overpressure

reduced by a foam shock-isolation media. In fact, theoretical approaches indicated that the plastic foam could impart pressures to the structures as high as an order of magnitude above the peak surface overpressures. Further investigation of such application of shock isolation was consequently suspended.

10.7 CONFIRMATION, CONTINUATION, AND RELATED APPLICATIONS.

The principal results obtained, those of the nature of the mode of principal response and the effectiveness of soil cover, were for a small sample of underground construction. Insufficient high amplitude results were obtained for damping estimations. Definition of the nature of higher than fundamental frequencies measured was not practical from the test sampling. Response to widely varying peak shock overpressures was not measured. Accelerations occurring in the soil adjacent and at varying ranges from the structures were not obtained, though such information would be of value for a comprehensive study of the nature of shock response. These factors, which narrow the scope of the results, indicate worthwhile extensions of the project testing. The rapidity and mobility of the testing methods employed by this project would permit a compilation of results with large size of sample.

Underground response theory could be evaluated in wide scope by non-destructive vibration testing of existing underground protective and civil construction.

A similar use, in that prediction of blast response could be made, would involve the use of high sensitivity equipment as used in this project for measurement of the lateral mode of vibration of bridges. In that model studies

do not provide the effects of friction and working of joints in the actual structure, and in that the forces of moving traffic or wind should excite the lateral mode sufficiently for measurement, a great mass of data could be obtained where little exists at present. The measurement of accelerations in vertical and horizontal components at various locations on the bridge would provide sufficient definition of mode that data could be collected simultaneously on vertical and transverse vibrations. A spectrum of data acquired by such means from bridges of varying types and span lengths would give design criteria for adequate lateral end anchorages and efficient location of reinforcement. Adequate anchorages would be those that allow the ability of the bridge to withstand lateral shock loadings to be determined by structural considerations rather than the more readily strengthened bearing conditions.

Structures of blast resistant design left essentially undamaged by the nuclear testing at the Nevada Test Site provide a broader representation of shape and construction of such design as would supplement results obtained from the structures tested by this project. Other uses for the non-destructive vibration testing would be for civil structures subject to transient or continuous dynamic loadings of traffic or machinery impact, wind, or wave.

APPENDIX I
VIBRATION MEASUREMENT ON EXISTING
STRUCTURES FEASIBILITY STUDY

I.1 INTRODUCTION

I.1.1 OBJECTIVE

The objective of this sub-project was to establish practical procedures for the determination of the major vibration characteristics of existing structures by non-damaging testing.

I.1.2 BACKGROUND

Vibration characteristics of main structural elements are important parameters in the determination of response to blast and shock loadings, design for resistance to the effects of nuclear weapons, and in certain non-defense applications such as analysis of response to bridge loadings or the vibrations of heavy machinery. In the case of structures subjected to loads in the typical blast overpressure decay curves, oscillatory motion is not the prime concern. In this situation the maximum response to the positive phase is generally critical, in that subsequent decaying vibrations are not likely to cause collapse should the structure withstand the initial displacement. The major factors in determining the initial and consequently maximum response are the mass of the structure and material being displaced, the stiffness of the structure, and the nature of the structural resistance to increasing load. Blast side-on overpressure has in itself no momentum; energy is thus imparted to the structural system by the pressure acting over a

finite displacement of the system. The mass and the stiffness are the principle factors determining the acceleration and, consequently, the distance through which the overpressure acts as it decays. The effective mass concerned and to a lesser extent the stiffness are difficult to measure on an in-place structure, particularly if the structure is buried. The stiffness and mass, however, determine the period of vibration of the structure and thus may be studied through analysis of the vibration characteristics.

Theoretical approaches have been presented for making approximations of the fundamental periods of response for various types of structures and structural elements. These theories have had a minimum of confirmation by tests on existing structures. Tests of underground structures for determining the variation in vibration characteristics as caused by differing weight and character of the soil overburden are non-existent. Proof of the validity or a revision, if indicated, of the theoretical approaches would be beneficial in allowing more efficient design and more confidence in the completed structures, and may provide the foundation for extrapolation of tests results to situations in rock.

I.1.3 THEORY

This sub-project was based on the concept that natural modes of vibration of a structure or element are independent of the means of excitation, or amplitude of vibration, insomuch as the mass remains unchanged and the structural elements remain elastic. Providing the measurement is made with sufficient accuracy and

sensitivity, a very small amplitude may be used and consequently the exciting force used need be only a relatively small fraction of the safe working load of the structures. An instrument which would provide a continuous record of velocity, displacement, strain, or acceleration could be used to analyze the vibrations and permit the calculation of several of the principal harmonics from one test. Placement of the exciting force in various positions could then be utilized to increase the amplitude of certain modes with respect to those of other harmonics and thereby permit easier interpretation and correlation of the results. The sub-project became one of determining whether the accuracy and sensitivity of available equipment would permit the measurement of the principal harmonics for various types of structures possessing a wide range of stiffness.

I.2 PROCEDURE

The procedure used to verify the assumption that harmonic analysis could readily be made on structural elements in place was to give structures an initial deflection which could be suddenly released. Structural members tested were: a simple steel beam, a massive one-way concrete slab, and corrugated steel culvert pipe. The testing procedures on these structural elements were as follows:

I.2.1 SIMPLE STEEL BEAM

A twenty-two and one-half foot, sixteen inch deep, forty-pound-per-foot wide flange section was selected for the test. The beam is a component of a continuous roof support system, shown in Figure I.2.1. The beam was selected as being a close approximation

of a simply supported beam, as the riveted butt joints at the ends of the beam are of a nature that end rotation due to the excited vibrations can take place within the slack of the connection. The roof load is transmitted through five bearing points to the beam, which essentially forms five concentrated masses for the purpose of theoretical vibration analysis. The initial deflection for the test was provided by suspending a weight of sixteen hundred pounds of lead from the beam. Vibrations were excited by suddenly releasing the load, in the tests on this beam, by means of a bomb release mounted as shown in Figure I.2.1. Three different loadings were used for the tests: the load divided and equally applied to the third points and the load concentrated at a quarter point and at a fifth point. The different loadings were used to vary the relative amplitude of different modes of vibration. Measurement of the vibrations was made by use of SR-4 strain gages on the lower flange at center and by mounting a Wianco ten-G range (322 ft/sec^2) accelerometer to the beam at various locations (Figure I.2.2). It was found that the strain gages were not sufficiently sensitive to adequately pick up the small amplitude of motion taking place. The accelerometer however provided a clear record of the motions and was used in five different combinations of accelerometer and loading positions.

TABLE I.2.1 - STEEL BEAM LOAD AND ACCELEROMETER POSITIONS

<u>Run</u>	<u>Loading Scheme</u>	<u>Accelerometer Location</u>	<u>Film Speed</u> (Inches/Second)
1	Symmetrical, 800# at Each Third Point	Flange, Mid Length	50
2	(")	(")	5
3	(")	Flange, Third Point	50
4	(")	(")	5
5	1600# at One Quarter Point	Flange, Point of Loading	50
6	(")	(")	5
7	First Panel Point	Flange, Point of Loading	50
8	(")	(")	5
9	(")	Flange, Mid Length	50
10	(")	(")	5

The procedure used, in which the load was applied to the beam by the use of turnbuckles which were used to change the geometry of the cables, proved to be practical and relatively quick (Figure I.2.1). Changing loading positions was made cumbersome by the use of weights to provide the deflection. The method did allow the amount of load applied to be accurately determined and consequently there was no danger of overloading the structure. The load selected was designed to give a maximum amplitude of vibration with a maximum acceleration under one G. One G was used as a limiting acceleration to avoid discontinuity or separation of the mass (roof system) and the supporting beam. The test on the steel beam showed that for field testing the use of weight in the amount employed and the suspended loading was impractical. The mounting of the weight

could be somewhat simplified by using a wheeled cart and the lifting could be done by chain hoist, but the problem of suspending the load from the structural member is apt to cause considerable difficulty, as would be the case with reinforced concrete, or buildings with suspended ceilings.

I.2.2 MASSIVE ONE-WAY SLAB.

A massive concrete magazine, part of a concrete gun emplacement (Figure I.2.3) was selected as having a stiffness greater than that of any concrete member likely to require vibration analysis. Vibrations induced in such an installation would thus form a proof of the applicability of the method to concrete structures. The slab forming the roof of the magazine is seven feet thick, reinforced across the nine-foot wide room as a one-way slab with nine-inch-deep, twenty-one-pound-per-foot I-beams on two-foot centers. The room itself was fifteen by nine by six and a half feet high. The installation of the loading column, piezoelectric accelerometer, and strain gage mountings (under the protective rubber wrappings) are illustrated in Figure I.2.4. The drain pit was utilized for placement solely to avoid cutting the loading column, which had been fabricated prior to selection of the test site.

Test procedure was to position the column, take the zero strain reading, then load the column by the screwjack to the desired load. The high amplification used on the signal from the piezoelectric accelerometer allowed considerable noise. The Sanborn direct-recording device used allows continuous inspection

of the gage signal and consequently permitted load release to be made at a time of minimum noise. The release device permits sufficient slack in the chain that the upward force is completely removed. The nature of the device is such that the load is removed within two and a half milliseconds, which time constituted rapid release in that the modes of vibration under study were excited. A total of six runs were made using different amplification and attenuation settings on the accelerometer signal. The system proved completely workable and was set up and operated by two men. The tests indicated that a guy system which would hold the column upright upon load release would be useful for operations in which the column was employed with a longer extension. The tests also showed that if the hook would retain the chain after release, which still allows complete load release, a considerable saving in minimum time between runs could be achieved.

Tests were run independently on the column to determine load release time and to calibrate the mounted SR-4 strain gages (Figure I.2.5). A load cell was installed on the column for the purpose of calibrating the strain gages, but its use on the moving member of the assembly during structures tests is considered to be too cumbersome. Characteristic load release measured is shown in Figure I.2.6.

The adjustable column as described gives very satisfactory results, enables application of a measured loading to a structure in a minimal amount of time, and permits rapid setup for repeated testing.

I.2.3 CORRUGATED-STEEL CULVERT PIPE

Corrugated-steel culvert pipe provided a sample in small scale which was very similar in material and shape to one of the most important types of blast resistant structures. Extensive testing was done on such pipe as it was readily available for both laboratory and field tests and variation due to placement circumstance could be measured. The pipe tested was 3/32-inch thick galvanized steel, four feet in diameter, riveted to form an integral perimeter. One ten-foot long section was tested in the field with the axis horizontal. Vibrations were induced by pre-loading into a desired shape by means of 3/16-inch wire rope and turnbuckles, as shown in Figure I.2.7 and then releasing the tension by use of a quick release device similar to that used on the loading column previously described. Vibration measurements were made with a Wiancko ten-G range accelerometer mounted inside the culvert close to the cable attachment point common to the different loading schemes. Three deflection modes were used in an effort to excite all the main harmonics. Measurements were dynamically recorded by the Mobile Blast Laboratory on Consolidated three-KC carrier light-recording equipment. This equipment permits continuous visual inspection of the galvanometer deflection due to the gage signal and consequently enabled sensitivity settings to be selected such that maximum readability of record could be achieved.

Laboratory vibration tests were made on a thirty-inch-long section of similar four-foot diameter corrugated-steel pipe. Loadings used were the same as those described above, with the axis of the

pipe horizontal as with the ten-foot section, and also with the axis vertical. In addition, the pipe was tested with the axis vertical with a circumferential application of the force as shown in Figure I.2.8, in an effort to induce measurable "hoop" vibrations. Mode of vibration for "hoop" vibrations may be described as having no tangential flexure, vibration occurring as variation between tension and compression with the radius uniformly expanding and contracting. Measurement of vibrations was made by use of piezo and Wiancko accelerometers and SR-4 strain gages applied tangential to the perimeter as in Figure I.2.9. Measurements were recorded on the Sanborn unit and by the Mobile Blast Laboratory. The loading systems were easily installed and allowed rapid re-testing and change of loading scheme. The systems used however, permitted large variations in the applied loadings with consequent danger of overloading the equipment and variation in the amplitude of the vibrations. Systems which would incorporate load measurement devices as does the loading column would be desirable for use in such testing. Aside from the lack of load measurement, the equipment proved very satisfactory for the tests performed.

I.3 RESULTS

I.3.1 DATA SOUGHT

Records obtained were used for measurement and identification of the periods of the principal modes of vibration. Arrival at general equations of vibratory motion for the structures tested was not attempted as being beyond the scope of this project. The

nature of records made, direct or mirrored-light recordings of galvanometer deflections, was such that visual analysis of periods could be readily made but no automatic translation of data for the digital computer was possible. Analysis with the object of arriving at equations of motion by measurement and visual interpretation for multi-degree of freedom systems such as those studied is difficult, and consequently such analysis requires digitizing and harmonic analysis by computer to be practical.

I.3.2 ANALYTICAL PROCEDURE

Recordings of accelerometer and strain signals were analyzed by direct visual interpretation. Each run, the result of the release of the imposed deflection, was individually examined. Measurement was made of all periods that could be separated. Grouping of the periods computed for a structure provided the means of identification by harmonic and allowed averaging of several readings. An illustration of the analysis of a recording is given by Figure I.3.1. The procedure outlined above provided relatively accurate determination of period for as many as the first five modes of vibration, depending on the stiffness of the structure and the sensitivity of the instruments employed.

I.3.3 MEASURED STRUCTURAL RESPONSES.

I.3.3.1 Simple Steel Beam - Examination of the records of ten separate tests on the beam provides several well defined groupings of period. Tabulated (Table I.3.1), these permit designation by mode and averaging of the calculations for all the runs in which that period could be readily calculated. Fluctuations

in reading is due in large measure to inaccuracy in separating those modes comprising the signal, resulting in missing or adding a cycle in the time increment studies. As separate modes predominate at different times and are amplified or reduced due to imposed deflection employed, the problem of interpretation was not difficult and fairly accurate cycle counts were possible. This may be seen by the close similarity of many of the readings from different runs. For some runs the same mode could be readily identified and followed for two different increments of record separated by a zone in which other modes caused the trace to be uninterpretable. The periods and the corresponding frequencies as computed from analysis of the records are as listed in Table I.3.1.

I.3.3.2 Massive One-Way Slab - Records of six runs were recorded for the vibrations due to the point loading described in the previous chapter. The runs were made with approximately the same initial deflection in the slab but at different settings of amplification, attenuation, and sensitivity on the instruments. The sensitivity and maximum recordable frequency on the Sanborn recording unit used is less than that of the Consolidated Equipment of the Mobile Blast Laboratory resulting in reduction in the amount of analysis feasible. As the test was intended as a proof that vibrations could be excited and measured, the equipment was adequate. Measurable vibrations were induced, a period of approximately four hundredths of a second appearing as the fundamental. As there were only two runs on which the various settings gave an optimum gage record as opposed to instrument noise, there was insufficient

confirmation data for designation and measurement of higher modes. In that the vibrations were induced and gave a record the proof test was considered as being successful. Use of the more sensitive recording equipment however, was indicated as being advisable for a more comprehensive test.

I.3.3.3 Corrugated-Steel Culvert Pipe - Records of induced vibrations were made of sixty-two runs for four-foot-diameter steel culvert-type pipe. Six runs were made on a ten-foot section in the field, employing three types of loading. The remainder of the runs were made on a thirty-inch-long section in the laboratory at different orientations, with various types of measurement devices and loading schemes, some runs recorded on the Sanborn machine and the remainder on the Consolidated equipment in the Mobile Blast Laboratory. Results of the tests are as tabulated in Tables I.3.2, I.3.3, and I.3.4. The results show the feasibility of obtaining the natural vibration characteristics from such loading means. Of particular interest is the obtaining of the period for the "hoop" vibrations. The period for such vibrations for an unloaded structure is generally computed as the circumference of a full circle of the radius of the arch divided by the sound velocity of the material. For the two-foot-radius steel section this period is computed to be slightly less than 0.77 milliseconds, assuming a sound velocity in the steel of 16,400 feet per second. Records made from four-point and circumferential loading tests provide an average period of approximately 0.80 milliseconds for the "hoop" vibration. As the radius for corrugated metal is indistinct and the sound

velocity in the steel employed is not exact it is considered that very close agreement was obtained. For larger radius structures and structures with lower sound velocity or with an applied mass, the "hoop" mode should become more readily and accurately measured. The tests showed that multi-point loading would be sufficient to excite the vibrations, the circumferential loading device being impractical for use on most existing structures. The accelerometer remains the most sensitive measuring device though the applied SR-4 strain gages were useful in identifying the hoop mode.

I.4 CONCLUSIONS

Simple harmonic measurements can be readily made on in-place structural elements by testing which is not damaging, unsafe, or overly involved. Principal requirement for satisfactory testing is sensitive measuring and recording equipment. Application of sufficient initial deflection to provide measurable vibrations may be made by inexpensive and readily portable equipment. Accuracy in measurement of periods by visual examination of records is improved by making multiple runs, varying applied deflection, and using different sensitivity settings in recording. This permits averaging from a larger sample, easier separation by modes, and measurement of vibrations which occur at wide ranges of amplitude.

Use of a computer is recommended for analysis when complex equations of the vibratory motion are desired. Data for such use should be recorded on magnetic tape so that digitizing may be done directly from the record for use in the computer. Concurrent

direct recording during the test would be desirable to insure collection of data as desired and for partial confirmation of computer results. Cases in which only an approximate fundamental period is desired may be instrumented with greater simplicity than those illustrated in this report, possibly even by the use of a reed gage.

The tests described, in showing that the basic modes of vibration are excited and are measurable at wide ranges of amplitude and character of the deflection device, confirmed the premise on which this sub-project was based. In addition, the various tests allowed the formulation of procedures and basic designs for equipment which would adequately, safely, and quickly accomplish such testing. The objective of the sub-project consequently was satisfactorily achieved.

170

CONCLUSION: Approximate Periods	FUNDAMENTAL	T^I	= 0.15	Seconds	(6.7 C.P.S.)
and Corresponding	2d Mode	T^{II}	= 0.052	"	(19 C.P.S.)
Frequencies	3d "	T^{III}	= 0.015	"	(67 C.P.S.)
	4th "	T^{IV}	= 0.0042	"	(240 C.P.S.)

TABLE I.3.2 - CORRUGATED-STEEL PIPE TEN-FOOT SECTION - ANALYSIS SUMMARY

MEASURED PERIODS

<u>Run</u>	<u>Loading</u>	<u>Measured Periods</u>			
1	Two-Point	.0650	.0076		
2	(")	.0642	.0148	.0076	.0033 .00318
3	Three-Point		.0146		.0034
4	(" .)	.0640	.0147		.0033
5	Four-Point	.062		.0075 .0075	.0046 .0045 .0047
6	(")	.064			

APPROXIMATE PERIODS AND THEIR
CORRESPONDING FREQUENCIES

T^I	=	.064	Secs (15.6 C.P.S.)
T^{II}	=	.0147	Secs (68 C.P.S.)
T^{III}	=	.0075	Secs (133 C.P.S.)
T^{IV}	=	.0046	Secs (218 C.P.S.)
T^V	=	.0033	Secs (300 C.P.S.)

TABLE I.3.3 - CORRUGATED-STEEL PIPE THIRTY-INCH SECTION -
SANBORN UNIT RECORDS SUMMARY.

MEASURED PERIODS (Piezoelectric Accelerometers)

<u>RUN</u>	<u>ORIENTATION</u>	<u>LOADING</u>	<u>PERIODS MEASURED (Seconds)</u>	
2-2	Axis Horiz ^{1.}	Two-Point	.0812	
			.0813	
2-6	(")	(")	.0815	
2-7	(")	(")	.0812	
			.0813	
3-1	(")	(")	.0812	
3-2	(")	(")	.0816	.024
4-1	(")	(")	.082	.0443
				.0435
H-1	Axis Vert. ^{2.}	Concentric	.0483	.015
H-3	(")	(")	.0467	
			.0477	
H-4	(")	(")		.00781
				.00777
				.0078
H-5	(")	(")	.051	
			.051	

1. Pipe Resting on Wood Pallet

2. Pipe Resting on Concrete Floor

Approximate Periods with Their
Corresponding Frequencies

T ^I	=	.0813	(12.3 C.P.S.)
T ^{II}	=	.048	(21 C.P.S.)
T ^{III}	=	.02 (Rough)	(50 C.P.S.)
T ^{IV}	=	.0078	(128 C.P.S.)

TABLE I.3.4 - CORRUGATED-STEEL PIPE THIRTY-INCH SECTION
CONSOLIDATED UNIT RECORDS PARTIAL SUMMARY

MEASURED PERIODS (SR-4) STRAIN AND WIANCKO ACCELEROMETERS
Axis Vertical, Three-Point Suspension (Figure 2.13)

<u>RUN</u>	<u>LOADING</u>	<u>EXCITATION</u>	<u>MEASURED-PERIODS (Seconds)</u>			
				.01475		
1	None	Ctr Struck		.01477		
3	None	Rim Struck	.0472			
9	None	Ctr Struck	.0473			
10	None	Rim Struck		.01498		
12	4-Pt	Cable Release (incomplete)		.01480	.00789	
13	4-Pt	Cable Release	.0471	.0413		
14	3-Pt	Ctr Struck		.0417		
15	3-Pt	Rim Struck		.0416		
16	3-Pt	Cable Release		.0422		
17	3-Pt	Cable Release				.0008
18	2-Pt	Ctr Struck		.0151		
20	2-Pt	Cable Release (incomplete)	.0463			
21	2-Pt	Cable Release		.0417	.00765	
22	Circumferential	Cable Release		.0416		
23	Circumferential	Cable Release (incomplete)				.0008
24	Circumferential	Ctr Struck		.0411		
25	Circumferential	Rim Struck		.0412		
26	Circumferential	Cable Release (incomplete)				.0008
27	Circumferential	Cable Release	.0416		.00768	.0008
28	Circumferential	Cable Release			.00757	
					.00754	
					.00824	.0008



FIGURE I.2.1- STEEL BEAM TEST

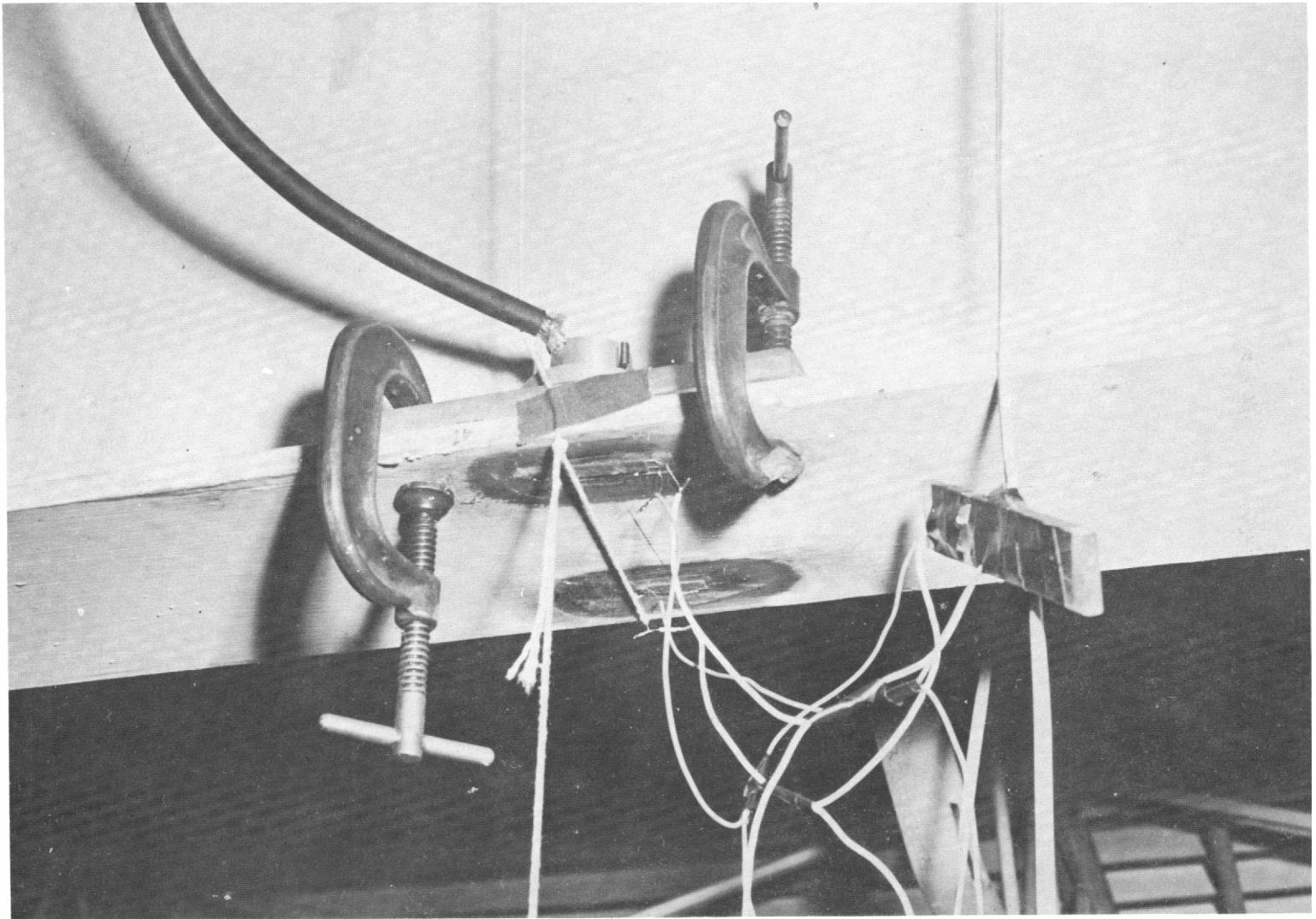


FIGURE I.2.2- STEEL BEAM GAGE MOUNTINGS

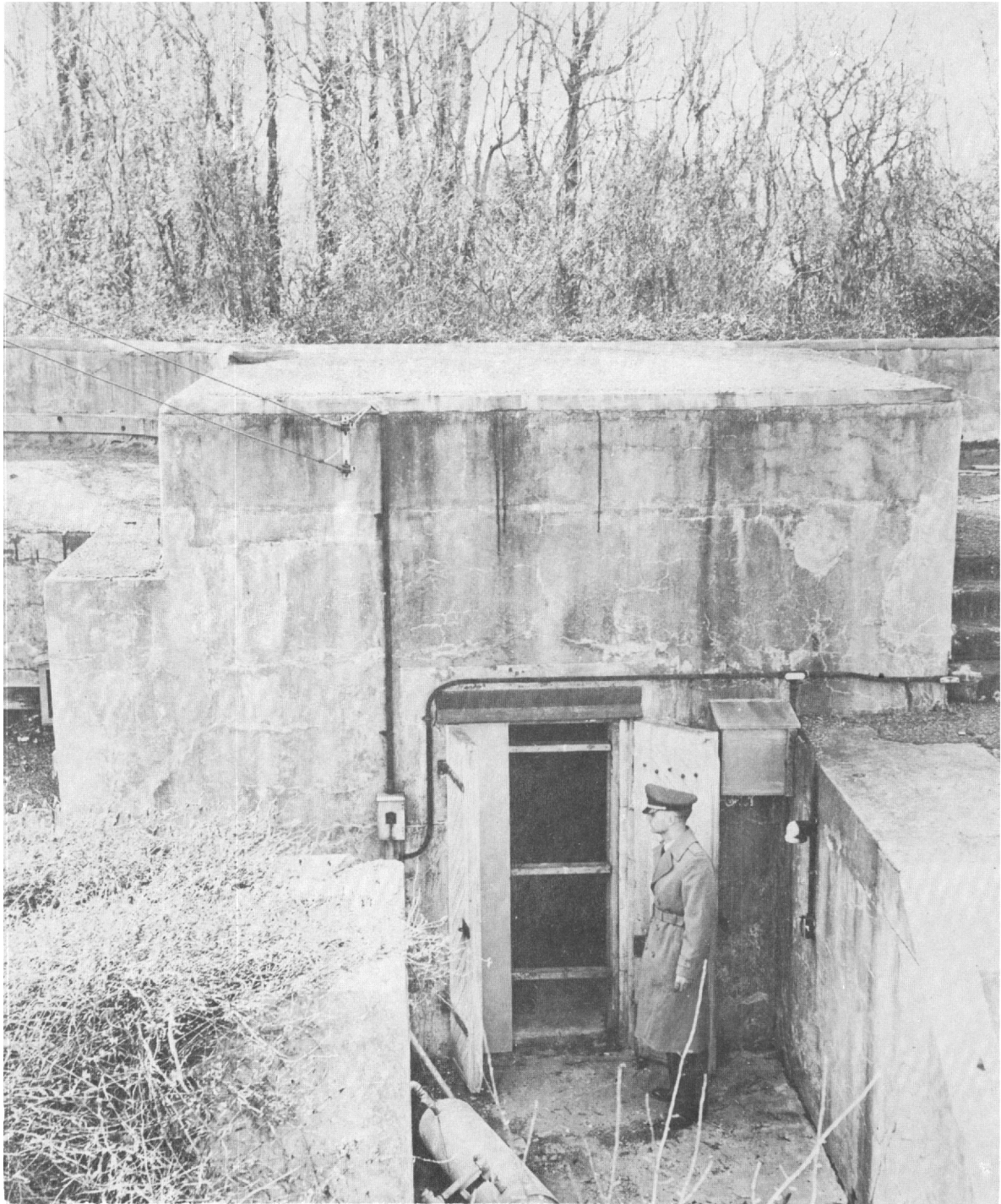


FIGURE I.2.3- CONCRETE MAGAZINE EXTERIOR

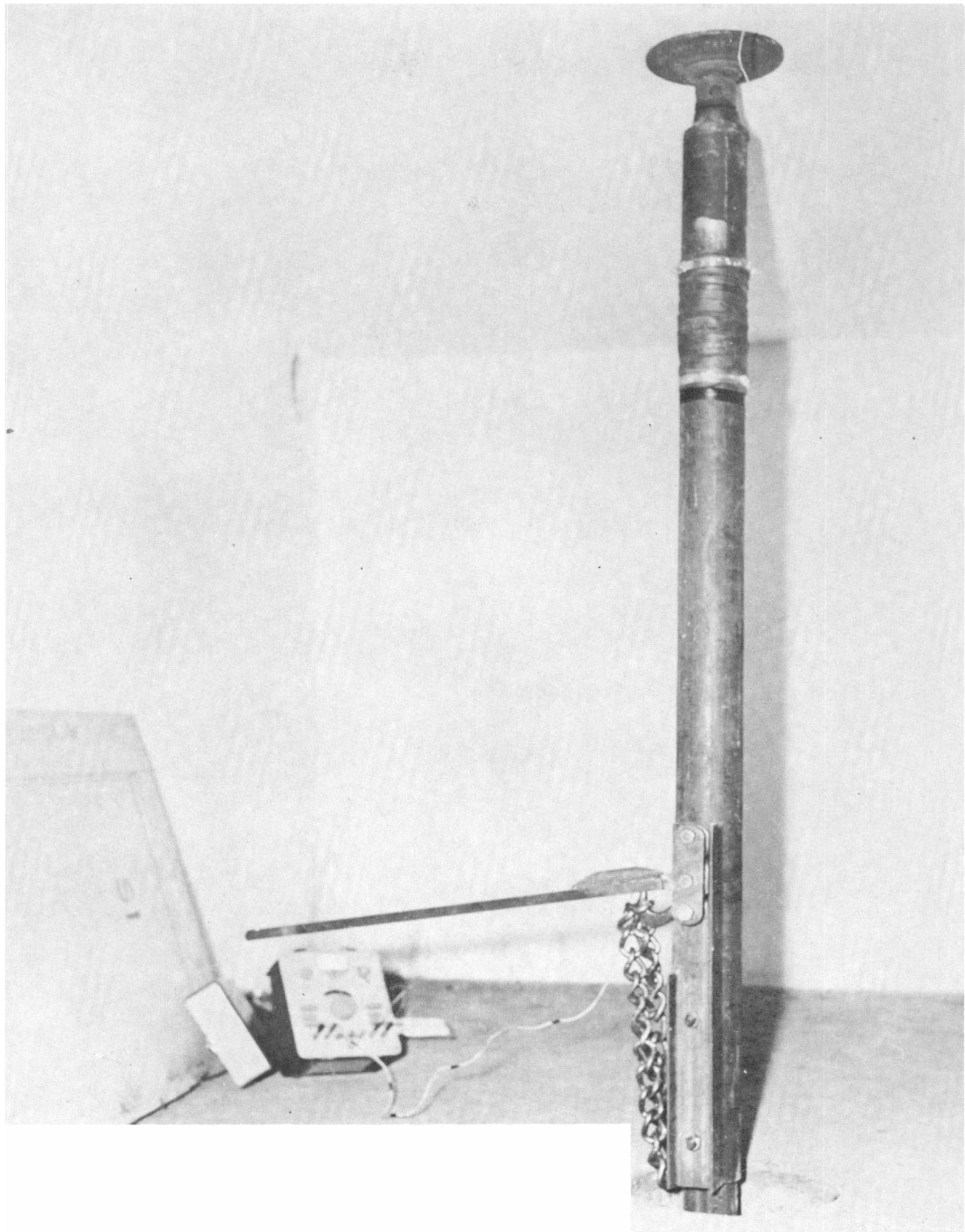


FIGURE I.2.4- LOADING COLUMN AND GAGE MOUNTINGS,
CONCRETE MAGAZINE

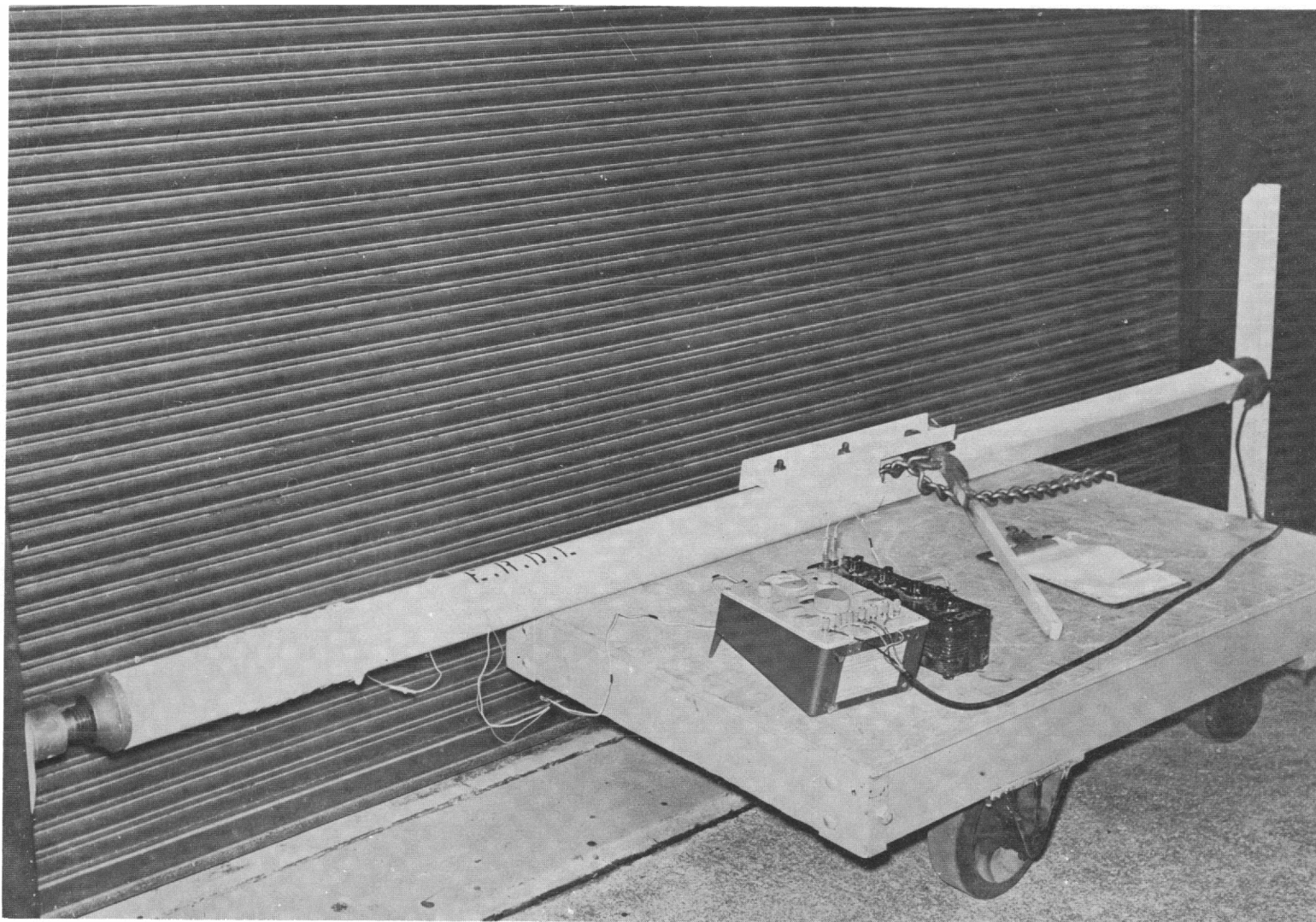


FIGURE I.2.5- LOADING COLUMN CALIBRATION AND RELEASE TEST

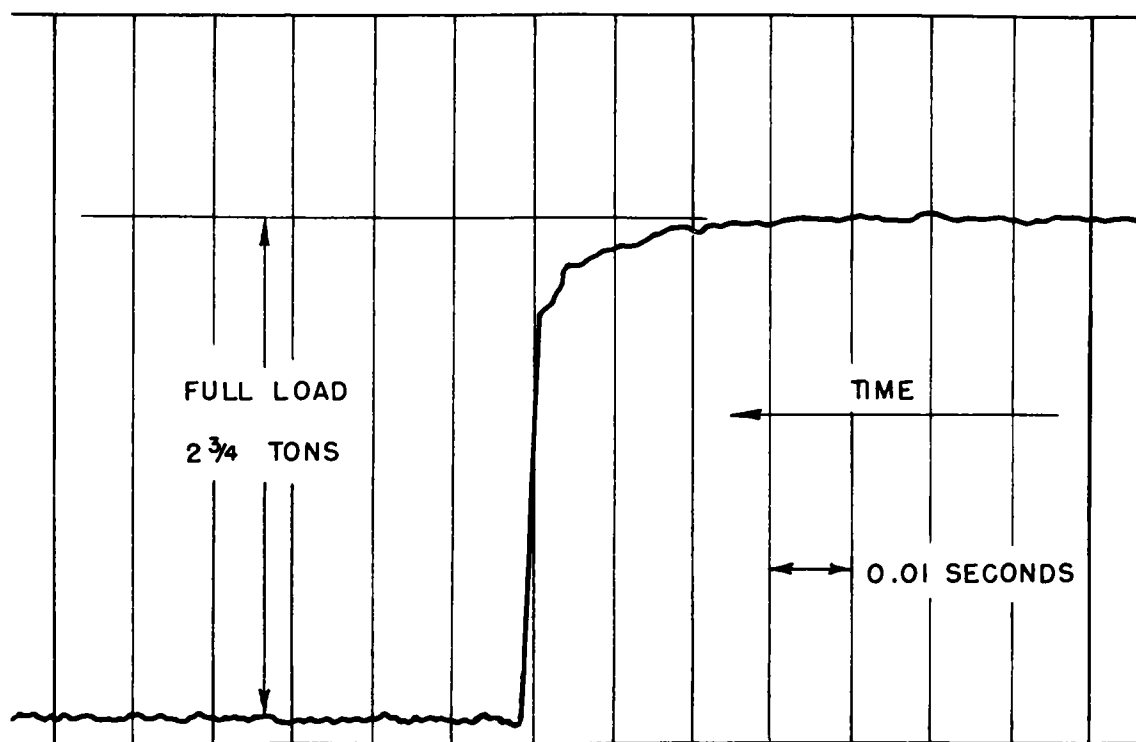


FIGURE I.2.6- COLUMN RELEASE CHARACTERISTICS

Trace of a mounted load cell.



FIGURE I.2.7- STEEL CULVERT FIELD TEST

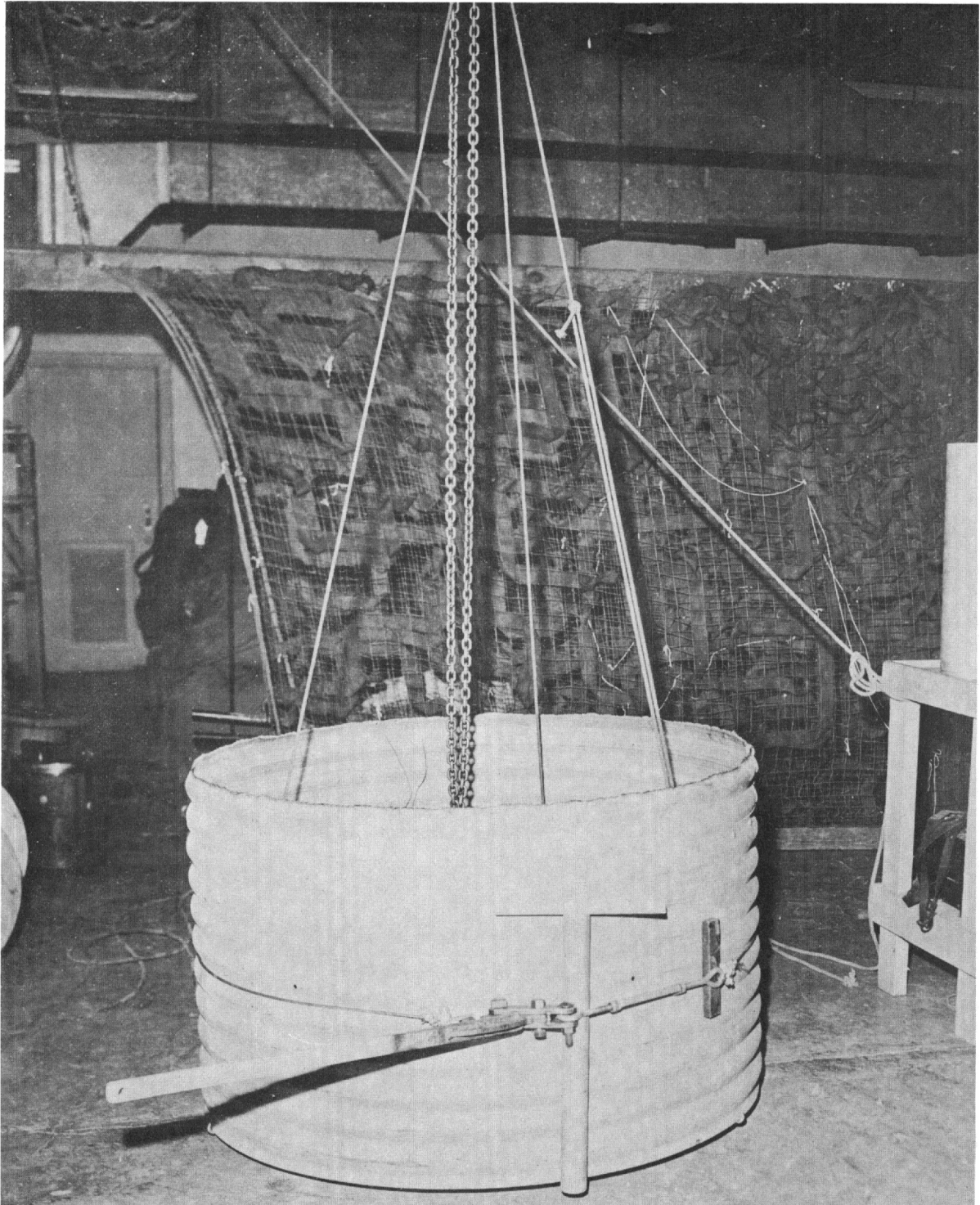


FIGURE I.2.8- CORRUGATED-STEEL PIPE WITH CIRCUMFERENTIAL LOADING

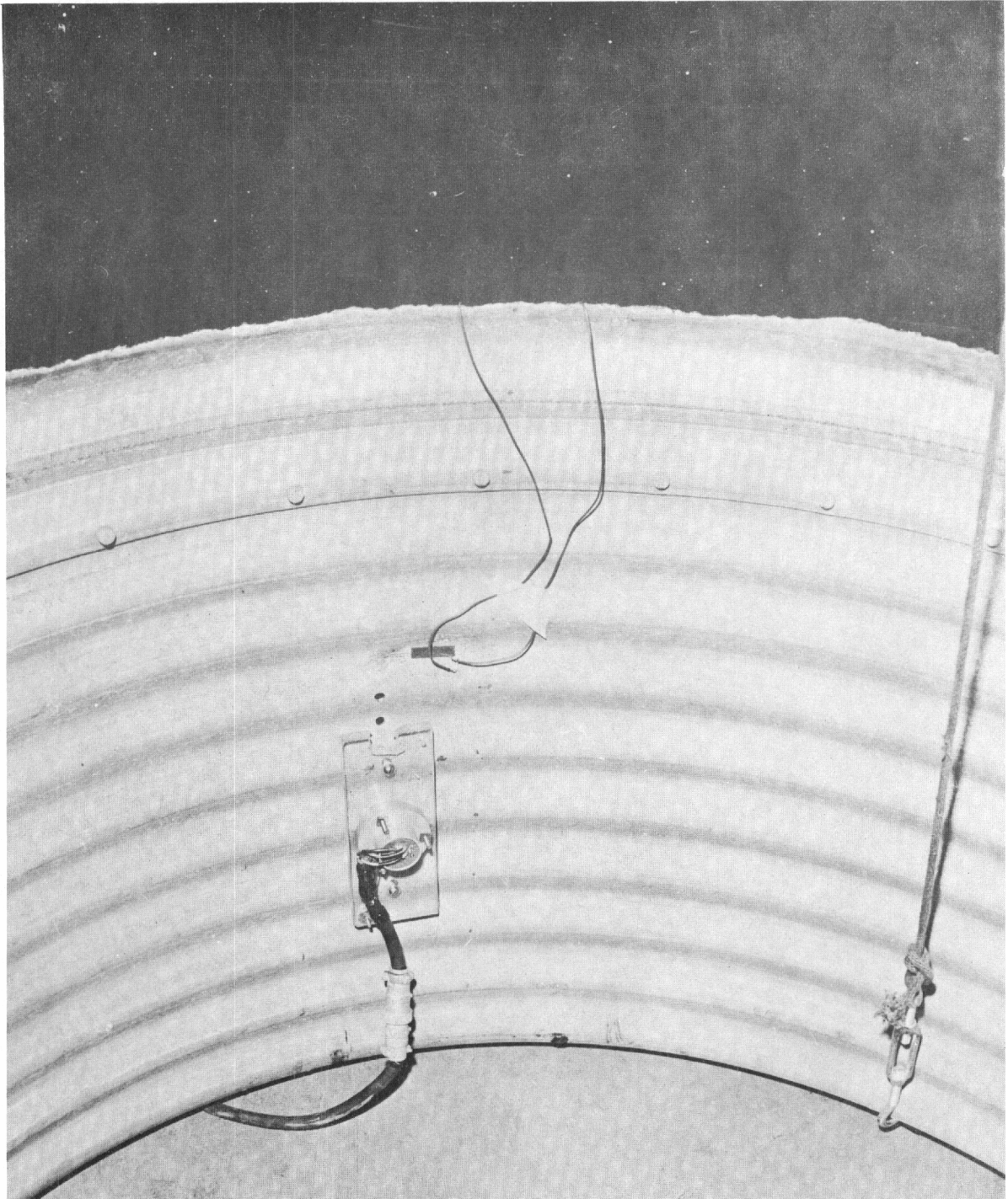


FIGURE I.2.9- CORRUGATED-STEEL PIPE GAGE MOUNTINGS

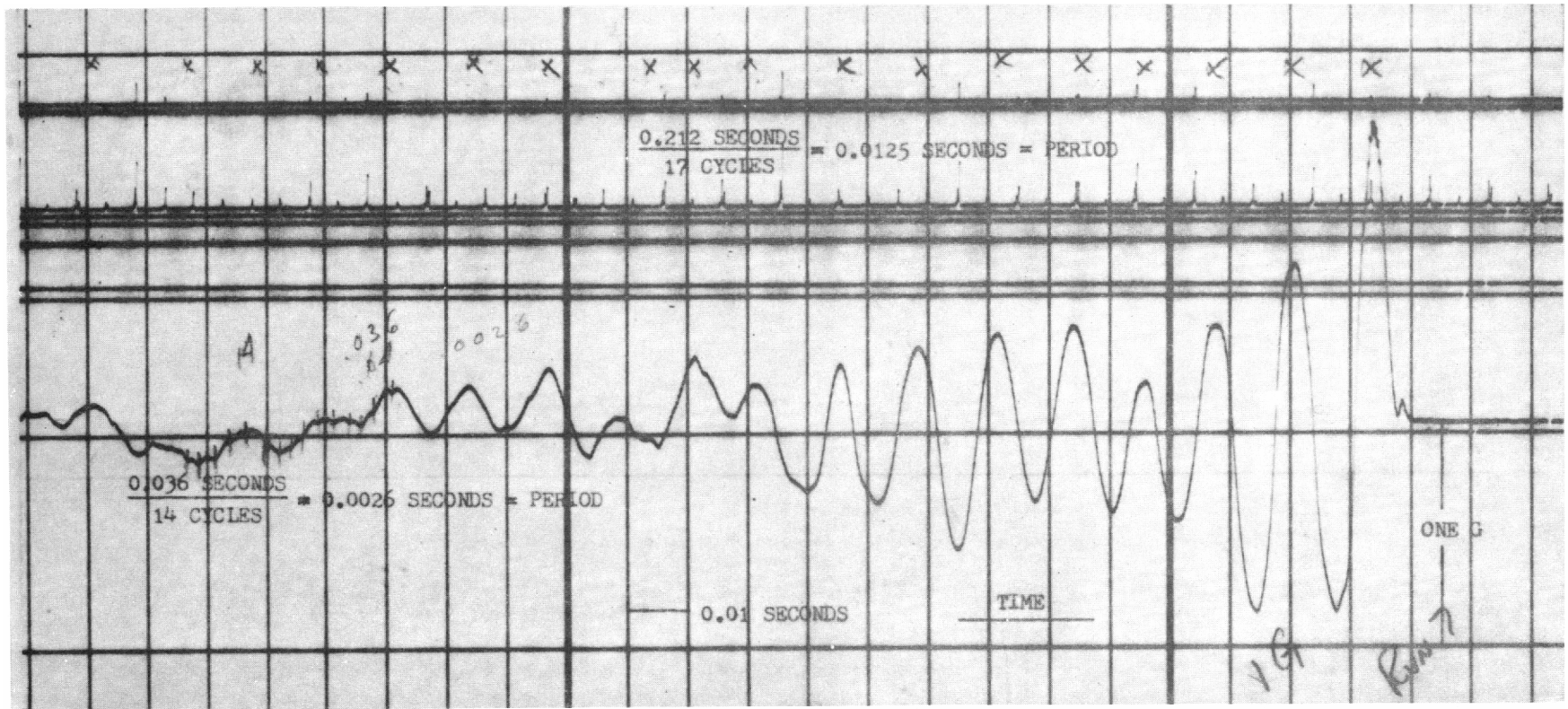


FIGURE I.3.1- STEEL BEAM SAMPLE RECORD ANALYSIS

APPENDIX II

SHOCK ISOLATION OF UNDERGROUND STRUCTURES

II.1 INTRODUCTION.

II.1.1 OBJECTIVE AND SCOPE.

The objective of this study was to determine whether an isolation medium of flexible plastic foam can afford protection against the damaging effects of blast loads on underground structures.

This sub-project consisted of a theoretical investigation of the nature of response of a flat-roofed underground structure overlain by an idealized plastic foam shock isolating medium.

II.1.2 BACKGROUND.

In past nuclear tests, underground structures designed to withstand blast loads were allowed to resist the full transmitted shock. These structures were designed to be strong enough to withstand this shock with no attempt made to reduce the magnitude of the shock transmitted to the structure.

Although it was determined by the nuclear testing that these structures could be effectively designed to resist the pressures to which they would be subjected, it would be desirable to have a simple means of increasing their overpressure resistance. Should such a means of increasing protection be found, future construction could be lightened, and existing structures could possibly be strengthened. It was anticipated that a simple and possibly effective means of providing the increased resistance for an underground flat-roofed structure might be a flexible plastic foam placed between the soil backfill and the roof in the manner shown in Figure II.1. The foam would be expected to temporarily

absorb some strain energy from the ground shock and reduce the rate at which the structure would have to absorb the transmitted energy.

II.1.3 THEORY.

Certain basic parts of the flat-roofed structure were isolated for the purpose of simplifying the response study. The system, simplified for harmonic analysis, consisted of the flat roof of the structure, assumed to act as an unyielding base for the foam; the layer of flexible plastic foam, which was assumed to act as a massless spring of varying stiffness; and, the backfill of soil over the plastic foam, taken as the vibrating single-degree-of-freedom mass. The length and width of the roof were assumed to be large enough that end effects of arching of the soil above it could be neglected.

In order that the system of roof, foam, and soil could be evaluated under dynamic loading conditions, without going to the expense of a full-scale test or a model test, a simple system lending itself to evaluation through the use of a computer was adopted. This comprised a mass, m , acted upon by a downward forcing function, p , and an upward forcing function, q . The function, p , consisted of the side-on overpressure plus a constant unit gravitational force. The mass, m , was defined as the mass of the soil backfill per unit horizontal area. The supporting reaction of the foam acting on the soil was expressed by the function, q , (Figure II.2). As the foam was assumed to be massless, q was also considered to be the pressure acting on the flat roof. Another simplification was made by considering

the roof to have an infinite stiffness. This was a reasonable assumption as the positive pressure pulse in the foam would be much longer than the period of vibration of the roof, with the result that q would not be materially reduced by roof deflection.

The function,

$$p = p_{so} \left(1 - \frac{t}{t_+}\right) \exp\left(-\frac{t}{t_+}\right) + mg \quad (1)$$

was used to relate p to the accepted expression for decaying overpressure (Reference 28), and the weight of the soil. The function p_{so} is the peak side-on overpressure; t , the time elapsed after the occurrence of the peak overpressure; t_+ , the length of the positive pressure pulse; and g , the acceleration of gravity (Reference 28 and Figure II.3).

The reaction, q , was obtained in three different ways. The basis of each was that q was a function of the displacement of the mass, m . In the first method values of q were chosen from the stress-strain diagram of an existing foam (Reference 30). In the second and third methods a function,

$$q = q_0 + k \left(\frac{x - x_0}{b}\right)^z, \quad (2)$$

was used to represent the stress-deflection characteristics of the foam, where q_0 was the static case reaction of the foam, which thus was essentially equal to mg ; x_0 was the static displacement of the mass, m ; x was the displacement of the mass, m ; b and z were the constants which determined the shape of the stress-deflection curve; and k , a proportionality constant, which was equal to one psi. In the second method q_0 , x_0 , b , and z were given values which produced a curve which had what were

assumed to be desired properties. The constants used with the third method were the results of a least squares curve-fitting procedure (Reference 29) applied to the stress-strain curves of two existing foams (Reference 27).

II.2 PROCEDURE.

II.2.1 GENERAL.

In general, the evaluation of the stress in the foam during response to the overpressure involved the solution of the differential equation.

$$m \frac{d^2x}{dt^2} = p - q. \quad (3)$$

In all cases the solutions were programmed for an IBM 650 digital computer. The Data Processing Section of ERDL received the required data in two forms. The first, for a step-by-step procedure, programmed a solution of equation (3). The second supplied information to an existing program for solving equations similar to (3). These forms are described in more detail below.

II.2.2 METHOD I.

In Method I the isolation properties of flexible polyurethane foam were studied using a step-by-step solution of equation (3). For these calculations the downward forcing function was changed to

$$p_{n+1} = p_{so} \left(1 - \frac{t_{n+1}}{t_+}\right) \exp \left(-\frac{t_{n+1}}{t_+}\right) + mg \quad (4)$$

where t_{n+1} was equal to t_n , the elapsed time since the shock arrival, plus a time step, h ; and p_{n+1} was the pressure at t_{n+1} .

The resistance function, q , was taken from the stress-strain diagram of the foam (Reference 30). This step-by-step procedure made use of the following equations (Reference 26):

$$a = \frac{p_{n+1} - q_{n+1}}{m}, \quad (5)$$

$$v_{n+1} = v_n + (1 - \gamma) a_n h + \gamma a_{n+1} h, \quad (6)$$

$$x_{n+1} = x_n + v_n h + \left(\frac{1}{2} - \beta\right) a_n h^2 + \beta a_{n+1} h^2 \quad (7)$$

where a was the acceleration of mass, m ; v , the velocity; and x , the displacement. The results of the procedure were as shown in Table II.1, where the values of p_{\max} and q_{\max} are listed for various combinations of peak side-on overpressure, foam thickness, and length of positive pressure pulse. No limit was placed on the maximum value of x in this first group of calculations although in actuality x could not be greater than the unloaded thickness of the foam.

II.2.3 METHOD II.

In Method II the resistance function, q , was assumed to have the properties of a hypothetical stress-deflection curve. The only information needed by the Data Processing Section were equations (1), (2), and (3) plus the selected constants. The computations were discontinued when x became greater than L , the unloaded thickness of the foam; or when v , the velocity of the mass, became negative. The results are listed in Table II.2, where p_{\max} and q_{\max} can be compared for various values of t_+ , p_{so} , b , and z .

II.2.4 METHOD III.

The final method used employed the equations and

constants mentioned in the second method. Here the stress-strain curves of Lockfoam No. 1 and No. 2 (Reference 27) were approximate by using least square curve fitting (Reference 29). The derived values of q_0 , x_0 , b , and z are listed in Table II.3 with the corresponding results for various values of t_+ and p_{so} . Again the computations were discontinued when x became greater than L or when v became negative.

II.3 DISCUSSION.

II.3.1 METHODS.

The value of the results depends upon the validity of the simplified model, which has limitations. For example, the unit soil mass does not show the complete picture. It is considered to be rigid in the model, but the soil may deform through consolidation and shear in unpredictable ways. Also, the pressure is not applied on the surface but reaches the entire backfill. At present the distribution of this pressure is uncertain.

The air trapped in the foam should cause the foam stress-versus-deflection curve to vary with the loading rate. An error caused by such variance would be most important in Method I where a static stress-strain curve was used.

The assumption that the roof was rigid is good. It could be made only if the natural period of vibration of the roof were much shorter than the length of the positive pressure pulse in the foam and if the amplitude of vibration of the roof were insignificant. As the stress in the foam during the pulse was low and constant at first, followed by a sharp increase and

decrease at the "bottoming-out" of the deflecting mass, this condition was fulfilled.

The IBM 650 digital computer equipment was well suited for the calculations because all problems involved trial and error solutions. Calculations of this kind contain many repetitions of a given set of operations which are cumbersome when done by hand but easily negotiated by this computer. All programs and data were read in on punched cards, and the results were read out in the same fashion. Then the results were printed by a listing machine to make them easier to read and interpret. Selected cases were plotted and were valuable in determining the effects of varying foam thickness, peak side-on overpressure, and length of positive pressure.

II.3.2 RESULTS.

In most cases the pressure reductions or increases due to the foam are of a nature that inaccuracies connected with the original assumptions may be neglected. In those cases in which the reduction or increase of the pressure due to use of the foam are small, only broad conclusions are justified. These results have been used in this report, but their limitations should be noted.

Determination of maximum pressure magnification or reduction can be made from Method III. In Method II this comparison must be modified by the limits placed on the deflection. When the displacement became a large percentage of the foam thickness "bottoming-out" should have occurred. If it did not, the results were discarded.

Another problem exists in Method I where no common limit was placed on the velocity. This limit should have been the negative velocity following the maximum displacement. Because it was not used, the maximum foam reaction was never reached. Had the calculations been continued to this point there would have been greater magnifications of pressure than those shown. As the magnifications computed were thus less than maximum, conclusions could be drawn without the true maximum having been determined.

II.4 CONCLUSIONS.

II.4.1 STRUCTURAL.

A structure designed to withstand high overpressures and long positive pressure pulses will have its capacity lowered by the addition of a foam isolation between the roof and the soil backfill. The peak force which the roof must resist will be increased. An increase in loading rate will accompany this load change. Although the tendency of the construction materials would be to have an increase in ultimate strength with increased loading rate, the purpose of the foam would have already been defeated.

In the realm of construction designed to resist low overpressures and short positive pressure pulses, the addition of the foam will reduce the peak pressure and time of loading for design purposes. It will also increase the capacity of existing structures. Caution must be used because the foam will increase the capacity only to a certain maximum load. Beyond this a reduction in capacity will occur, even to the extent where

loads on the structure due to shock overpressure may be many times greater than those on a similar non-cushioned structure.

II.4.2 APPLICATION TO SHOCK TUBE OR BLAST SIMULATOR.

The characteristics exhibited by the foam-mass combination suggest that it could find application in a shock tube. For a given impulse generated in the tube a more desirable pulse configuration could be obtained by using selected mass, foam thickness, and foam deflection characteristics in an apparatus which would isolate the model being tested from the shock chamber. Axial compression of the foam by a piston-like mass at the end of the shock chamber would be desirable and such a scheme is shown in Figure II.4. Possible effects of this scheme on the original pulse are an amplification of the peak pressure, an increase in loading rate, and an increase or decrease in the duration of positive pressure.

II.5 RECOMMENDATIONS AND FUTURE WORK.

II.5.1 DESIGN.

The results show that with a particular combination of blast intensity and foam isolation no pressure amplification or attenuation takes place. Structures which undergo higher pressure intensities must withstand pressures which are still higher with foam isolation, while structures which are subjected to lower pressure intensities may have these pressures attenuated by the same isolation. Until the dividing line is established, the use of foam isolation is not recommended.

II.5.2 COST.

Another aspect of foam isolation is its cost relative

to conventional types of construction. A comparison must be made before any decisions concerning the advantages of one type of construction over another are possible. An example of the questions to be answered is: Are the maintenance costs and expense of the special equipment used in placing the foam and the cost of the foam itself going to be greater than the cost of the extra material used to provide similar protection by heavier conventional construction?

II.5.3 ARCHES.

Flat-roofed structures isolated by foam are only a starting point in this investigation. Entirely different results may be obtained from the analysis of buried structural arches similarly isolated. Soil arching would be very important in such situations.

General solutions have been found for arch deflections, and an investigation of the soil arch is now in progress. When a solution to this problem is obtained, a theoretical study of the interaction of the soil with the foam isolation might provide an evaluation of the structural protection that could be obtained.

TABLE II.1 MAXIMUM VALUES OF FORCING AND REACTION
FUNCTIONS VS CONTROLLING CONSTANTS, METHOD I

$$\gamma = 1/2, \beta = 1/6$$

Case	Foam	t_+ (sec)	x (in)	L (in)	p_{so} (psi)	p_{max} (psi)	q_{max} (psi)
1	Urethane Foam	.190	1.2	10	30	31	653
2		.570	1.2	10	30	31	169
3		.950	1.2	10	30	31	378
4		.228	1.2	10	15	16	413
5		.684	1.2	10	15	16	548
6		1.140	1.2	10	15	16	442
7		.317	1.2	10	5	6	76
8		.951	1.2	10	5	6	110
9		1.585	1.2	10	5	6	118
10		.190	3.6	30	30	31	459
11		.570	3.6	30	30	31	511
12		.950	3.6	30	30	31	538
13		.228	3.6	30	15	16	193
14		.684	3.6	30	15	16	467
15		1.140	3.6	30	15	16	240
16		.317	3.6	30	5	6	40
17		.951	3.6	30	5	6	94
18		1.585	3.6	30	5	6	109

$q_0 = 0.90$ psi.

b does not apply.
z does not apply.

TABLE II.2 MAXIMUM VALUES OF FORCING AND REACTION
FUNCTION VS CONTROLLING CONSTANTS, METHOD II

Case	Foam	b	z	t_+ (sec)	p_{so} (psi)	p_{max} (psi)	q_{max} (psi)
19		12	5	.190	30	35	45
20		12	5	.190	5	10	6
21		12	5	.950	30	35	*
22		12	5	.950	5	10	22
23		12	7	.190	30	35	67
24		12	7	.190	5	10	6
25		12	7	.950	30	35	197
26		12	7	.950	5	10	29
27		18	5	.190	30	35	*
28		18	5	.190	5	10	5
29		18	5	.950	30	35	*
30		18	5	.950	5	10	*
31		18	7	.190	30	35	*
32		18	7	.190	5	10	5
33		18	7	.950	30	35	*
34		18	7	.950	5	10	*

Hypothetical Foam

$x_0 = 3 \text{ in.}$

$q_0 = 5 \text{ psi.}$

$L = 30 \text{ in.}$

* Values meaningless

TABLE II.3 MAXIMUM VALUES OF FORCING AND REACTION
FUNCTIONS VS CONTROLLING CONSTANTS, METHOD III

Case	Foam	b	z	t_+ (sec)	q_0 (psi)	p_{so} (psi)	p_{max} (psi)	q_{max} (psi)
35	(1)	10.26	5.63	.190	9.7	15	25	25
36	(1)	10.26	5.63	.190	9.7	30	40	63
37	(1)	10.26	5.63	.950	9.7	15	25	84
38	(1)	10.26	5.63	.950	9.7	30	40	169
39	(2)	2.55	1.76	.190	9.0	30	39	35
40	(2)	2.55	1.76	.190	9.0	15	24	20
41	(2)	2.55	1.76	.950	9.0	30	39	74
42	(2)	2.55	1.76	.950	9.0	15	24	40

- (1) Lockfoam No. 2
(2) Lockfoam No. 1

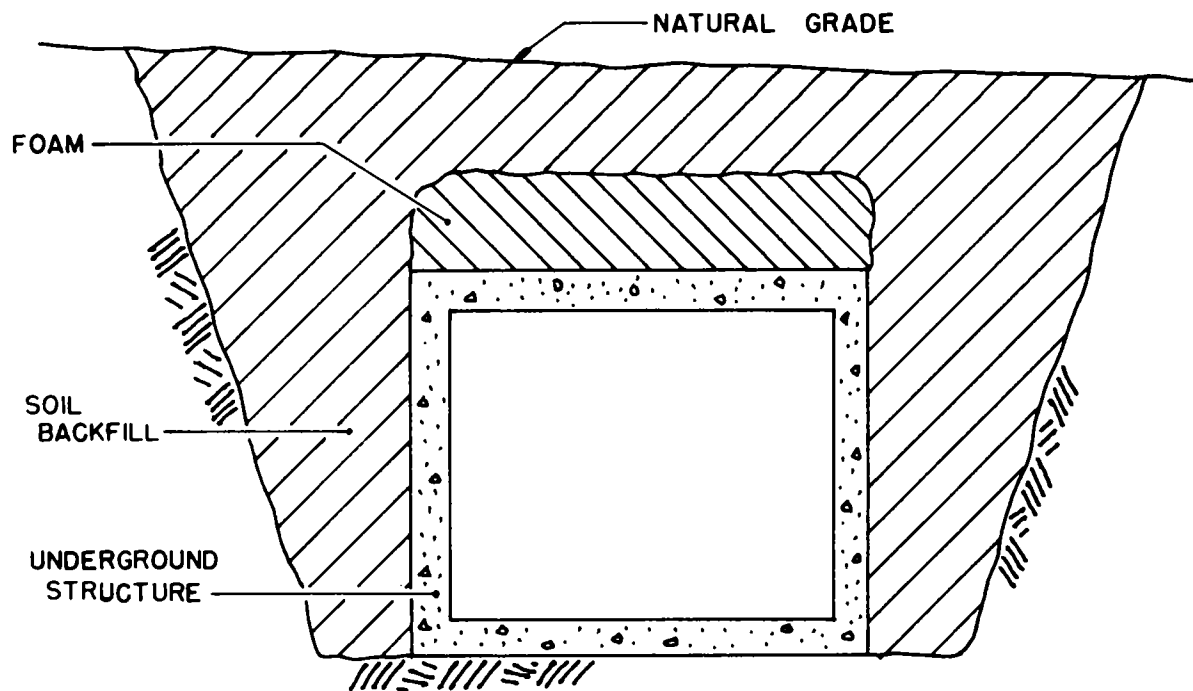


FIGURE II.1 TYPICAL FOAM ISOLATION INSTALLATION

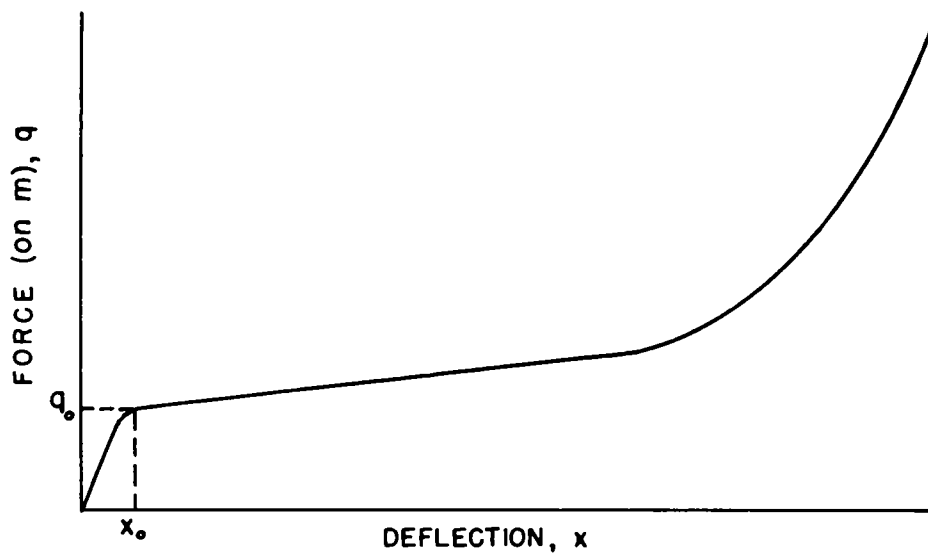


FIGURE II.2 TYPICAL FOAM FORCE-DEFLECTION CURVE

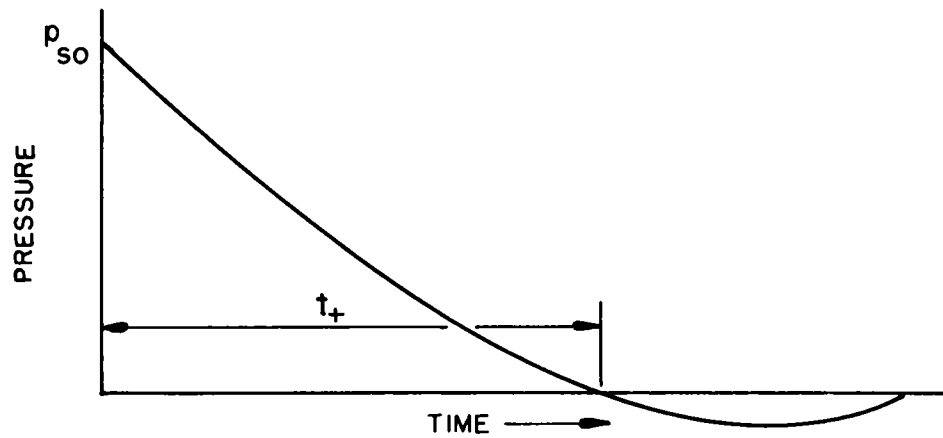


FIGURE II. 3 AIR PRESSURE PULSE

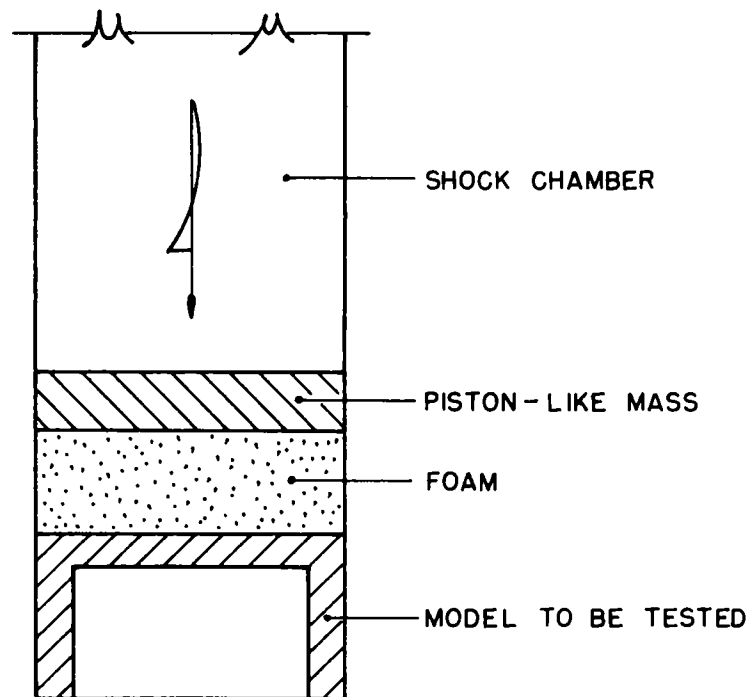


FIGURE II. 4 POSSIBLE USE OF FOAM IN A SHOCK TUBE

APPENDIX III
TABULATED AND GRAPHIC PERMANENT DISPLACEMENT RESULTS

TABLE III.J - SURFACE PERMANENT DISPLACEMENTS¹, BLANCA

STATION	POSITION ²			RANGE FROM G.Z.			PERMANENT TRANSLATION					AZIMUTH		DIVERGENCE OF DISPL. FR. RADIAL
	North	East	Elev.	Horiz.	Absolute	Vert.	North	East	Vert	Net Horiz.	Absolute	Radial From GZ	Net Displ.	
GZ	886,990	635,350	6138		GROUND ZERO, BLANCA	EVENT								
2J	888,657	636,902	6293	2278	2283	155	-0.10	+0.06	+0.11	0.12	0.16	43	149	+ 106
DEN	888,570	636,660	6388	2052	2068	250	+9.43	+9.01	+2.55	13.04	13.29	40	44	+ 4
3J	888,562	636,536	6425	1969	1990	287	+2.30	+3.99	+0.96	4.61	4.70	37	60	+ 23
4J2	888,466	636,281	6532	1745	1789	394	+1.55	+4.01	+1.03	4.30	4.42	32	69	+ 37
4JJ	888,402	635,978	6624	1546	1620	486	+0.36	+3.99	+0.65	4.01	4.06	24	85	+ 61
BOG	888,491	636,153	6579	1702	1758	441	+1.13	+3.88	+1.06	4.04	4.18	28	74	+ 46
5J	888,409	635,924	6674	1531	1622	536	+0.42	+4.59	+0.91	4.61	4.70	22	85	+ 63
SUN	888,488	635,816	6747	1569	1683	609	+0.72	+4.25	+1.02	4.31	4.43	17	80	+ 63
LOX	888,478	635,557	6861	1502	1667	723	+0.56	+3.43	+0.54	3.48	3.52	8	81	+ 73
7J	888,496	635,488	6890	1512	1689	752	+0.52	+3.28	+0.42	3.32	3.35	5	81	+ 76
2L	887,935	637,162	6205	2044	2045	067	+2.79	+5.06	+1.40	5.78	5.95	62	61	- 1
AXE	887,923	637,099	6241	1982	1985	103	+3.02	+4.90	+1.23	5.76	5.89	62	58	- 4
DUX	887,710	636,777	6316	1598	1608	178	+13.32	+18.65	+6.32	22.92	23.77	63	54	- 9
3L2	887,724	636,772	6312	1600	1610	174	+13.27	+18.48	+6.27	22.75	23.60	63	54	- 9
3L1	887,733	636,772	6309	1604	1613	171	+13.24	+18.38	+6.20	22.65	23.49	62	54	- 8
WHY	887,980	636,422	6454	1459	1493	316	+8.26	+12.51	+1.55	14.99	15.07	47	57	+ 10
4L2	887,889	636,296	6448	1305	1341	310	+9.04	+14.78	+1.67	17.33	17.41	46	59	+ 13
5L	887,776	635,677	6724	851	1033	586	+2.72	+5.07	+1.32	5.75	5.90	23	62	+ 39
TAR	887,774	635,589	6767	820	1033	629	+7.23	+5.69	+1.92	9.20	9.40	17	38	+ 21
7L2	887,739	635,549	6796	775	1017	658	+1.37	+3.02	+1.38	3.32	3.59	15	66	+ 51
AL	887,618	635,333	6911	628	996	773	+4.71	+3.90	+1.84	6.12	6.39	358	40	+ 42
2N	887,521	637,112	6283	1840	1846	145	+2.59	+4.96	+1.11	5.60	5.70	73	62	- 11
3N	887,481	636,650	6372	1390	1409	234	+11.83	+20.46	+2.90	23.63	23.81	69	60	- 9
7N2	886,911	635,848	6862	504	882	724	+7.17	+34.71	-1.37	35.44	35.47	99	78	- 21
NET	886,900	635,854	6856	512	882	718	+7.01	+34.44	+5.33	35.15	35.55	100	78	- 22
2P	886,324	637,565	6296	2313	2318	158	-1.15	+2.03	+0.37	2.33	2.36	107	120	+ 13
3P	886,379	637,343	6371	2085	2098	233	-2.95	+6.11	+0.26	6.78	6.79	107	116	+ 9
4P	886,404	636,995	6460	1746	1776	322	-5.64	+9.67	+1.79	11.19	11.34	110	120	+ 10
HEX	886,472	637,019	6477	1748	1780	339	-5.34	+10.13	+2.19	11.45	11.66	107	118	+ 11
5P2	886,525	636,391	6719	1140	1280	581	-6.84	+32.39	+5.69	33.10	33.59	114	102	- 12
7P1	886,076	635,775	6923	1008	1278	785	+1.15	+12.12	-18.04	12.17	21.76	155	85	- 70
3S	885,439	636,757	6423	2094	2113	285	-2.64	+4.04	+1.78	4.83	5.14	138	123	- 15
SEX	885,507	636,697	6452	2003	2028	314	-3.70	+3.50	+1.63	5.09	5.35	138	137	- 1

1 All readings in feet or degrees (Azimuth clockwise from grid North)

2 Nevada State grid, Central Section

TABLE III.1 (Continued) - SURFACE PERMANENT DISPLACEMENTS¹, BLANCA

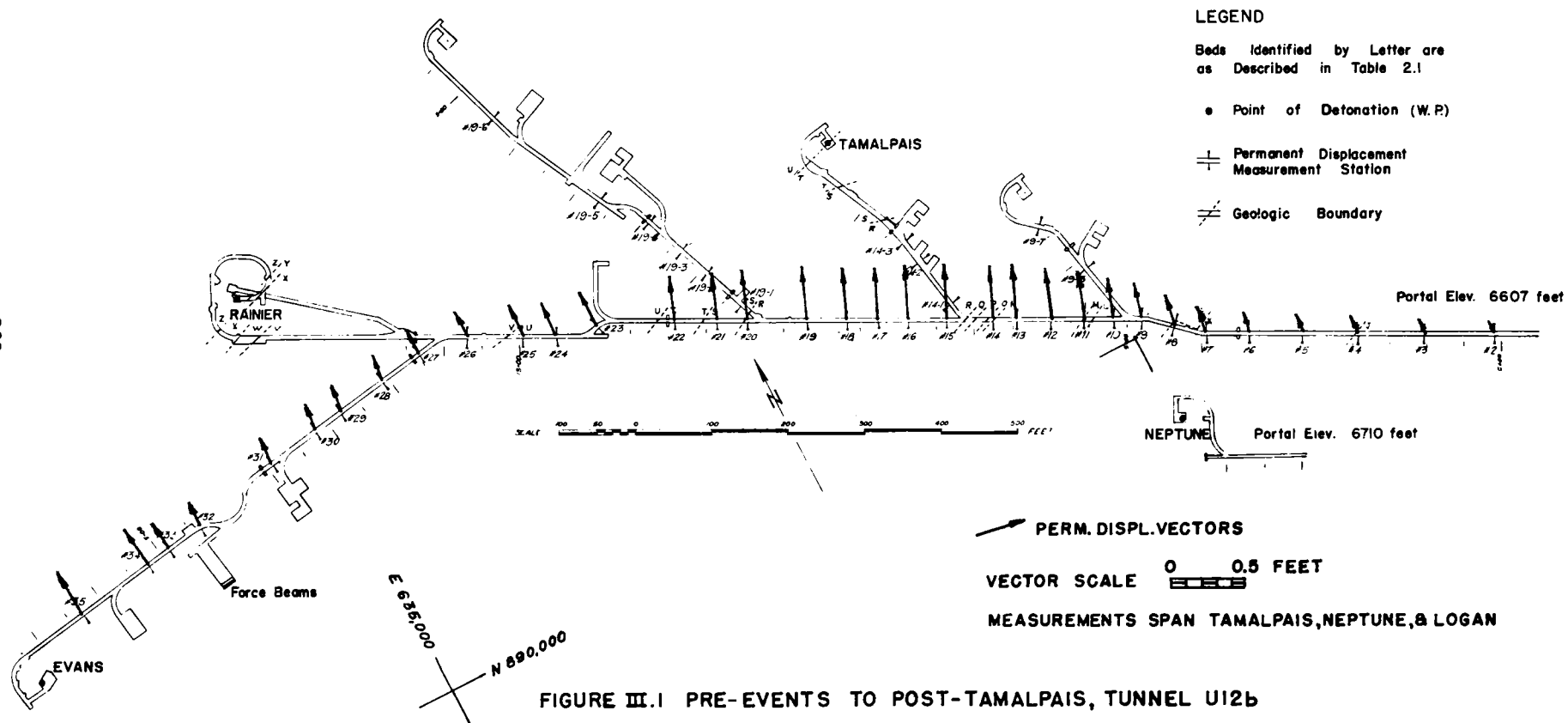
STATION	POSITION			RANGE FROM G.Z.			PERMANENT TRANSLATION					AZIMUTH		DIVERGENCE OF DISPL. FR. RADIAL
	North	East	Elev.	Horiz.	Absolute	Vert	North	East	Vert	Net Horiz.	Absolute	Radial From GZ.	Net Displ.	
LS-1	885,518	636,514	6529	1872	1913	391	-7.37	+9.10	+3.82	11.71	12.32	140	129	- 11
7S-1	885,368	635,789	6879	1680	1836	741	-0.36	+0.53	-0.07	0.64	0.64	165	124	- 41
SUCK	885,423	635,710	6934	1608	1794	796	-0.40	+0.46	-0.08	0.61	0.61	167	131	- 36
TEX	885,157	637,498	6235	2824	2825	097	-0.27	+0.07	-0.04	0.28	0.28	130	165	+ 35
2T	885,143	637,031	6313	2497	2504	175	-0.95	+1.97	+0.12	2.19	2.19	138	116	- 22
3T	885,016	636,824	6391	2464	2477	253	-0.40	+0.49	-0.10	0.63	0.64	143	129	- 14
REX	885,166	636,962	6347	2434	2443	209	-1.13	+2.79	+0.57	3.01	3.06	139	112	- 27
4T	884,882	636,393	6577	2352	2393	439	-0.49	+0.13	-0.14	0.51	0.53	154	165	+ 11
DEX	884,886	636,237	6644	2283	2339	506	-0.36	+0.12	-0.14	0.38	0.40	157	162	+ 5
5T	884,793	636,160	6713	2342	2411	575	-0.33	+0.10	-0.17	0.34	0.38	160	163	+ 3
7T-1	884,819	635,872	6842	2233	2341	704	-0.20	-0.03	-0.12	0.20	0.24	166	189	+ 23

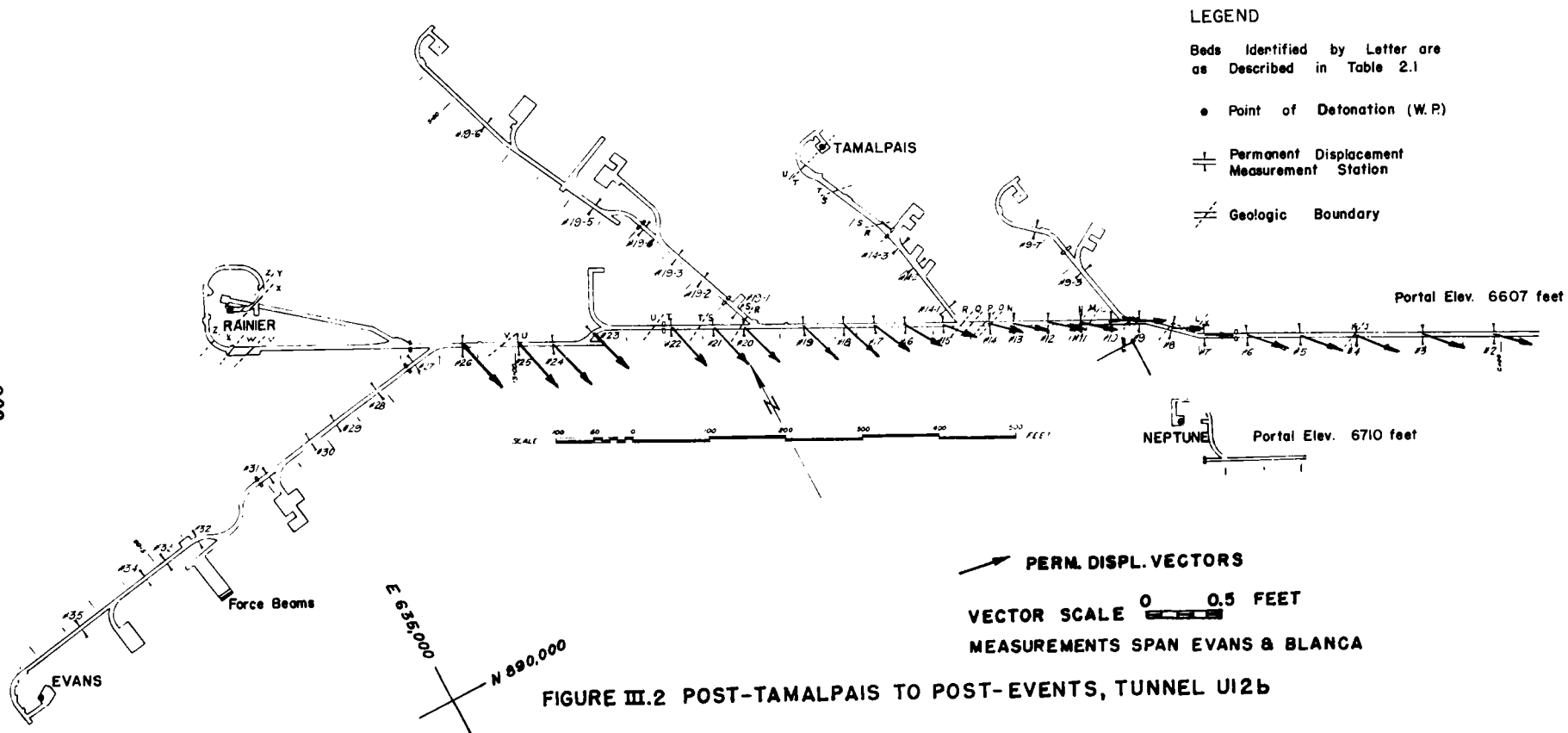
TABLE III.2 - SURFACE PERMANENT DISPLACEMENTS¹, TAMALPAIS

STATION	POSITION ²			RANGE FROM GZ			PERMANENT TRANSLATION					AZIMUTH		DIVERGENCE OF DISPL. FR. RADIAL
	North	East	Elev	Horiz	Absolute	Vert	North	East	Vert	Net Horiz	Absolute	Radial From GZ	Net Displ	
GZ	890,402	635,788	6616	GROUND ZERO, TAMALPAIS EVENT										
4F	889,365	635,883	6713	1041	1046	97	+0.14	+0.01	+0.86	0.14	0.87	175	4	-171
LIP	889,358	635,844	6729	1046	1052	113	+0.17	+0.12	-0.02	0.21	0.21	177	35	-142
5F	889,465	635,736	6798	938	956	182	+0.35	+0.03	-0.02	0.35	0.35	183	5	-178
ANN	889,497	635,701	6830	909	934	214	-0.02	+0.22	-0.12	0.22	0.25	185	95	-90
NEW	889,499	636,059	6717	943	948	101	+0.12	+0.10	-0.01	0.16	0.16	163	40	-123
BAT	889,655	636,034	6747	786	797	131	+0.13	+0.13	-0.01	0.18	0.18	162	45	-117
SAC	889,803	636,374	6687	838	841	71	+0.07	+0.11	-0.01	0.13	0.13	136	58	-78
5D	889,835	636,338	6691	790	793	75	+0.11	+0.06	-0.01	0.13	0.13	136	29	-107
ED	889,924	636,109	6796	576	603	180	+0.02	+0.21	-0.08	0.20	0.22	146	84	-62
7D	889,957	636,106	6798	547	576	182	+0.06	+0.21	-0.01	0.22	0.22	144	74	-70
DON	890,116	636,423	6652	696	697	36	+0.05	+0.22	-0.08	0.23	0.24	114	77	-37
SIT	890,310	636,583	6560	800	802	-56	-0.02	+0.17	-0.01	0.17	0.17	96	96	0
5C1	890,272	636,524	6577	747	748	-39	-0.03	+0.16	+0.275	0.16	0.32	100	101	+1
6C1	890,317	636,468	6626	685	685	10	-0.02	+0.16	+0.01	0.16	0.16	97	97	0
JO	890,312	636,458	Not Obsv	676			-0.02	+0.02	0	0.03		98	135	+37
6C2	890,264	636,431	6648	658	658	32	-0.02	No Change	+0.01	0.02	0.02	102	180	+78
7C	890,263	636,367	6680	595	599	64	-0.06	+0.11	0	0.13	0.13	103	118	+15

1. All readings in feet or degrees (Azimuth clockwise from grid North)

2. Nevada State grid, Central Section





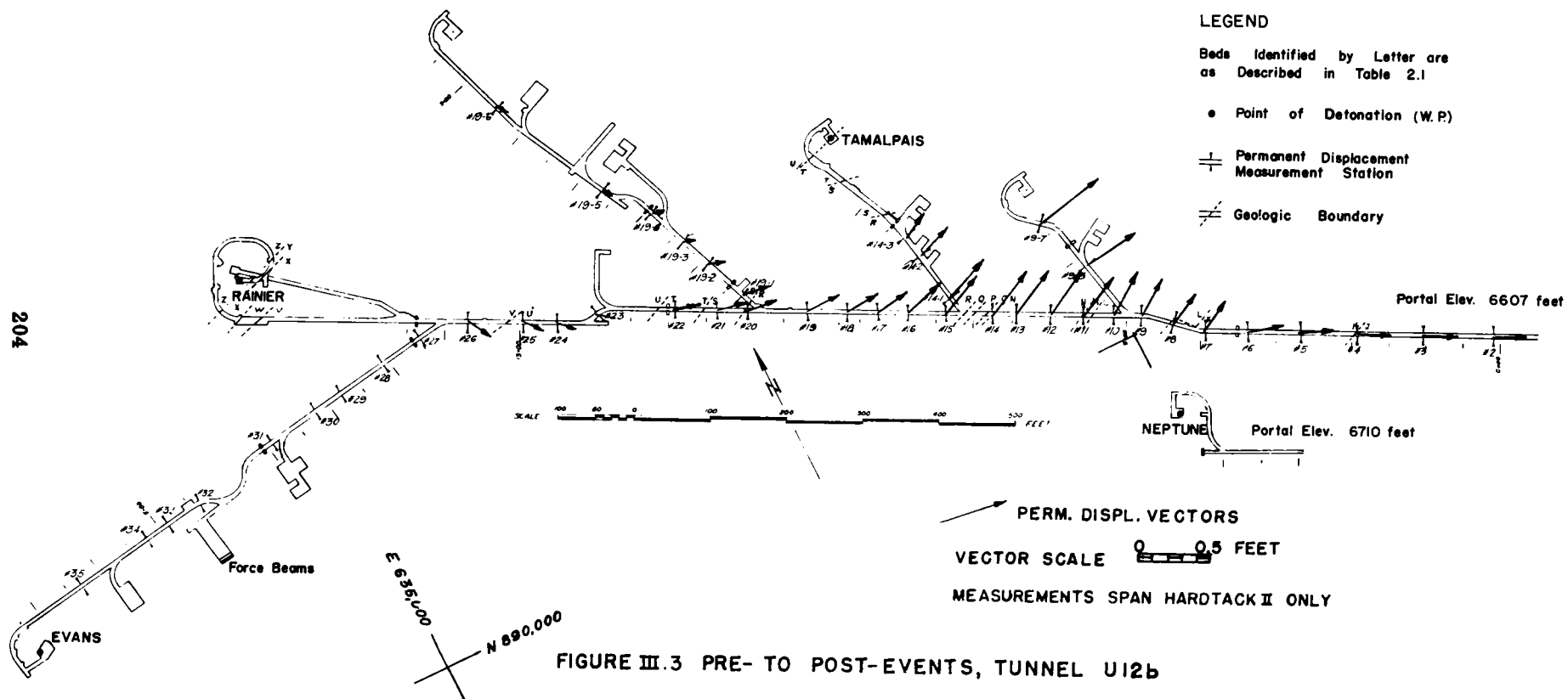
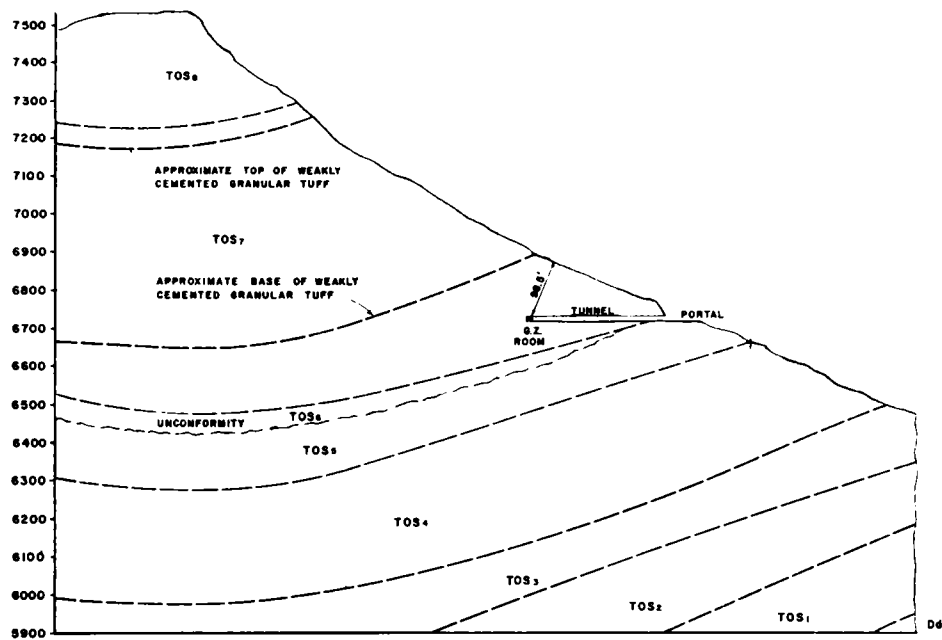


FIGURE III.3 PRE- TO POST-EVENTS, TUNNEL U12b



DESCRIPTION OF BEDDINGS

- TOS₈ - WELDED TUFF; RHYOLITE TO QUARTZ LATITE
- TOS₇ - BEDDED TUFF; MOSTLY ALL TUFFS ARE LOOSELY CEMENTED AND "SANDY" LIGHT GRAY TO GRAYISH BROWN
- TOS₆ - WELDED TUFF; LIGHT GRAY TO BROWNISH GRAY
- TOS₅ - BEDDED TUFF; WELL CEMENTED; LIGHT YELLOW GREEN
- TOS₄ - BEDDED TUFF; WELL CEMENTED; LIGHT GRAY TO BUFF, SOME PINK
- TOS₃ - BEDDED TUFF; WELL CEMENTED; RED AT TOP AND BASE, PINK TO BUFF INTERBEDS
- TOS₂ - BEDDED TUFF; MOSTLY LIGHT GRAY TO BUFF
- TOS₁ - BEDDED TUFF; PURPLISH TO PINKISH RED
- D₄ - LIMESTONE; HARD, DENSE, CRYSTALLINE; MEDIUM TO DARK GRAY

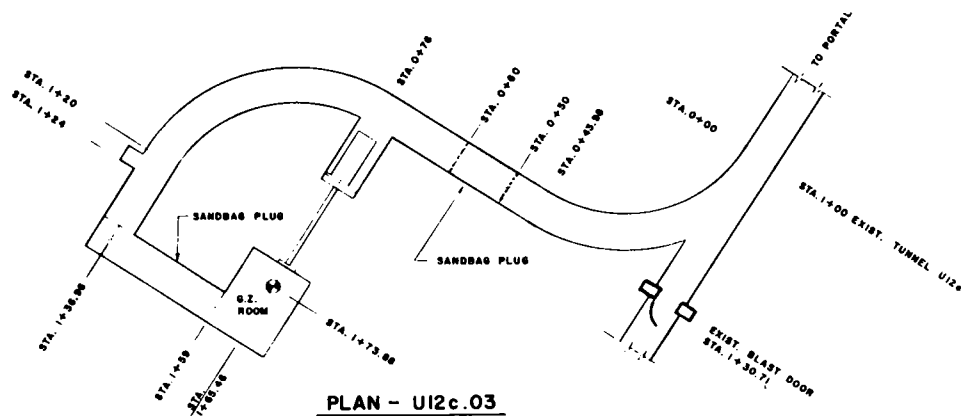


FIGURE III.4 GEOLOGIC SECTION,
TUNNEL UI2C
(REFERENCE 3)

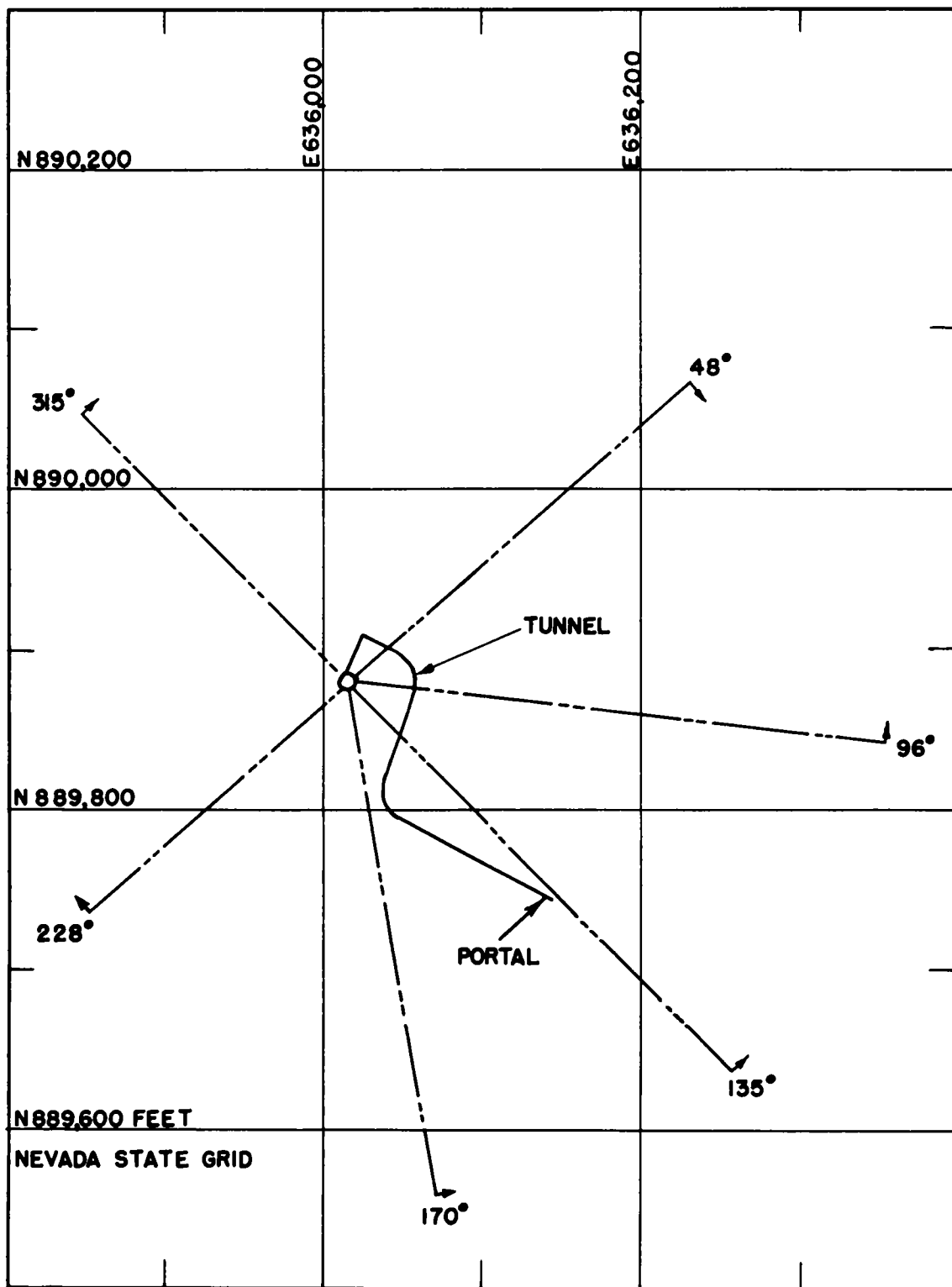


FIGURE III.5 NEPTUNE CRATER SECTIONS PLOT PLAN

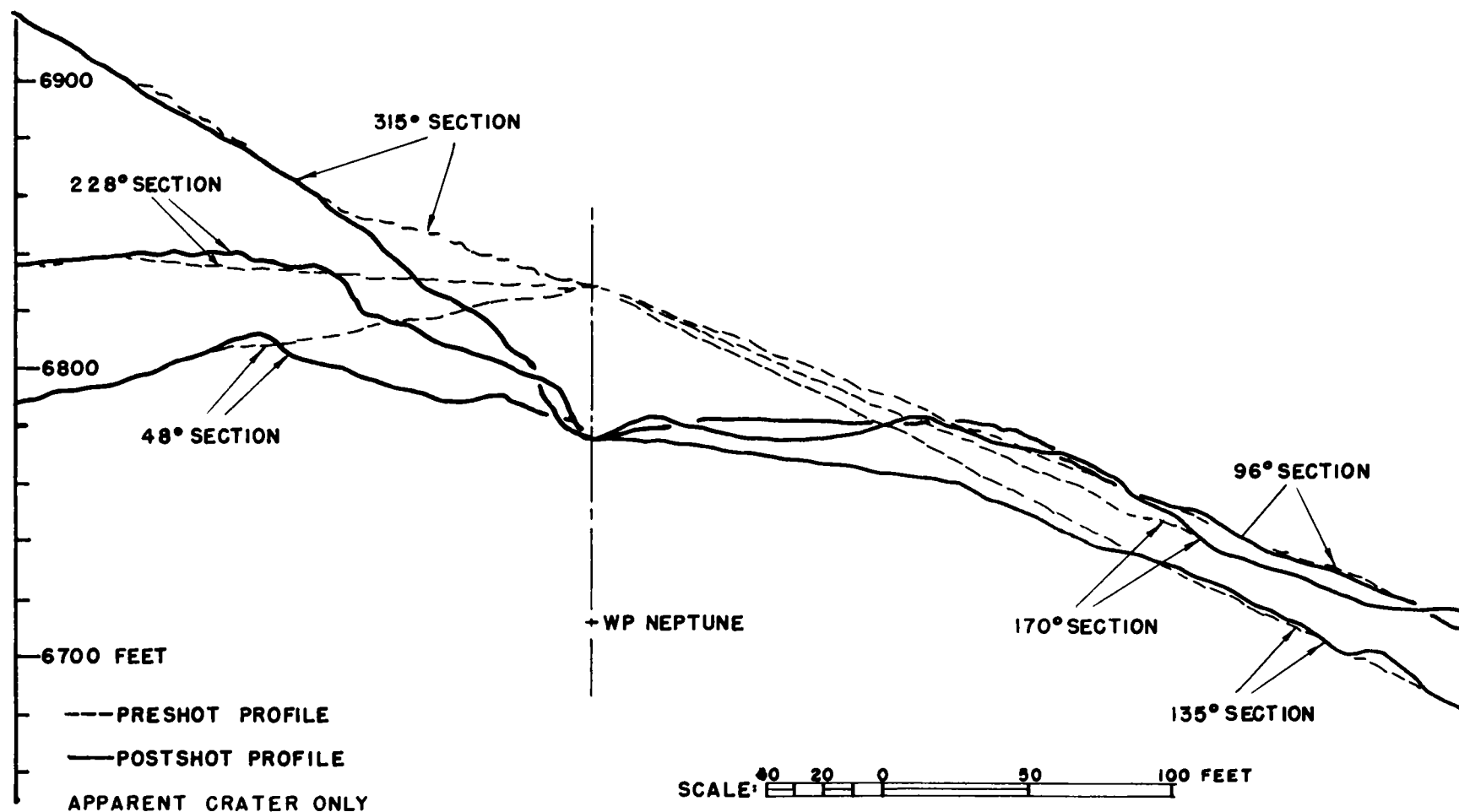


FIGURE III.6 NEPTUNE CRATER SECTIONS

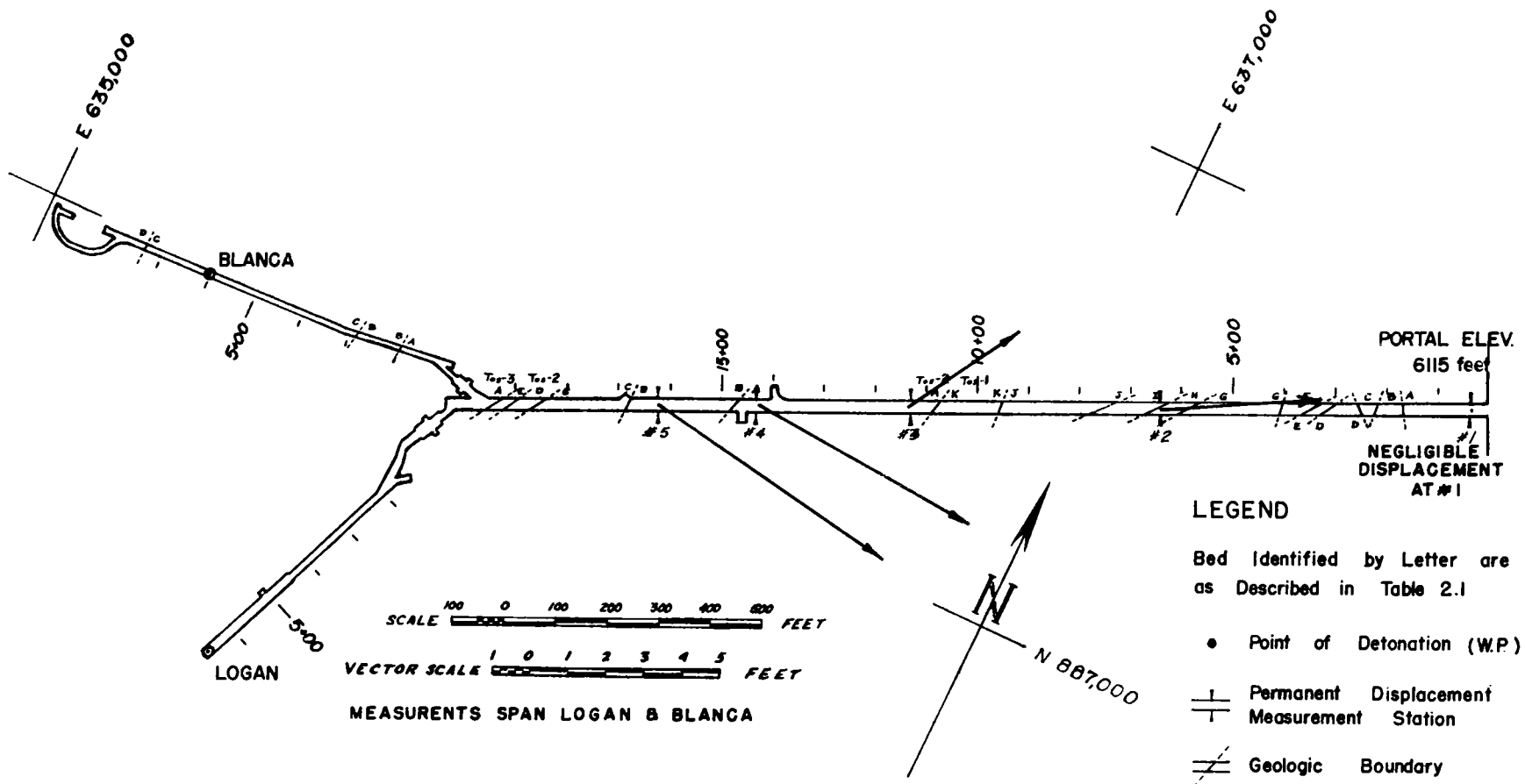


FIGURE III.7 PRE-EVENTS TO POST-EVENTS, TUNNEL U12e

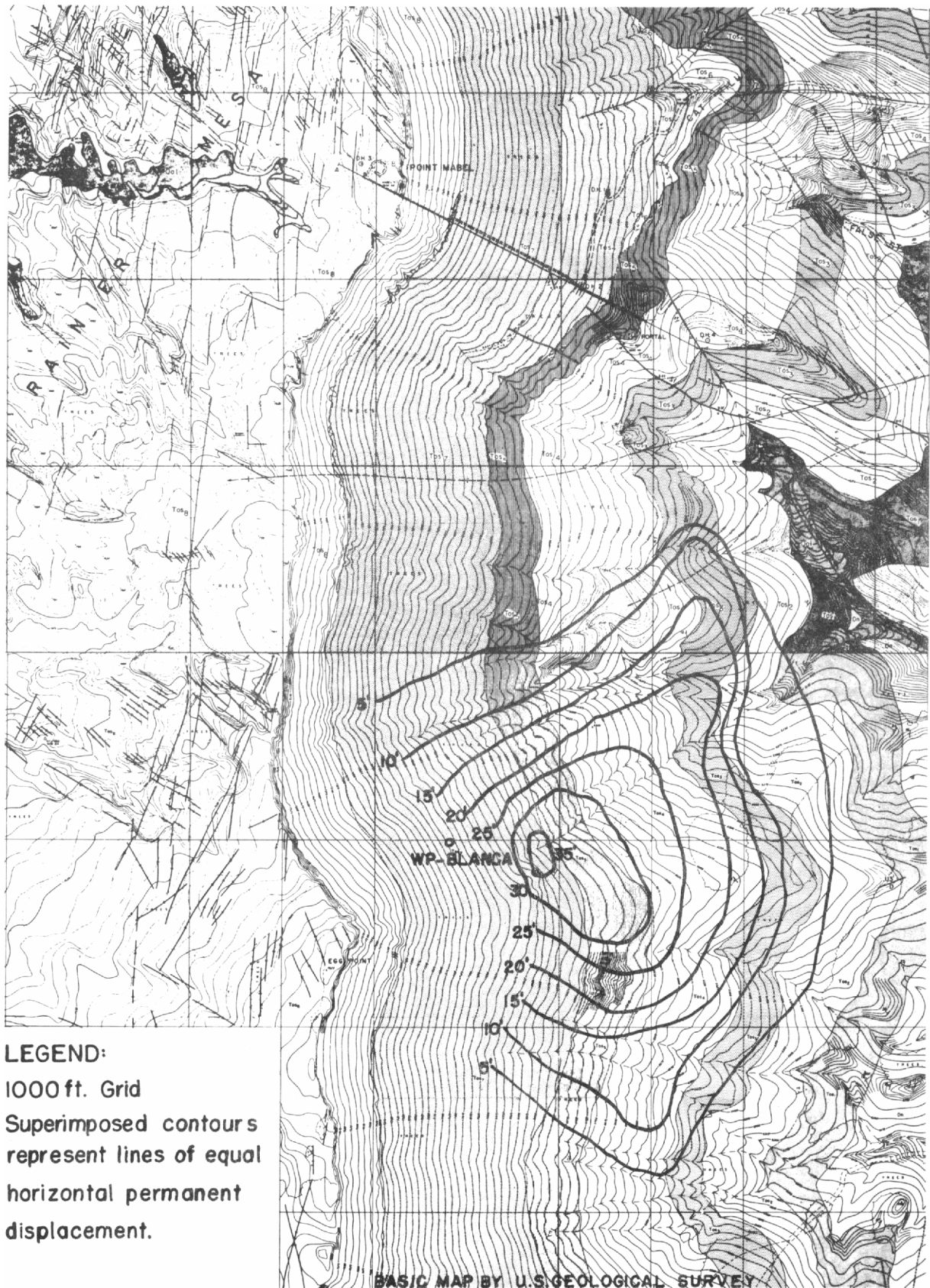


FIGURE III.8—SURFACE HORIZONTAL DISPLACEMENT CONTOURS,
BLANCA

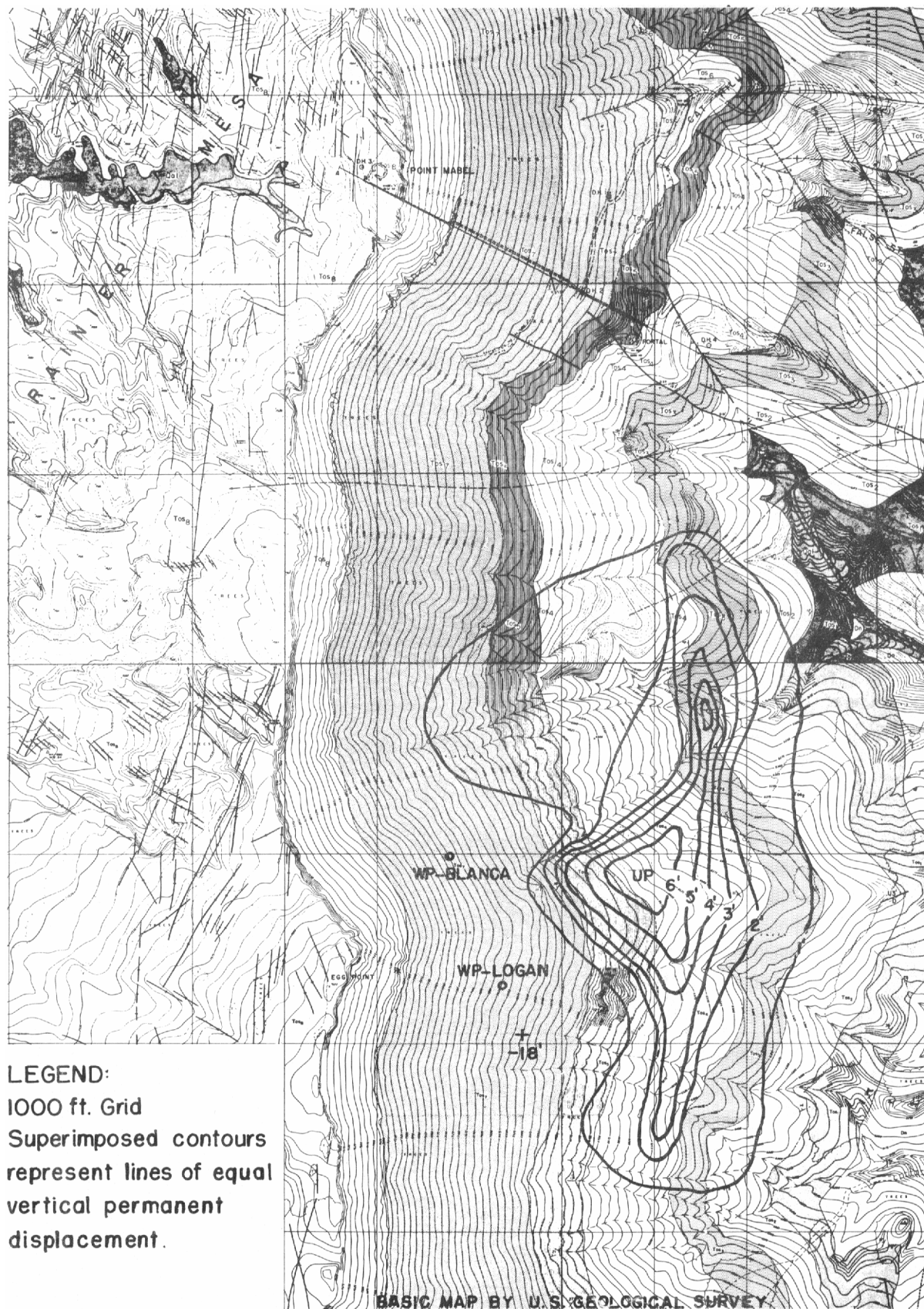


FIGURE III.9—SURFACE VERTICAL DISPLACEMENT CONTOURS, BLANCA

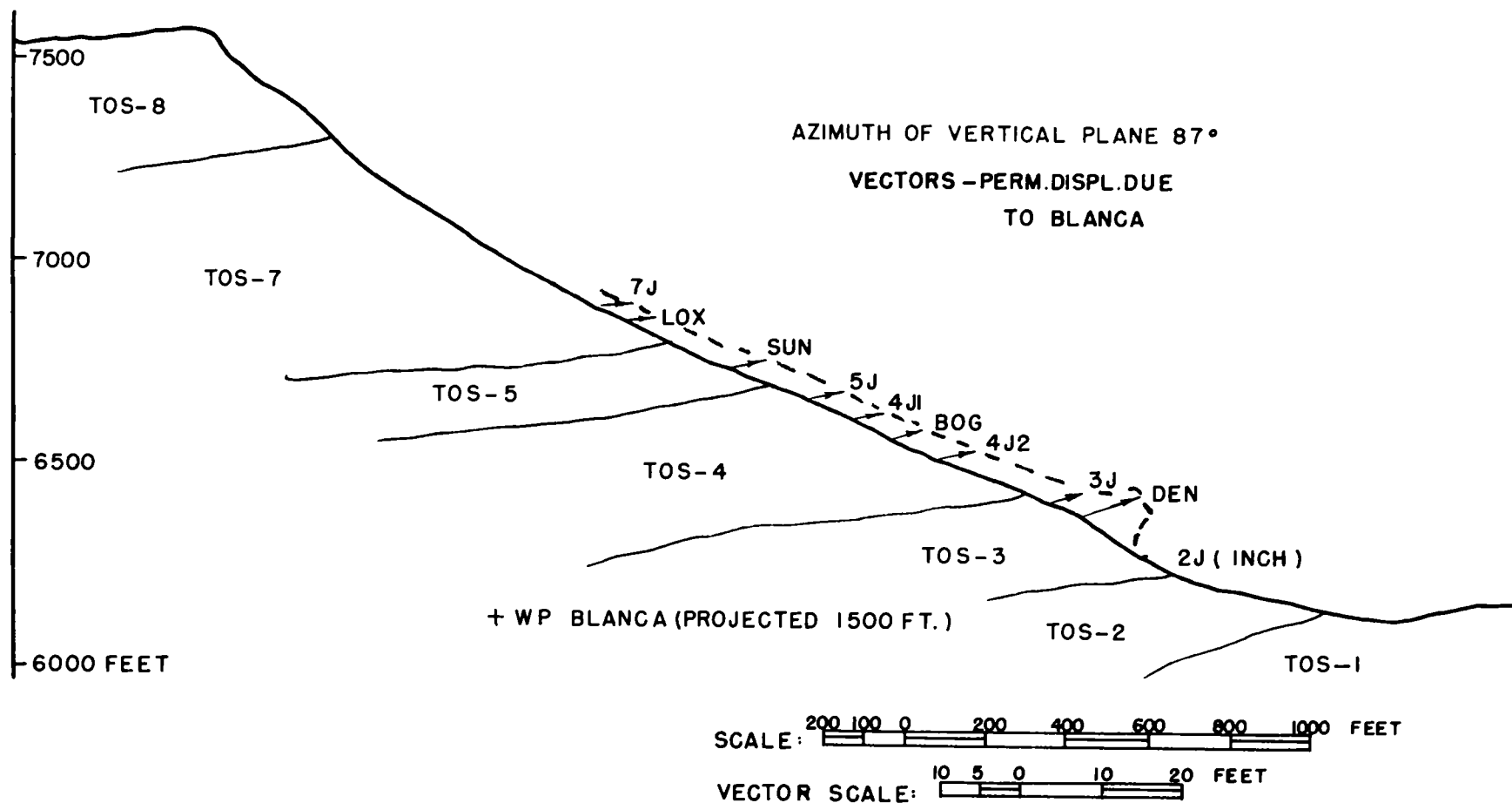


FIGURE III.10 SECTION ALONG LINE-J

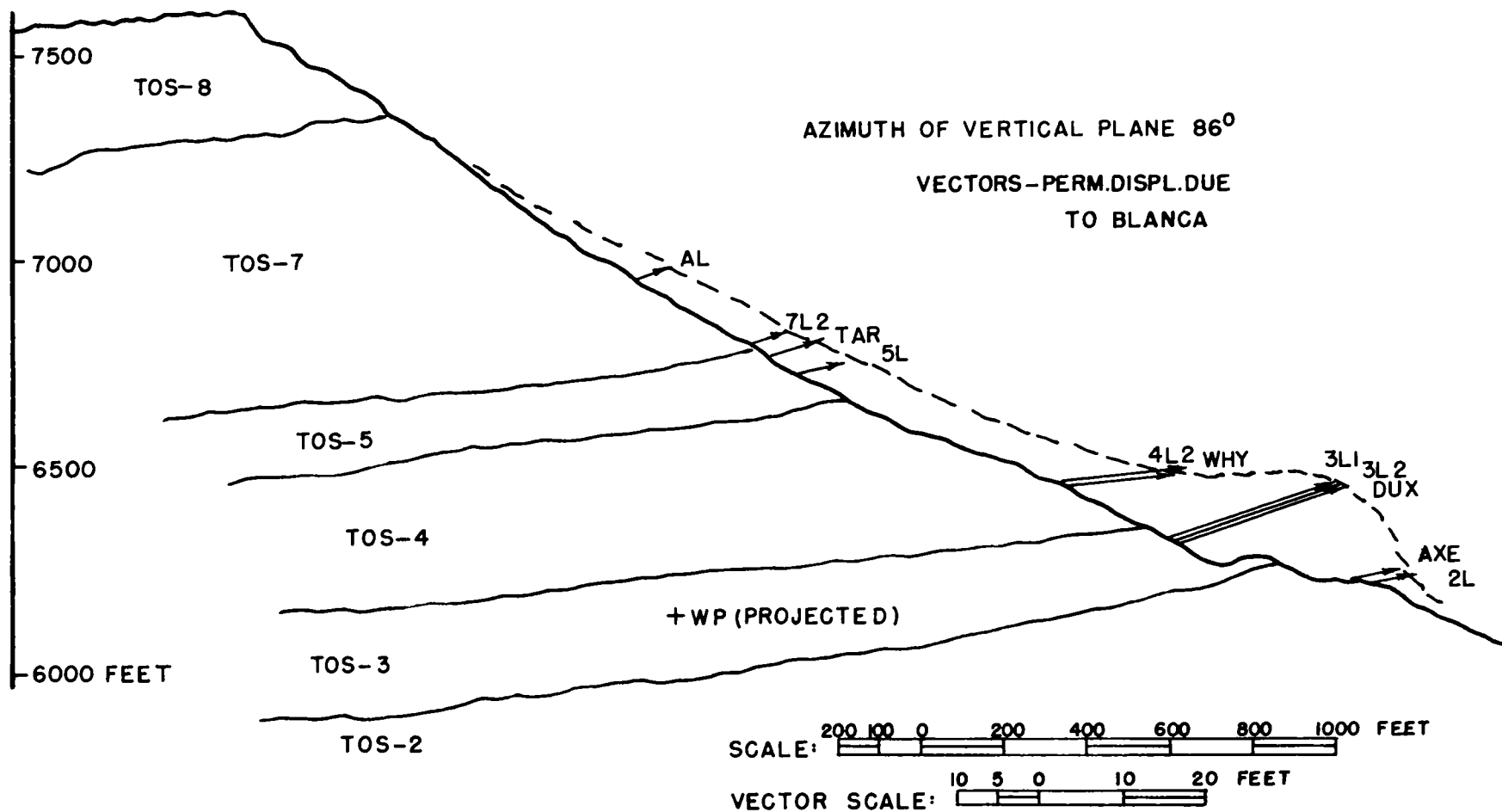


FIGURE III.11 SECTION ALONG LINE-L

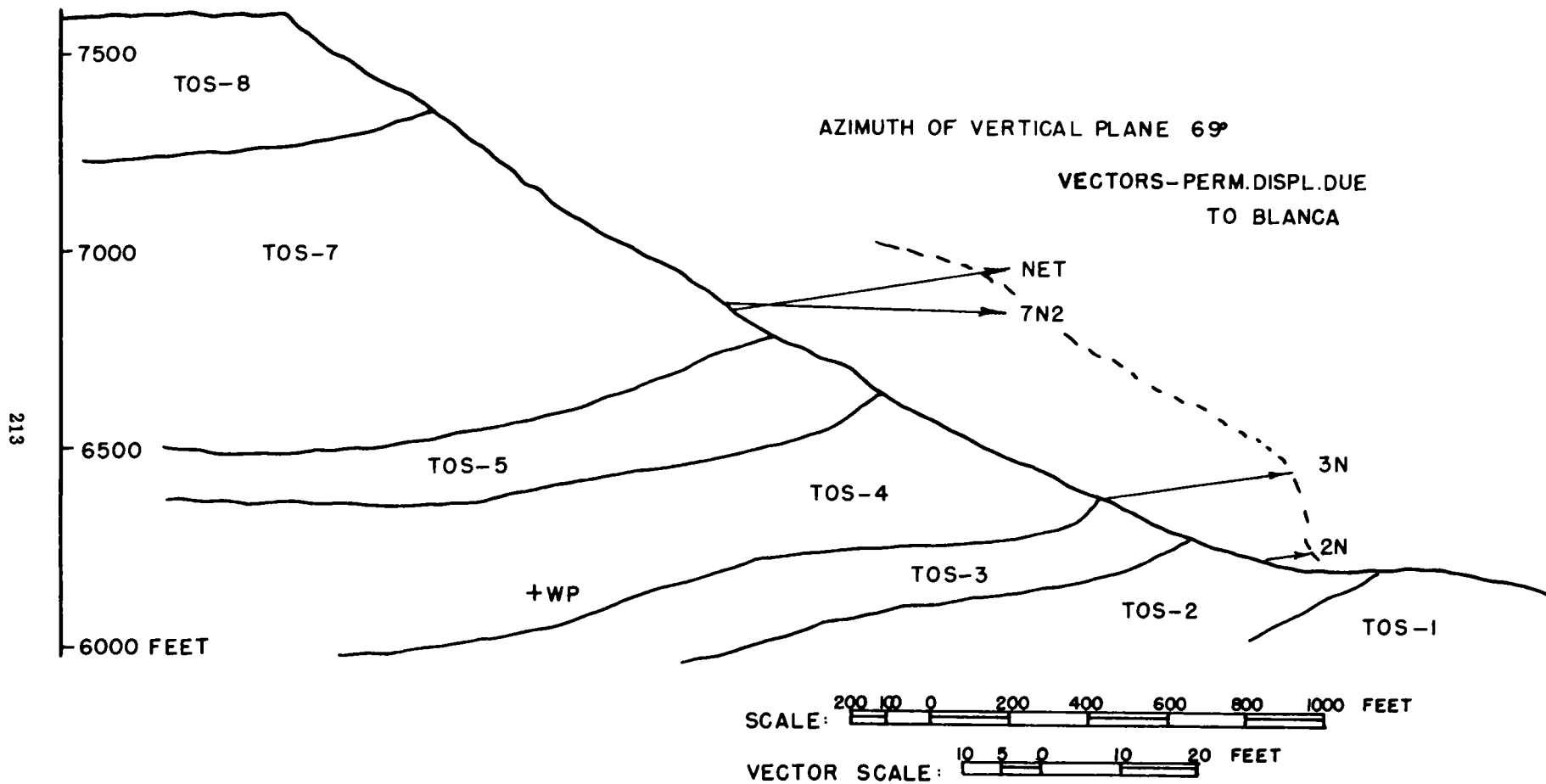


FIGURE III.12 SECTION THRU WP-BLANCA

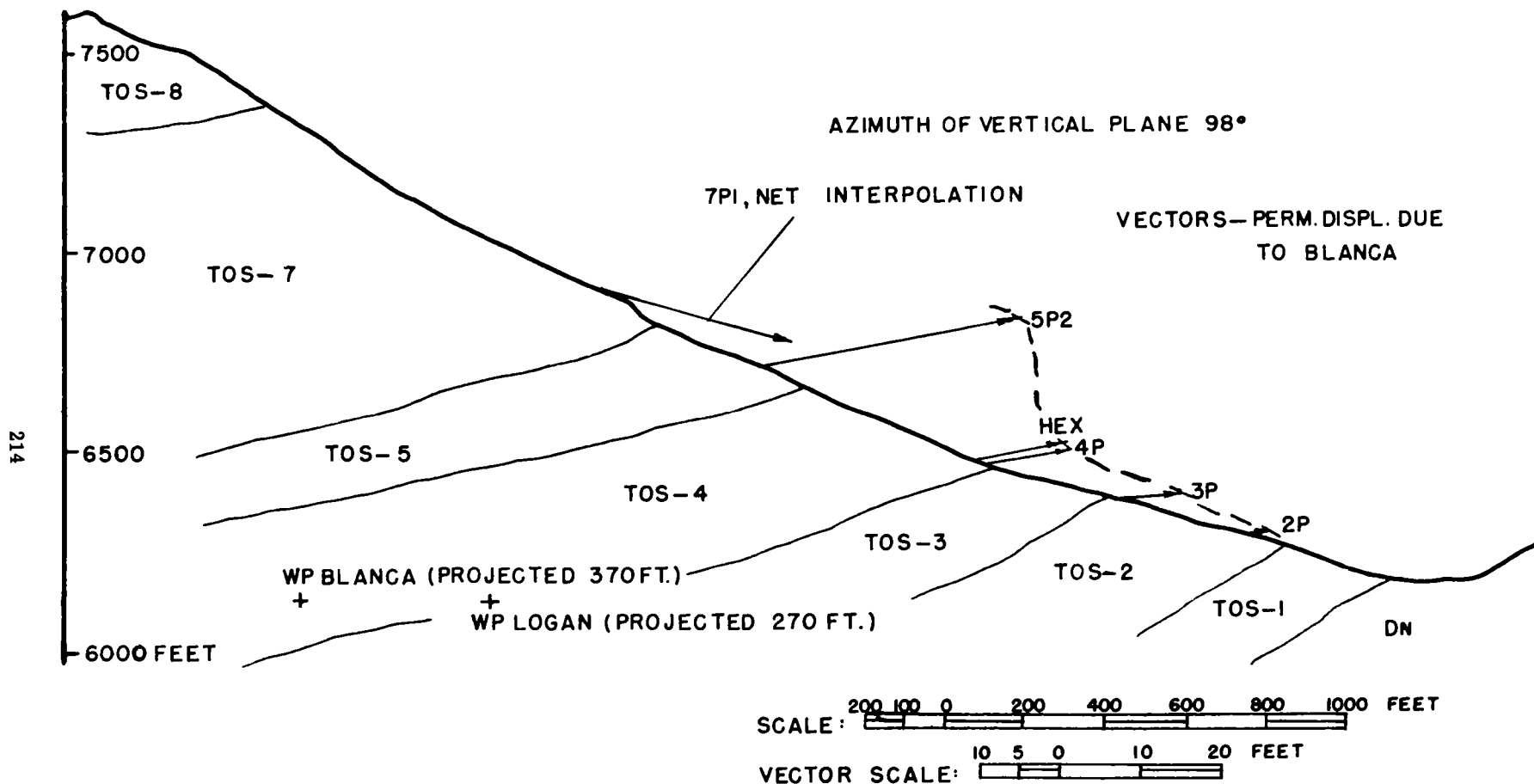


FIGURE III.13 SECTION ALONG LINE-P

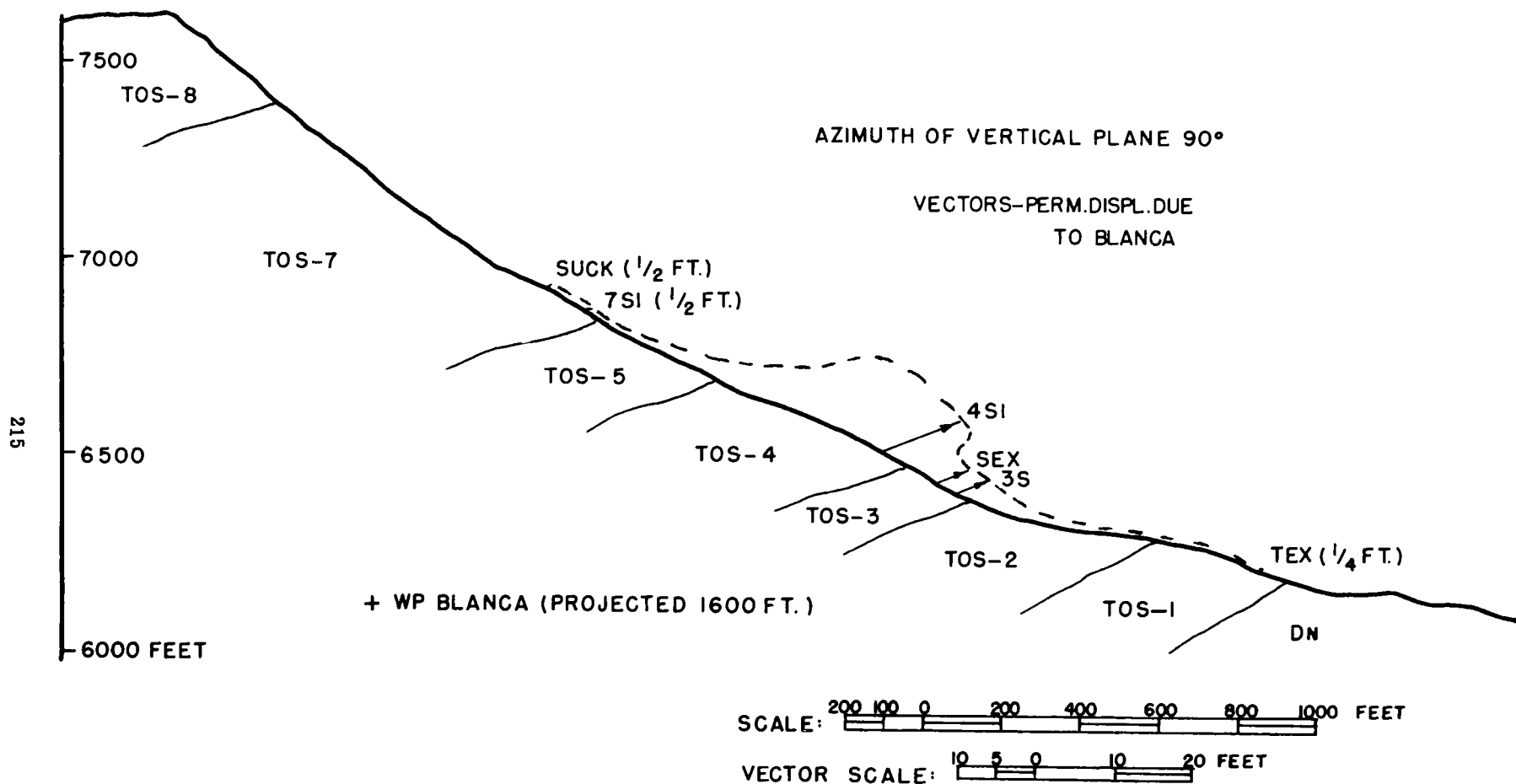


FIGURE III.14 SECTION ALONG LINE-S

REFERENCES

1. M. V. Anthony; "Ground Motion Measurements," Operation Hardtack II, ITR-1704 (1959).
2. Walter Helm; "ITR-1712," Operation Hardtack II.
3. G. W. Johnson and C. E. Violet; "Phenomenology of Contained Nuclear Explosions," UCRL-5124 Rev.I (1958).
4. F. A. Pieper, A. C. Tiemann, and R. H. Sievers, Jr.; "Subsurface Accelerations and Strains from an Underground Detonation. Part II," ERDL, WT-1531 (1958).
5. W. R. Perret; "Subsurface Motion from a Confined Underground Detonation. Part I," Sandia Corporation, ITR-1529 (1957).
6. J. W. Cattermole, "Geology of the USGS Tunnel and Underground Effects of the High Explosives Tests, Nevada Test Site," U. S. Geological Survey Trace Elements Investigations Report 715 (TEIR-715).
7. W. R. Hansen and R. W. Lemke; "Geology of the USGS and Rainier Tunnel Areas, Nevada Test Site," U. S. Geological Survey Trace Elements Investigations Report 716 (TEIR-716) (1957).
8. A. B. Gibbons; "Geologic Effects of the Rainier Underground Test, Preliminary Report," U. S. Geological Survey Trace Elements Investigations Report 718 (TEIR-718) (1958).
9. Engineer Research Associates, Inc., "Underground Explosion Test Program, Technical Report No. 5, Sandstone," 15 February 1953.
10. USC and GS "Plane Coordinate Projection Tables, Nevada," Special Publication No. 318, Dept. of Commerce, 1954.
11. R. M. Foose and R. B. Hoy; "Air and Ground Inspection Techniques for the Detection of Underground Explosive Tests," Stanford Research Institute, ITR-1715 (1959).

12. M. A. Chaszeyka and F. B. Porzel; "Study of Blast Effects in Soil, Final Report," Armour Research Foundation Project No. D119 (1958).
13. Engineering Research Associates, Inc., "Underground Explosion Test Program, Technical Report No. 4, Granite and Limestone," 30 August 1952.
14. D. L. Martin, "Nuclear Cratering Phenomena (U)," unpublished ERDL technical report.
15. O. K. Ehlers, F. A. Piper, and A. C. Tiemann, "High Explosive Equivalence for Underground Detonation of Operation Plumbbob," unpublished ERDL technical report.
16. R. V. Proctor and T. L. White, "Rock Tunneling with Steel Supports," Commercial Shearing and Stamping Co. (1946).
17. J. L. Merrit and N. M. Newmark, "Design of Underground Structures to Resist Nuclear Blast," University of Illinois, April 1958.
18. "Design of Structures to Resist the Effects of Atomic Weapons," Manuals-Corps of Engineers, U. S. Army:
 - a. "Principles of Dynamic Analysis and Design," EM 1110-345-415, 15 March 1957.
 - b. "Structural Elements Subjected to Dynamic Loads," EM 1110-345-416, 15 March 1957.
 - c. "Arches and Domes," EM 1110-345-420, draft.
 - d. "Buried and Semi-Buried Structures," EM 1110-345-421.
19. G. H. Albright, "Evaluation of Earth-Covered Prefabricated Ammunition Storage Magazines as Personnel Shelters," Operation Plumbbob, ITR-1422 (1957), Confidential, formerly Restricted Data.

20. G. H. Albright, "Evaluation of Buried Conduits as Personnel Shelters," Operation Plumbbob, ITR-1421 (1957).
21. T. G. Morrison and M. R. Johnson, "Full Scale Field Tests of Dome and Arch Structures," Operation Plumbbob, WT-1425, draft, Confidential, formerly Restricted Data. [Also, see ITR-1425 (1957).]
22. J. J. Meszaros, H. S. Burden, J. D. Day, "Instrumentation of Structures for Air-Blast and Ground-Shock Effects," Operation Plumbbob, ITR-1426 (1957).
23. G. H. Brittain and E. H. Scharres, "Dome-Structure Response Instrumentation," Operation Plumbbob, ITR-1525 (1957).
24. E. Cohen and E. Laing, "Response of Dual-Purpose Reinforced-Concrete Mass Shelter," Operation Plumbbob, ITR-1449 (1957).
25. "Building Code Requirements for Reinforced Concrete," American Concrete Institute, ACI 318-56 (1956).
26. N. M. Newmark, "Analysis and Design of Structures to Resist Atomic Blast," Bulletin of the Virginia Polytechnic Institute, Vol. 49, No. 3 - Part 2, January 1956.
27. A. Ali, "Dynamic Stress-Strain Characteristics of Various Materials," The University of Texas Structural Mechanics Research Laboratory, Austin, Texas, June 3, 1957.
28. "The Effects of Nuclear Weapons," United States Atomic Energy Commission, June 1957.
29. W. Kaplan, "Advanced Calculus," Addison-Wesley Pub. Co., Inc., Cambridge, Mass. (1953).
30. "Introduction to Flexible Urethane Foam," The Dayton Rubber Co., Dayton, Ohio (1958).

